Modeling the Hydrologic Effects of Longwall Mining on the Shallow Aquifer System using MODFLOW with Telescopic Mesh Refinement

Final Project Report to Office of Surface Mining

Project P.I. Colin J. Booth

Institution: Northern Illinois University

Authors: Colin J. Booth and Christopher B. Greer
Department of Geology and Environmental Geosciences
Northern Illinois University
DeKalb, IL 60115
cbooth@niu.edu

Date: Final report: August 25, 2010
Format Revisions: January 5, 2011

Contents

List of Figures with captions

List of Tables

Executive Summary

Longwall mining is an efficient and economical form of underground coal mining that has substantial impacts on surface and near-surface hydrologic systems. The hydrologic mechanisms involved are now relatively well understood in principle, but techniques to model and predict the impacts using standard groundwater modeling software have not been developed.

The objective of this project was to develop an approach by which the widely used groundwater flow model MODFLOW could be applied to simulate the hydrogeologic impact of longwall mining subsidence in the upper part of the overburden. By restricting the model to the shallow system above the intermediate confining zone that is common to virtually all longwall profiles, we avoid issues of mine drainage, variably saturated flow and extreme fracturing that characterize the lower part of the overburden and make MODFLOW unsuitable.

The project used the Groundwater Vistas ® interface (GV) (version 5) to the MODFLOW codes.

The principal problems to address were thus:

(1) *The high hydraulic gradients and rapid spatial variation of hydraulic properties in the overburden above the longwall panels.* This issue was addressed by the use of Telescopic Mesh Refinement (TMR), using the TMR conversion feature in GV that transfers the basic physical and hydraulic framework from a regional model to a more refined local model.

(2) *Changes in hydraulic properties due to fracturing as a site is undermined and subsides, affecting the groundwater flow system*. These can be summarized as

(a) Rapid increase in fracture porosity through fracture openings and bedding separation in the early tensile phase of subsidence, which causes rapid transient head drops, especially in confined bedrock aquifers. This cannot be handled in MODFLOW by storage coefficient manipulation. However, we represented this effect by using well sinks, a standard modeling feature, to simulate the rapid loss of water into the new void space. A partial reversal in the compression phase is simulated by source wells.

(b) Fracture-induced increases in hydraulic conductivity (K) and storage coefficient (S) in the subsidence area over the panel during the initial tensile phase, followed by partial reduction during the compression and settlement phases. There is no mechanism in MODFLOW or GV to include these changes in a continuous simulation. In this study, we approximate the advance of the longwall mine panel in short discrete steps and then manually adjust the pre-defined property zones in each layer.

(c) Subsidence of ground and layer elevation, up to about 2 m above the 3-m extraction in the study area. This was not simulated in the demonstration model as it would require cell-by-cell adjustments in the elevation property matrix for each layer at each discrete advance step, a major manual effort between each run, with uncertain stability of the outcome. Further procedure research is needed for this problem.

A demonstration model was constructed to simulate the hydrologic behavior over a four-panel section of a longwall mine in Jefferson County, Illinois, for which extensive field data are available from an earlier field study.

Study Site

The Jefferson County (Rend Lake) site is located in south-central Illinois (Figure 1.0). It consists of gently rolling topography with only about 15 m (50 ft) of local relief, drained by several small streams that now flow into Rend Lake reservoir. The Rend Lake mine extracted the Herrin (No. 6) Coal, which averaged about 3 m thick at depths of about 222m. The overburden strata at the site largely consist of shales and siltstones, but the principal units of hydrogeologic interest are the Mount Carmel Sandstone at a depth of about 21-23 m, and the overlying shale and glacial clay-till with some sand and gravel lenses. The Mount Carmel consists of a lower channel sandstone and an upper sheet sandstone separated in the study area by a shale-siltstone unit 0-6 m thick.

The site was studied in detail between 1988 and 1995, especially over the last two panels. The 3-m extraction produced about 2 m of ground subsidence. Hydraulic conductivities in the sandstone, originally around 10^{-6} m/s, were increased by about an order of magnitude in the central subsidence trough and by one to two orders in the residual tension zone along its edges.

Potentiometric responses to the mining of panels 3 and 4 were monitored starting in mid-1988. The observed heads (initially measured in the range 100-110 m AMSL) declined rapidly ahead of the approaching mine face and subsidence zone, due to drawdown transmitted outwards from the primary head drop occurring in the zone of active tensional fracturing. The most rapid drop and minimum values are in the early tensile phase of subsidence. After a low of 42 m below ground surface (BGS), water levels partially recovered during the compression phase and then reached about 10 m BGS by the end of monitoring in 1995 and 6 m BGS in 2008.

Regional Model

The Regional and Local Models (RM, LM) represent the upper 60-70 m of the 220-m overburden system. Both consist of the same 8 layers including the sandstone aquifer, the immediately underlying shale and limestone, and the overlying shale and glacial drift. The regional model (RM) area is about 53 km^2 and encompasses natural boundaries of the sandstone paleochannel to the west, north and southeast, the Rend Lake Fault Zone east of the mine, and Rend Lake reservoir across the eastern area. .

A steady-state regional model (RM) with 34,200 cells (57 rows x 75 columns x 8 layers) was developed in Groundwater Vistas® (GV) and calibrated to a reasonable approximation of the potentiometric heads across the area against a limited data base of water levels. The key calibration targets were the water levels in the Panel 4 study area.

The final calibration was reached using 10 hydraulic conductivity property zones (some layers had more than one zone), constant-head external boundaries in the more permeable aquifer units

and no-flow external boundaries in the low-permeability units, a complex configuration of the Rend Lake Fault System, and stream-drains in the surficial layer that permitted the discharge of shallow water and kept shallow water levels down to acceptable levels.

Local Model

A Local Model (LM) was created from the RM using the TMR conversion process in Groundwater Vistas. The LM consisted of 146,624 cells of uniform size 20 m x 20 m, arranged as a grid of 158 columns x 116 rows. The 8-layer configuration and same layer thicknesses were used directly from the RM. The LM covers the study area of the four longwall panels (each 183 m wide and up to 1,737 m long), barrier pillars, a subsidence region around the panels and an external estimated radius of hydrologic influence extending about 600 m outside the subsidence area. The total area of the LM is about 7.3 km^2. Storage coefficients for transient simulation were specified from field and literature values. Base hydraulic conductivity zones were mapped in from the RM and modified locally in the subsidence zones as described below. The final demonstration model has constant-head external boundary conditions set by the RM, and internal stream/drain boundaries in (layers) L1 and L2.

As noted above, two mechanisms of hydrologic impact of longwall subsidence were simulated: the rapid increase in fracture porosity that occurs in the early stages of subsidence resulting in rapid head drops, and enhancement of hydraulic conductivity and storage coefficient resulting from fracturing and bed separation. The modeling approaches were based on the conceptual model of the mechanisms involved as well as constraints in MODFLOW and GV.

The transient fracture porosity increase was simulated by well sinks. Equivalent "pumping" rates were determined from estimates of the total volume of new void space per grid cell divided by the estimated time of rapid subsidence during which they were created.

The K and S increases were simulated by a discretely advancing package of three stress zones: an advance zone (A) of slight increase; a tensional zone (B) of major increase during the principal subsidence phase, and a compression zone (C) in the later subsidence stages, during which some of the earlier increase was partially reversed. Modification values in the three stress zones were respectively 2x, 10x and 7.5x the base K and S values in most property zones; these are of course uncertain (though suggested by field data) and subject to further calibration. The final zone configuration is an interior rectangle in the central subsidence area over the panel with residually enhanced zone-C properties, surrounded by a margin with residually greater enhanced zone-B properties.

The simulations require separate model runs for each mine advance, because of the inability of MODFLOW to change K and S values during a run. Between each run, the user must manually advance each stress zone and well-sink simulation package to the next position, a somewhat laborious process although one that could be handled routinely once the basic model structure has been designed. At each successive run, the initial heads are input from the final heads of the previous run; thus, the previous model file must be accessible to the active file. The first model that initializes the heads in the sequence is the steady-state LM derived from the original RM.

In the demonstration model, panels 1 and 2 were modeled coarsely by a single transient model with 10 continuous stress periods (total 200 days) for the well sinks and a predetermined K and S configuration. The advances of Panels 3 and 4 were modeled in more detail with individual runs, each of 100-m advances in 6 days. The sequence was completed with a recovery simulation to 1800 days after the end of mining.

Results

The overall pattern of simulated potentiometric levels was very similar to values observed over Panel 4 during the 1988-1995 study. The precise timing and values of the simulated responses were not exactly equivalent (simulated drawdowns were about half those observed), but they were in the right range and could be adjusted to a better solution in a calibration process with the appropriate combination of K and S modifications and well-sink values. The model is considered successful as a demonstration of techniques that can be used to apply MODFLOW to longwall mining.

The well-sink approach was successful in simulating the transient cone of depression that forms in the subsiding area due to the rapid opening of bedding planes and fractures. This is a simple way to represent a key mechanism that has not previously been modeled in the longwall situation. The precise values of drawdown would still require calibration-type adjustments of the well-sink parameters and K and S modification factors. Nevertheless, the simulated values were in an appropriate general range of observed drawdown both at the center of the subsiding area and as transmitted to adjacent panels.

The concept and use of stress zones in discrete steps to modify the hydraulic properties as the mine face and subsidence front advances is also new and was also successful procedurally. It is a viable though time-consuming way to apply MODFLOW to the longwall mine subsidence problem. Again, the difficulty is the uncertainty about the magnitudes and distribution of property changes. The general pattern of the simulated heads in the demonstration model was consistent with field observations and expectations, but reproduction of precise values at specific locations would need more calibration.

The major inconsistency between the simulated result and observed field condition was the overall head elevation (above datum). Simulated heads were some 10 m higher than field heads at all times except for the final recovered static level, on which the steady-state Regional Model was original calibrated. Whether this is a problem of incorrect initial steady-state levels, insufficiently intense stress from the panels, or possibly incorrect storage coefficient values (which are not calibrated in the steady-state RM) is a problem for further work. In addition, the radius of influence of the potentiometric depressions produced by mining extend farther out than originally expected, touching the boundaries of the LM, and it may be that more of the RM needs to be included in the LM during the TMR process.

Future Work.

For the specific model developed in this study, a more complete LM sensitivity analysis and calibration study are required. However, these are issues of interest primarily for the background

case study rather than the demonstration purpose of the project. More generally, experimentation is needed on incorporating elevation changes due to subsidence into the discrete stepwise advance routines of the LM, which can be worked in GV, and developing feedback linkage from the Local Model to the Regional Model, which cannot.

The techniques demonstrated in this modeling project can be applied to other areas. Substantial supportive work in obtaining site information and in developing the conventional regional model would be needed, but application of TMR and the procedures developed for the LM would be relatively straightforward.

1. Introduction

1.0 Introduction

This study was designed to apply an established groundwater model tool (MODFLOW with Telescopic Mesh Refinement (TMR)), using readily available interface software, to simulate the impacts of longwall mining on the shallow aquifers above an underground longwall coal mine.

Longwall mining is an efficient and economical form of underground coal mining that has substantial impacts on surface and near-surface hydrologic systems. In its present form, it has been used extensively in the Appalachian coalfield and Mid-Continent region since the late 1970's and early 1980's. Longwall has risen and fallen with the economics of the coal industry, but has shown recent resurgence in Illinois, for example.

However, longwall mining impacts the surface and near-surface system because of the extensive influence of subsidence and strata movement. Effects on wells, water resources and surface drainage are common concerns of the public when longwall mining is proposed in an area.

From many studies conducted since the 1980's, the hydrologic mechanisms and impacts of longwall mining are now well understood in principle. In practice, however, they are of considerable contention and misunderstanding among the public, and even technical personnel in environmental or engineering consulting companies are commonly unfamiliar with this complex interface of mining engineering and hydrogeology, The typical groundwater modeling tools used in more common hydrogeological problems have not been applied to longwall mining hydrology, and in the absence of guidelines or well-documented applications of accessible models, it is unlikely that technical personnel would develop such applications. Thus, it is difficult for consulting companies or regulatory agencies to make site-specific predictions or characterizations regarding the hydrologic impacts of longwall mining. Techniques to model and predict these complex impacts using software and methods that are readily available are long overdue.

The overall objective of this study was thus to produce a well-documented approach, backed by a thorough case study, which can be used as a guide by engineering and hydrogeological companies and regulatory agencies for the application of modeling to evaluate and predict the hydrologic impact of longwall mining. The development and case study information are produced for the mid-continent region, but could be applied to other coalfield areas.

This project addresses issues of zoning, permitting, and planning longwall mining, and the goals of the Applied Science Program in developing, demonstrating and transferring essentially established technologies to the environmental problems related to mining, to help State regulatory authorities in permitting mines and protecting the public and the environment during mining and reclamation.

The report presented here includes an introduction to the OSM-sponsored project, review of longwall mining hydrology and modeling techniques, summary of the Illinois study site used for model development, description of the regional model (RM), and description of the local model (LM) produced from the RM using the TMR conversion in Groundwater Vistas. The LM was then used to develop new approaches to simulating the impact of longwall mining on the shallow aquifer system in MODFLOW, particularly the representation of the effect of fracture porosity increases through well sinks and the subsidence-induced modification of hydraulic properties using stress zones traveling in discrete steps.

1.1 Objectives

The specific objectives of the project are:

(1) Develop and apply the use of MODFLOW with TMR to the problem of modeling the hydrological effects of longwall coal mining on overlying aquifers. This application is restricted to aquifers in the shallow part of the overburden system, not to deep aquifers in the immediate roof zone. Mine inflow is not modeled.

(2) Develop and demonstrate the MODFLOW-TMR application using a well-documented longwall site studied in Illinois for which we have extensive field data for both impact and recovery stages.

(3) Prepare appropriate documentation describing the application of MODFLOW-TMR that can be used by others in predicting site-specific longwall impacts on aquifers.

The project was originally intended to take 12 months from summer 2007 to summer 2008. The start was postponed to Fall 2008 due to budgetary constraints and then numerous personnel changes substantially delayed progress further. OSM permitted no-cost extensions through to summer 2010.

1.2 Approach

Particular aspects of the approach, discussed in more detail in later sections, are:

(1) This study focuses on the shallow groundwater system, not the hydraulically more complex, heavily fractured, variably saturated deep zone immediately above the mine. The shallow system is suitable for MODFLOW-type porous media modeling and is typically separated hydraulically from deep mine drainage effects by a confining zone in intermediate levels of the overburden.

(2) The major problems modeling the groundwater behavior in the shallower subsidence zone above the longwall mine are:

> (i) Changes in hydraulic properties and elevations due to subsidence and related fracturing;

(ii) Rapid loss of water into suddenly opened fracture space;

(iii) Steep hydraulic gradients and rapid transient head changes in the affected strata.

Handling these problems in a numerical model requires a finely discretized grid over a local area that is nevertheless part of the natural groundwater system over a broader regional area. TMR provides an established approach for this problem. The regional model (RM) and local model (LM) are hydraulically linked by common boundary conditions.

(3) The model development and calibration are based on a well-documented case study of longwall mining in Jefferson County, Illinois that was investigated in detail by the PI (from NIU) and the Illinois State Geological Survey in 1988-1995. Data available from this study include monitoring and measurement of ground subsidence, strata movement, potentiometric changes, and hydraulic properties before and after subsidence. The development is based on this Mid-Continent setting but the end result should be adaptable to any region with longwall mining.

The original intention was to use two types of MODFLOW interface software: Visual MODFLOW® by Waterloo Hydrologic Inc. (now Schlumberger Water Services, Inc.) and Groundwater Vistas® by Environmental Simulations Inc. Both are widely used in the environmental industry and thus likely to be familiar to target users; both are relatively straightforward, well validated, and regularly updated; and both were licensed for use in the institutional department. However, a necessary upgrade of Visual MODFLOW resulted in operating restrictions that made the software impractical for use (it required Administrator-level privileges that are not permissible on student-accessible computers) and so the decision was made to use only Groundwater Vistas.

The MODFLOW programs produced by the USGS comprise FORTRAN source codes in the public domain. Although available for use or modification, these codes use input/output structures that are difficult and impractical to use for any complex modeling problem. In contrast, commercially available visual interface software permits input, output, and operation of the many capabilities of MODFLOW through standard WINDOWS-based operation. Groundwater Vistas (GV) is a screen-based visual interface by which the user creates and modifies the model framework (grid, layers, hydrogeologic properties, stresses, boundary conditions, etc.), selects and sets up an appropriate flow model (e.g. MODFLOW-2000, etc.) to run on the model framework, generates the visual presentation of the simulation results, and also supports numerous enhancements such as auto-calibration, post-processor transport models, etc. The capabilities and choices in GV are enormous but the procedures to utilize them are complex.

1.3 Student Training

The following students from the Department of Geology and Environmental Geosciences have received support, training and practical experience while working on this project:

Graduate students (experience with data manipulation, numerical modeling using MODFLOW, conceptual understanding of longwall mining hydrology, and field work):

Eduard Breuer (Research Assistant, 2007-2008)
Christopher Greer (Research Assistant, 2009-2010)

Undergraduates (experience with data manipulation, spreadsheet work, graphics preparation, and reference research):

Ryan Adams (Student help, 2010)
Michael Bramnik (Student help, 2010)

1.4 Presentations

The following presentations based on project results have been made to geologists, engineers and environmental scientists in the Midwest region:

2010 Booth, C.J. and C.B. Greer. Modeling the hydrologic effects of longwall mining on shallow bedrock aquifers using MODFLOW with TMR: GSA Abstracts with Programs, vol. 42 (2) #171447. Geological Society of America North Central/South Central Meeting, Branson, Missouri, April 11, 2010.

2010 Booth, C.J. and C.B. Greer. Modeling the hydrologic effects of longwall mining on shallow bedrock aquifers using MODFLOW with TMR. Illinois Groundwater Association, Lisle, Illinois, April 22, 2010

October 2010: Booth, C.J. and C.B. Greer: Modeling the Hydrologic Effects of Longwall Mining on Shallow Aquifers Using MODFLOW with TMR, Midwest Ground Water Conference (MWGWC), Columbus, OH. In topical session: "Groundwater Issues Related to Development of Energy Resources" (October 6, 2010).

Abstracts for these presentations and the PowerPoint® presentation for the IGA meeting and MWGWC meeting were provided to OSM. Further presentations are intended.

2. Review of Longwall Mining Hydrology and TMR Modeling

2.1 Hydrogeological effects of longwall mining

Longwall mining completely extracts large rectangular panels of coal, typically 150-300 m wide and several kilometers long, resulting in the rapid collapse of the unsupported roof and consequent subsidence of the overlying strata and ground surface. A complex suite of hydrogeological responses results from these movements. Fracturing and bed separations change the fracture porosity and permeability of the overburden strata.

Extensive dewatering and drainage to the mine occur in the heavily fractured strata immediately above the mine, Wells bottoming in this deep zone typically lose water either permanently or until the mine floods after closure. Above this zone, at some intermediate level in the overburden, there is normally a relatively unfractured low-permeability aquitard zone that prevents shallower aquifers from draining to the mine (Singh and Kendorski, 1981). This zone may be subdivided into a lower dilated zone of increased horizontal permeability and an upper constrained zone of little to no change in permeability (Kendorski, 2006); both retain confining properties and protect the shallower aquifers. The heights and thicknesses of these zones in the overburden depend on overburden geology, depth of mining, width of the panel, extraction thickness and other factors.

Hydrologic responses in the strata above the aquitard zone result from *in situ* changes in hydraulic properties produced by subsidence, and generally not from loss of water to the mine. Typical responses are well documented and include lowering of water levels in shallow bedrock aquifers, often followed by recovery, and changes in stream flows, hydraulic gradients, and well yields (e.g. Rauch, 1989; Johnson, 1992; Matetic and Trevits, 1992; Werner & Hempel, 1992; Hutcheson et al., 2000a, 2000b; Booth, 2002).

Besides drainage to the mine, which is not normally significant for shallow aquifers above the confining zone, there are four principal mechanisms causing head drops above longwall panels:

(1) The opening of joints and separation of bedding planes in early subsidence suddenly increases the initial fracture porosity. As the void volume opens, water levels drop, producing a potentiometric low in the active subsidence area over the advancing longwall front. Increased fracture porosity causes rapid potentiometric head drops in confined bedrock aquifers, but has little effect in aquifers that are unconsolidated (because they do not depend on fracture porosity) and/or unconfined (because unconfined storage coefficients are much larger than confined coefficients).

(2) Drawdown (lowered water level) spreads outward through the aquifer as water drains toward the primary potentiometric low in the subsidence area. Although this is a secondary effect, the drawdown spreads ahead of mining and is thus the first and farthest effect seen at observation wells. It is transmitted farther and occurs more gradually in more transmissive units, whereas in poorly transmissive units it occurs more rapidly and closer to the site and time of undermining.

The lateral transmission of drawdown through aquifers controls the "radius of influence" of the hydrologic effect of longwall mining.

(3) Increased fracture permeability within the subsided zone reduces hydraulic gradients, lowering water levels upgradient, but also moderates the potentiometric lows generated in the subsidence area.

(4) In areas with moderate to high topographic relief, significant and often permanent head drops result from drainage of upper aquifers through fractured aquitards. This mechanism is particularly important for perched or hilltop aquifers in the Appalachian coalfield (Johnson, 1992; Werner & Hempel, 1992), but relatively unimportant in low-relief settings like Illinois.

Recovery of water levels in shallow aquifers is commonly observed within a few months to a few years after mining. Early partial recovery may occur rapidly in shallow bedrock units during the subsidence compressional phase when fractures and bedding separations close back up. Longer-term recovery depends on the flow of water into the transient potentiometric depression in the subsidence zone. This is dependent on site-specific factors such as an adequate source of recharge, a transmissive aquifer system, and the absence of continued major drainage to lower units.

2.2 Modeling the hydrologic effects of longwall mining

Previous Models. Application of groundwater models to the longwall mine problem has been very limited because of the difficulties in simulating the complex interaction of mining stress fields, changing hydraulic properties, and hydrologic impacts. Fully integrated models of the hydrological impact of longwall mining require linkage of strata deformation to the mining process (mining engineering and rock mechanics), changes in hydraulic properties to the deformation, and changes in groundwater flow to these controls. Furthermore, conditions in the deep fractured and caved zones include radically changing hydraulic properties, local boundary conditions, variably saturated regions, and mine voids and large fractures in which the Darcian porous media assumptions used in most models may not be valid.

Finite-element models that link strata deformation and hydraulic property changes through poroelastic theory and then simulate the groundwater flow patterns were developed at Penn State University in the 1990's (e.g. Liu and Elsworth, 1997; Kim et al., 1997). One variant, a 2D profile model that simulated the hydrologic response of a study site in Ohio, was developed for the US Bureau of Mines (Matetic et al., 1995). However, these research-level FE models have not been developed into accessible software for the modern PC and are not available for practical use.

The most widely used, well-validated, versatile, groundwater flow computer model, with several available commercial interface packages, is undoubtedly the USGS finite-difference model MODFLOW (McDonald and Harbaugh, 1988) and its variants (MODFLOW-88/96, MODFLOW-2000, MODFLOW-2005, etc.). Winters (2004) applied MODFLOW to a large-scale basin system in Pennsylvania that involved numerous mine complexes including mostly

flooded longwall mines. The mines were modeled as high permeability horizontal layers with a fractured overburden, and the application was on a large enough scale that porous media equivalence was probably satisfied. However, using standard MODFLOW models for the mine zone and the intensely fractured, variably saturated region with probable non-Darcian conduit flow is problematic. Recently, Merrick (2009) found that application of MODFLOW-SURFACT (a commercial variant of MODFLOW that simulates unsaturated flow) was more successful than standard MODFLOW in simulating the deep fractured zone and unsaturated conditions around a longwall mine in New South Wales, Australia. The model did not address transient hydraulic property changes or permeability changes in the shallow aquifer zone, but it demonstrated viability for the near-mine fractured and unsaturated conditions.

Current Approach. The approach to modeling used in the present study is based on the assumption that the intermediate confining zone (almost invariably present except in very shallow mines) allows us to separate the overburden into two model domains: the deeper zone, including the lower fractured zone and mine boundary, that is unsuitable for standard MODFLOW, and the shallow aquifer zone that is suitable for MODFLOW.

The shallow zone is typically dominated by saturated porous media flow, drainage to the mine is not an issue, and leakage to deeper zones can be simulated if necessary through appropriate lower boundary conditions. Several commercial software interfaces (e.g. Visual MODFLOW®, Schlumberger Water Services; Groundwater Vistas® (Environmental Simulations Inc.) are available and widely used. Nevertheless, several problems must be resolved, including the lowering of heads due to rapid fracture porosity increase, the dynamically changing hydraulic properties during subsidence, and the transient advance of the subsidence zone. Other problems include the steep hydraulic gradients and sharp spatial changes in hydraulic properties around the mined area.

2.3 Review of TMR

This project develops the application of available MODFLOW-based modeling techniques to simulate the hydrologic effect of longwall mining on the shallow aquifer zone, using Telescopic Mesh Refinement (TMR). It does not simulate the flow conditions in the deep mining zone, which are better addressed by other types of coupled models.

A problem in finite-difference (FD) numerical models like MODFLOW is that finely discretized grids are needed to simulate local areas of special interest or rapid spatial changes in head, but that to use a fine grid over the entire model domain is computationally very demanding. Mehl et al. (2006) provide a recent overview of possible approaches to the problem. The simplest solution is one FD model with variable grid spacing (fine spacing in the area of interest or of greatest hydraulic change, increasingly coarser spacing farther away). However, this approach is computationally inefficient, in that it requires too much refinement in inconvenient grid areas, and it also generates numerical errors. It is particularly unsuited to the problem of longwall mining, since the zones of rapid hydraulic change are both elongated and changing in time.

Telescopic mesh refinement provides a more efficient approach in which a coarse grid is used to define the "regional" model, and the results of that model are used to specify the head and flux boundary conditions of a finer "local" model. Anderson and Woessner (1992) describe TMR as a way to resolve the tradeoff between the number of nodes and the required level of detail. Mehl et al. (2006) distinguish between traditional TMR without interactive feedback, and recent methods that involve numerical coupling of the local and coarse grids, either directly or iteratively.

Although not previously used with longwall mining, TMR was being used in other hydrogeological problems as long ago as the 1980's. Ward et al. (1987) applied the technique to a hazardous waste site near Dayton, Ohio. A steady-state 2D model at the regional scale used natural physical and hydraulic boundaries of the system, and was then used to set boundary conditions for a steady-state 5-layer model at the local scale, which in turn produced a more detailed 6-layer model at site scale. Buxton and Reilly (1986) used TMR with a regional model extended to the physical limits of the aquifer, and two transient 3-D local models nested within the larger model.

Leake and Claar (1999) present USGS procedures and programs for TMR using MODFLOW. Hunt et al. (2000, 2001) used TMR with Groundwater Vistas MODFLOW to connect the Dane County Regional Model (DCRM) in Wisconsin down to a site-scale model. The DCRM, with a grid spacing of 400 m, was used to assign constant-head boundary conditions for a refined model that had 100-m grid spacing. Initial parameter estimates were transferred from the DCRM to the TMR model and then further refined (e.g. by using Hydrologic Response Units to determine recharge values).

TMR has also been used with other model types. For example, Székely (1998) used "Windowed Spatial Zooming" on a finite-difference model with an iterative interface linking "parent and child" meshes across their boundaries by equating heads and fluxes. Keating et al. (2003) used nested TMR coupled through specified flux and specified head boundaries with a finite element model.

Leake et al. (2003) evaluated methods that can be used to interpolate smaller boundary forms and heads for larger scale block-centered FDM's such as MODFLOW. Mehl et al. (2006) reviewed recent methods of coupling the local and coarse grids. These more recent iterative coupling methods were not used in this project, which is focused on the special problems of longwall hydrology. However, there is clearly potential for further work building on this project.

3. Description of Jefferson County Study Site

3.1 Site Description, Geology and Hydrogeology

The Jefferson County (Rend Lake) site is located in south-central Illinois about 12 miles (19 km) southwest of the town of Mount Vernon. The study area straddles the Waltonville and Ina (Illinois) USGS 7.5-minute quadrangle topographic maps (1:24 000 scale). The Rend Lake mine extracted the Herrin (No. 6) Coal (Pennsylvanian: Carbondale Formation) in several longwall areas adjacent to and under Rend Lake reservoir. This study focuses on a set of four longwall panels on the eastern side of the lake (Figure 3.1). The site is part of the Mount Vernon Hill Country and consists of gently rolling topography with only about 15 m (50 ft) of local relief, drained by several small streams that flow into the former Big Muddy River system and now Rend Lake.

Structurally, the area lies on the western flank of the Fairfield Basin. Regional dips are around 2-3 m/km, generally ENE. The site itself is apparently unfaulted but the important Rend Lake Fault System (Keys and Nelson, 1980) runs SSE-NNW just east of the longwall panels, which were truncated to avoid it. This fault zone is discussed further in the Regional Model section below.

The coal seam extraction, averaging about 3 m thick, was at depths around 222m (725 ft). The overburden strata at the site largely consist of shales, plus siltstones, clays, sandstones, and thin coals and limestones (Figure 3.2). The principal units of hydrogeologic interest are the Mount Carmel Sandstone (Bond Formation) and overlying shallow bedrock and glacial drift. The Mount Carmel occurs at a depth of about 21-23 m (69-75 ft) at the panels, totals about 23 m (75 ft) in thickness, and consists primarily of two sandstone benches separated in the study area by a shale-siltstone unit variously 0 - 6 m (0-20 ft) thick. The thicker, lower bench is a coarse-grained channel facies while the upper bench is a finer grained sheet facies. The benches join together about a half-mile east of the site, which is located on the western part of a broad bend of an apparent paleochannel (Mehnert et al., 1997). The edge of the channel is about one mile (1.7 km) west and 1.5 miles (2.5 km) north of the site.

The sandstone is overlain by 15-18 m (49-59 ft) of shale and 3-10 m (10-33 ft) surficial cover of glacial deposits. The shale thins westward and in places a sandstone unit subcrops directly beneath the drift, evident in a few boreholes. In this study, this sandstone has been interpreted as a separate unit from the Mt. Carmel. Generally, the upper 35 ft (10.5 m) of bedrock is weathered shale or sandstone, underlain by a mostly continuous layer of unweathered shale. The glacial deposits are primarily clay till over the site, but discontinuous sand and gravel units are present locally, and thicker sand and gravel probably occurs to the east in the valley deposits of the former Big Muddy River, now occupied by Rend Lake.

Two cross sections (Figures 3.3 through 3.5) show the regional geology above approximately 30.5 meters (100 feet) elevation above mean sea level surrounding the Rend Lake study site, illustrating the shallow geology. Beneath the Mount Carmel sandstone, the shales and the Carthage Limestone, are continuous in this regional area. Minor coal seams exist throughout

these formations and tend to be discontinuous above the Carthage Limestone and more extensive below.

Groundwater flow in the regional area generally follows the topography of the ground surface, flowing from the higher ground surface elevations west of the study area to the lower elevations at Rend Lake to the east.

3.2 Rend Lake Mine and Results of the 1998-1995 Field Study

The Jefferson County/Rend Lake site was studied in detail between 1988 and 1995, first under the Illinois Mine Subsidence Research Program (IMSRP) and then as part of an investigation supported by OSM. Information about the site and results of the studies are available in numerous publications including the IMSRP report (Mehnert et al., 1997), OSM report (Booth et al., 1997) and conference and journal articles (e.g. Booth et al., 1998). The investigations were the basis of several M.S. theses at NIU Department of Geology (Spande, 1990; Pattee, 1994; Miller, 1996, Bertsch, 1997) in which site information and study results are recorded.

The study was conducted over the last two panels of a four-panel section of the mine. The 3-m extraction produced about 2 m of ground subsidence, over 90% of which occurred within 3 months of mining (Mehnert et al., 1997). At the edge of the panel, deformation occurred mainly as shear in weaker beds or on the interfaces between strong and weak beds. Over the center of the panel, tensile failure also occurred at the strong-weak interfaces, indicating bedding separations.

Field tests (Mehnert et al., 1997; Booth et al., 1997, 1998) before and after subsidence showed that the sandstone is a moderately permeable aquifer with initial hydraulic conductivities around 10^{-6} m/s. Permeabilities in the sandstone increased by about one order of magnitude in the central subsidence trough and by about two orders in the residual tension zone along its edges. At some individual horizons, the permeability increased several orders of magnitude due to bedding separations, some of which were evident as lost circulation and bit drops.

Potentiometric responses to the mining of panels 3 and 4 were monitored in several piezometers starting in mid-1988. The initial water levels in the sandstone had already been lowered to around 20 m (66 ft) BGS, near the top of the aquifer, presumably because of previous mining of panels 1 and 2, but pre-mining water levels were probably no deeper than about 10 m (33 ft) BGS, as indicated by the eventual post-mining recovery. At both panels, the observed heads declined rapidly ahead of the approaching mine face and subsidence zone, due to drawdown transmitted outwards from the primary head drop occurring in the zone of active tensional fracturing. For example, at panel 4, the water level was near the top of the upper sandstone bench (21 m BGS) at the start of monitoring in 1988, gradually lowered due to approaching mining, then dropped rapidly just before site subsidence in February 1989, reaching a low of 42 m (138 ft) BGS during maximum tension, about 6 m (20 ft) above the base of the aquifer.

The water levels subsequently recovered to about the top of the lower bench during the compression phase and then, as water flowed back into the aquifer, to a fully confined state in

1990 and to about 10 m BGS by the end of monitoring in 1995. Later pumping tests during the fully confined phase (Booth et al., 1997, 1998) indicated that leakage from the overlying shale probably entered the upper sandstone bench but was prevented from reaching the lower bench by the intermediate shale unit.

Water samples were collected from the site throughout the study period (Booth et al., 1998; Booth and Bertsch, 1999). The natural water quality in the Mt Carmel Sandstone, shown by samples from a nearby well unaffected by mining, was a marginally fresh Na-HCO_3-type. Pre-subsidence water on-site was marginally brackish Na-HCO_3 -type with TDS 1200-1300 mg/l and sulfates around 260 mg/l. During the post-mining recovery, the sulfate levels increased to a maximum of 1273 mg/l and TDS to 2755 mg/l, most likely due to flushing of soluble sulfate salts produced by the oxidation of sulfides during the earlier unconfined phase.

In addition to investigations of the sandstone aquifer, the water levels were monitored throughout the study period in a number of shallow wells into the shallow drift materials and also into the overlying shale unit on and around the mined site. Potentiometric monitoring and hydraulic tests were also conducted during mining in several piezometers in the drift and one piezometer into the deeper shale. There is thus a large hydrogeological database for this site.

3.3 Recent Field Update

A field visit to the site was made in July 2008. The model area was toured to gain site understanding. The landowner was contacted to obtain permission to locate, monitor and sample the old test well (P350) into the sandstone aquifer over the final study panel. The well was open and accessible. The water level was 19 ft (5.8 m) below ground, i.e., it had remained at approximately the same recovered level since readings were last taken some 13 years ago. This therefore appears to be the fully recovered level for the sandstone aquifer and the value can be used in model calibration. Samples were taken and analyzed. Sulfate levels were only 413 mg/l, essentially a return to pre-mining levels from the 2,000+ mg/l levels after mining, indicating that long-term flushing of the aquifer has occurred.

4. Regional Model

4.1 Model Software

MODFLOW is the U.S. Geological Survey's three-dimensional finite-difference groundwater model, first published in 1984 (McDonald and Harbaugh, 1984) and updated several times. In this study we used the commercial software Groundwater Vistas™ (Environmental Simulations, Inc., 2007), version 5.19, as interface to MODFLOW. Groundwater Vistas (GV) allows the choice of several of the MODFLOW variants. In version 5, MODFLOW-2000 (Harbaugh et al., 2000) is the default system; this was used to develop the three-dimensional regional groundwater flow model for the region surrounding panels 1 through 4 of the Rend Lake mine. MODFLOW-88 was used for most of the development of the Local Model.

4.2 Scope and Relationship of Regional and Local Models

The basic framework of the Regional Model was set up initially using a digitized topographic surface map in GIS inputted to the property value matrix in GV as the top of Layer 1 (L1). Thicknesses of the geological strata were obtained from a variety of sources including information from the 1988-1995 study and borehole logs obtained from the Illinois State Geological Survey. Layer elevations were set up in the appropriate GV property value matrices from the combination of topographic elevation and thicknesses.

The Regional and Local Models (RM, LM) represent the upper 60-70 m of the 220-m overburden system. Layers include the Mt. Carmel Sandstone, the immediately underlying shale and Carthage Limestone units, and the overlying shale and glacial drift. The regional model (RM) has an area of about 53 km^2 encompassing natural boundaries of the sandstone paleochannel to the west, north and southeast, a major fault zone in the bedrock, and the large man-made Rend Lake reservoir to the east (Figure 4.1) The four longwall panels (each about 600 ft (183 m) wide) and their barrier pillars (200 ft (61 m) wide) occupy about 1.6 km^2 area. However, the subsidence zone extends about 93 m from the edge of the panel at the surface, based on the 23^o angle of draw, and the effective radius of transmitted hydrologic influence is estimated at about 600 m (based on other study sites), so that the LM extends out to boundaries encompassing an area of 7.3 km^2. The creation and specification of the LM are discussed in more detail in section 5.

4.3 Regional Model Geometry

A steady-state regional model (RM) with 34,200 cells (57 rows x 75 columns x 8 layers) was developed in Groundwater Vistas® (GV) and calibrated to a reasonable approximation of the potentiometric heads across the area. Eight layers of varying thicknesses (Figure 4.2) represented the following:

1.	Drift	4.6 m (15 ft)
2.	Weathered shale/sub-cropping sandstone unit	10.7 m (35 ft)
3.	Non-weathered shale	12.2 m (40 ft)
4.	Upper bench (sheet facies) Mt Carmel Sandstone	6.1 m (20 ft)
5.	Mid-Mt Carmel shale/siltstone confining unit	6.1 m (20 ft)
6.	Lower bench (channel facies) Mt Carmel Sandstone	12.2 m (40 ft)
7.	Shale (undifferentiated)	22.9 m (75 ft)
8.	Carthage (Shoal Creek) Limestone	3.1 m (10 ft)

Each layer was constructed with mapped zones of different permeability values to represent different lithologic units present in the same layer interval and to permit more flexible calibration.

4.4. Model Stresses and Boundary Conditions

Wells. No wells were used in the Regional Model.

Streams/Drains. Since the purpose of the RM is to provide a framework starting point for TMR, not to fully simulate the regional system hydrology, modeling of the small streams crossing the area was not originally intended. However, during the later calibration process it was found necessary to incorporate the small streams in the surface layers in order to bring the simulated heads down to acceptable levels.

These small stream valleys cut locally through the landscape and provide groundwater discharge points that do not otherwise appear in the model. They are shown as mostly ephemeral on the USGS topographic map, but most probably serve as discharge points for very shallow groundwater or vadose interflow in the surficial till layers while not holding sufficient water to replenish the groundwater system at times of lower groundwater levels. Therefore, they were modeled by the DRAIN option, which allows drainage to the stream from groundwater but not the reverse.

The DRAIN option is a head-dependent boundary condition that calculates the flux by Darcy's Law, for which the drain geometry and conductivity must be specified. A minimal stage (0.5 m), streambed thickness (0.5 m) and streambed conductivity (0.01 m/d) were specified. The effect on calibration is discussed below.

Recharge. A uniform recharge of 2.7×10^{-5} m/d (= 1 cm/year) was eventually applied in the calibration. This is a somewhat low value but may be reasonable considering that the drift that blankets the area is poorly permeable clay till. The dominant soil type is the Bluford Series which is considered slowly permeable, somewhat poorly drained, and unlikely to remove ponded water by infiltration (Trent, 1996). A low value also probably reflects the effect of the extensive shallow stream incision across the areas of principal interest as discussed above.

Boundaries: Boundary conditions are applied to the external edges of the model grid and to internal features within the model area.

The external edges of a MODFLOW model are no-flow boundaries by default. In many cases the external boundaries can be placed far enough away from the area of interest that their condition is relatively unimportant to the hydrologic phenomena under study. However, external boundaries may also exert significant control on head configurations, especially for steady-state simulations with minimal hydrologic stresses. Thus, it is necessary to experiment with boundary conditions.

Initial boundary conditions. In the initial RM development, a relatively simple boundary configuration was used.

* The external edge boundaries were initially treated as general-head boundaries but were later changed to constant-head boundaries for simplicity and ease of calibration. Head values were based on field relationships at the study site. These BC's were changed again in the final calibration (see below).

* In the top layer (L1), the model is bounded in the east by Rend Lake, treated as a constant-head boundary.

* In the bedrock layers, the eastern boundary is the Rend Lake Fault Zone, initially treated as a no-flow boundary but substantially modified during calibration to become a modified permeability zone in most of bedrock layers L3-L6; it remained a NFB in L7-L8.

4.5 Development and calibration of the Regional Model

Calibration is an integral part of model development. In summary, calibration consists of successively adjusting the various parameters that control groundwater flow (boundary conditions, permeability values and distributions, recharge, etc.) until an acceptable simulation of the system is achieved. Acceptability is determined both by the reasonableness of the simulation and by comparison of simulated heads against known field values. The system parameters may be constrained by field data and scientifically reasonable values, but they are nevertheless always inadequately known. Calibration is thus a process of hypothesis testing of the conceptual model of the system.

Because of the numerous different parameters that affect head distributions, calibration is a non-unique process. Most simulated solutions could be achieved through several different combinations of parameters. Nevertheless, constraining a simulation by reproducing even limited field values provides a degree of confidence such that the calibrated model can then be used for other applications such as prediction of future conditions or response to hypothetical stresses.

In this study, the regional model was calibrated against limited site water-level data through adjustments of recharge, permeability values of ten different designated permeability zones, horizontal/vertical anisotropy, boundary conditions, and drains. The RM was then used as the base for TMR transformation to a local model and experimental simulations of work on mining impacts. Field observations of the potentiometric head responses to mining in the 1988-1995 study were used to constrain and adjust the mine impact mechanism models.

Calibration data. Despite the considerable data available at the Local Model (LM) scale, data are scarce and imprecise on the RM scale. There is an adequate borehole geology database to build the geological framework of the model, but values of groundwater level are few and are subject to uncertainties of elevation, seasonal and long-term variation, and impact of previous underground mining. However, for the purpose of testing the TMR approach the RM merely needs to provide a reasonable approximation of heads across the area of interest. Available data for both RM and LM include:

* Water levels in approximately 20 private shallow wells (drift, upper bedrock) across and surrounding the LM study area, measured during the 1988-1995 field investigations. Ground elevations were determined from the 7.5-minute topographic maps but locations were accurately field verified so that most head elevations are reasonably accurate. However, water levels vary seasonally and between years (e.g. 1988 was a severe drought year whereas 1989 was wet). The approximate median levels were targeted in the RM steady-state calibration. In most cases, the water-level data were not distorted by mining, either because the wells were sufficiently far from the mine at the time, or were drift wells.

* Water levels in piezometers set in various units (primarily the Mt Carmel Sandstone) over and adjacent to longwall panels 3 and 4. All piezometers were accurately surveyed for location and ground elevation at the time of construction. In most cases water levels were continuously monitored using automatic transducers for periods at least up to undermining. Mining of panels 1-3 had already impacted these water levels. However, long-term recovery data over panel 4 measured several years after mining probably indicate typical natural levels.

Calibration of the RM focused on reproducing a reasonable pattern of heads over the RM area, with specific targets over the panel-4 area as follows (Table 4.1):

Table 4.1 Calibration targets at P350 location, Panel 4

Layer	Unit	Water levels (m BGL)	Approx. Heads (m AMSL)
L1	Drift	1-2 m	131 m
L2	Weathered bedrock	3-4 m	129 m
L3	Unweathered shale	4-6 m	127 m
L4	Upper Sandstone	7-8 m*	125 m
L5	Confining unit	7-8 m*	125 m
L6	Lower Sandstone	7-8 m*	125 m
L7	Shale	unknown	
L8	Carthage/Shoal Creek Lst	unknown	

* During the active mining phase, piezometric heads in the upper sandstone (L4) were in the range 1.5-2.5 m higher than heads in the lower sandstone. There are no comparable data available for the pre-mining or fully recovered periods, but it is hypothesized that this was largely due to mining, hence not a target in the unmined RM.

The levels in the sandstone are adjusted for subsidence. The long-term recovered level in well P350 was about 6 m BGL but the ground had subsided 2 m during undermining, hence the static pre-mining level would have been about 8 m below pre-mining ground elevation, or about 125 m AMSL.

Permeabilities (hydraulic conductivities) were based on site data from the 1988-1995 field investigations and modified layer-wise during calibration (see Table 4.2 for values). A high anisotropy (Kh/Kz) value (1000x) was used to achieve coarse calibration of heads in this model. This is probably due to the relatively coarse nature of the layer discretization rather than to point values of anisotropy this high. Grouping of individual layers produces an overall transverse anisotropy, thus coarse grouping of much finer-scaled stratification in this setting probably creates a significant layer-anisotropy effect. Later stages of the calibration generally reduced the Kh/Kz anisotropy slightly to between 100x and 1000x. No lateral anisotropy was specified (thus Kh = Kx = Ky).

Table 4.2 Initial Hydraulic Conductivity Values Used in Regional Model
Two sets of data provided where layer has two zones.

Layer	Unit	High K (m/d) (e.g. sandstone)		Low K (m/d) (e.g. till or shale)	
		Kh	Kz	Kh	Kz
L1	Drift	N/A	N/A	0.432	0.00864
L2	Weathered bedrock	0.864	0.00864	0.864	0.00864
L3	Unweathered shale	0.432	0.000864	0.0432	0.0000864
L4	Upper Sandstone	0.432	0.000864	0.00432	0.0000864
L5	Confining unit	0.432	0.000864	0.00432	0.0000864
L6	Lower Sandstone	0.432	0.000864	0.00432	0.0000864
L7	Shale	N/A	N/A	0.00432	0.00000864
L8	Carthage Limestone	N/A	N/A	0.00864	0.0000864

Modified Calibration and Conceptual Model.

The first attempts to develop a local model (LM) from the RM via the TMR capability of the GWV software revealed previously unnoticed dewatered zones in the lower layers that were clearly incorrect. It was therefore necessary to return to the RM, reconsider the conceptual model, and recalibrate.

External Boundaries. Experimental runs were conducted with a variety of internal and external boundary configurations. A hydrogeologically more sophisticated set of external edge boundary conditions was developed:

L1 Drift: distant constant-head boundaries [set 1.5 m BGL].

L2 Weathered bedrock subcrop: no-flow boundary (NFB) in shale, constant-head boundary (CHB) [at 3 m BGL] in sub-cropping sandstone.

L3 Non-weathered shale: NFB, but CHB in local sandstone area [at 4 m BGL]

L4 Upper sandstone sheet facies: CHB in sandstone unit [at 6 m BGL]; NFB's in the shale facies.

L5 Mt Carmel shale/siltstone confining unit: NFB in shale, CHB [at 6 m BGL] in sandstone.

L6 Lower sandstone channel facies: CHB [6 m BGL in western areas and at 118 m AMSL (from well R18, slightly east of the RM area; see discussion on Rend Lake fault Zone below) on the eastern boundary. NFB's where L6 comprises shale.

L7 Shale: no-flow boundaries

L8 Carthage/Shoal Creek Limestone: no-flow boundaries.

These boundary conditions reflect that low-permeability units typically serve primarily as vertical-flow leakage layers between higher permeability aquifer units, and thus are more appropriately bounded laterally by hydraulic NFB's. Constant-head boundaries are set at the aquifer edges as a matter of convenience; they are distant from the focus of the model and there is limited field information regarding their values.

***Internal boundaries*:**

Minor water bodies are set as constant head cells in Layer 1. However, artificial lagoons adjacent to coal mines are not simulated, since they will be clay-lined and not in continuity with the groundwater system.

Rend Lake was simulated by constant heads at the lake elevation value (405 ft, 123. 5 m AMSL) in L1 beneath the lake. It is reasonable to consider this unit as being in approximate hydraulic equilibrium with the lake. Potential groundwater exchange with the lake is allowed by setting the L2 unit as variable head cells.

Rend Lake Fault System: The Rend Lake Fault System (RLFS) (Keys and Nelson, 1980) is a series of closely spaced, generally normal faults trending NNW/SSE across the entire area, occasionally offset in step-wise fashion. Individual throws are up to about 55 ft (17 m), mostly downthrown to the east. The faults form the eastern edge of this section of the mine, because of the coal seam offsets. They are inactive and cut through all the bedrock units. The hydrologic role of the fault system is unknown. Faults can vary from highly conductive where active groundwater flow solution has occurred to poorly conductive because of sealing by clay and fault

gouge. However, one certain effect is that thin conductive horizons will be disrupted by the fault throw.

In the initial RM described above, the RLFS was set as a barrier boundary and all bedrock units to the east were defined as inactive from the model viewpoint. However, this produced unacceptable head and flow patterns by forcing significant upward discharge in all the bedrock units on the western side of the fault zone. The RLFS treatment was refined in the revised RM as follows:

L1: Fault does not affect surficial drift.

L2: In this weathered bedrock layer the RLFS may be a permeable zone. It is therefore not specified as a boundary, and L2 is continued east of the RLFS as a variable head unit.

L3: The RLFS is probably a barrier in this shale unit, but lateral flow is in any case likely to be insignificant. Here the RLFS is modeled as a zone with higher vertical than lateral hydraulic conductivity. The L3 unit is allowed to be variable head active east of the RLFS to allow for vertical leakage in that region of the RM.

L4 & L5: Upper sandstone and confining unit. The RLFS is likely to have offset the conductive zones in the thin sheet facies (where present) and so is modeled as a thin zone of cells blocking lateral flow but allowing vertical flow, as in L3. However, L4 and L5 remain active cells east of the Fault.

L6: The lower sandstone unit is thick enough to maintain continuity across the fault. This channel facies continues eastward in a fairly narrow but thick band bounded to the north and south by shale. The RLFS is thus not modeled in layer L6. The eastward continuation of an active flow system in the sandstone is indicated by field measurements from the later field study at sandstone well R18, 200-ft (61-m) deep at Nason Point (Bertsch, 1997). The water level in the well was more or less steady at 28 ft below well top, a head elevation of about 387 ft (118 m) AMSL, approximately 7 m lower than the steady-state recovered head at P350. The reliable water supply and its relative freshness (TDS < 1,000 mg/l) in R18 suggest an active circulation in the sandstone east of the RLFS.

L7 & L8: The shale and limestone layers are likely to have thin conductive zones totally offset by the faults. The RLFS is treated here as an effective barrier. The units east of the fault are of no hydrologic significance for the model and are treated as inactive.

Final calibration of the regional model (pre-mining steady state)

During the final stages of the calibration process, simulated heads in the channel sandstone (L6) were still approximately 2 m too high while simulated heads in the glacial deposits (L1) were reasonable. Further attempts to lower the L6 values through adjustments of hydraulic

conductivity and anisotropy were unsuccessful. However, the addition of drains in L1 to simulate the small draining streams allowed the adjustment of hydraulic conductivities in L4-L7 to reduce the L6 simulated heads to acceptable levels while keeping the L1 simulated heads from rising above ground surface.

Table 4.3 Hydraulic Conductivity Values in Final Calibration of Regional Model Two sets of data provided where layer has two zones.

Layer	Unit	High K (m/d) (e.g. sandstone)		Low K (m/d) (e.g. till or shale)	
		Kh	Kz	Kh	Kz
L1	Drift	N/A	N/A	0.432	0.0432
L2	Weathered bedrock	0.432	0.0432	0.0864	0.00864
L3	Unweathered shale	0.0864	0.00864	0.0000864	0.000000864
L4	Upper Sandstone	0.0864	0.00864	0.0000864	0.000000864
L5	Confining unit	0.0864	0.00864	0.0000864	0.000000864
L6	Lower Sandstone	0.0864	0.00864	0.0000864	0.000000864
L7	Shale	N/A	N/A	0.0000864	0.000000864
L8	Carthage Lst	N/A	N/A	0.00432	0.000432
L3-5	Fault Zone	N/A	N/A	0.00864	0.432

The final distribution of hydraulic conductivity values is represented in two cross sections (Figure 4.2). The distribution of blue cells representing low permeability units versus green cells representing sandstone in these sections matches the distributions in the geologic cross sections in Figures 3.4 and 3.5.

Head simulation across the mined area

Contour plots of simulated heads in L1 and L6 are presented in Figure 4-3 (a) and (b) respectively. Simulated water table elevations in L1 are highest in the west (greater than 150 m AMSL) at the topographic high and decrease with lower surface elevations to the west and east, with the lowest elevations adjacent to Rend Lake at 123.5 m (405 ft) AMSL. The simulated water table contours indicate gaining conditions of the streams in particular locations. The L1 simulated head at the P350 location in Panel 4 within the LM study area is close to the observed head of approximately 131 m AMSL.

Simulated potentiometric surface elevations in L6 are also highest in the west (greater than 145 m AMSL) beneath the topographic high within the shale and decrease toward the lateral contact with the channel units of the Mt. Carmel sandstone. The simulated gradient is much lower in the higher-permeability sandstone, with flow from the center of the model area out towards the constant head boundaries in the southwest corner and south and east edges of the RM. The L6

simulated head at the P350 location in the middle of Panel 4 within the LM study area is close to the observed head of approximately 125 m AMSL.

4.6 Sensitivity Analysis

Groundwater flow models are sensitive to different degrees to the hydraulic parameters input into the model. Various parameters, chosen based on their apparent effects on the model during calibration, were increased and decreased by a factor of 10 to examine the effect on the calibration targets at the P350 location in L1 and L6 (Table 4.4). Simulated heads that were more than +/-1 m from the targets are in bold.

Table 4.4 Sensitivity Analysis of Regional Model

Parameter Adjustment	L1 Head (m AMSL) (target = 131)	L6 Head (m AMSL) (target = 125)
Calibrated values	132.0	125.9
Recharge up by 10x	**146.4**	**130.1**
Recharge down by 10x	**128.6**	125.0
Sandstone K up by 10x (L3-L5)	132.0	**123.2**
Sandstone K down by 10x	132.0	**128.7**
Shale K up by 10x (L3-L7)	131.8	**128.3**
Shale K down by 10x	132.0	125.3
Anisotropies up by 10x (Kz -)	132.2	124.9
Anisotropies down by 10x (Kz +)	131.8	**128.2**
Fault simulated as Inactive	132.0	125.5

The RM appears to be most sensitive to areal recharge from precipitation, particularly the L1 surficial layer. The channel sandstone heads in L6 are also quite sensitive, particularly to adjustments in the sandstone hydraulic conductivity values. Increases in either shale hydraulic conductivity or global vertical hydraulic conductivities allow too much water into the lower sandstone. The lack of sensitivity to eliminating flow through the fault in L3-L5 indicates that the calibrated hydraulic condition within those cells was sufficiently low to reasonably simulate the effects of the fault on the heads within the LM area.

5. **Local Model**

5.0 Local Model Development

After the calibration of the Regional Model, a Local Model was established through the TMR transformation process available in GV (Groundwater Vistas ®). There is no way to learn the use of complex modeling software such as GV except by using it. A detailed operating guide here would be impossibly large; the user should refer to the GV manual (Environmental Simulations, Inc.) provided with the software. However, we include some specific command sequences involved in particular aspects of the LM development.

The approach finally resulting from this model development is successful but depends on considerable time-consuming manual involvement in the simulations due to the limitations of MODFLOW in accommodating hydraulic property changes. We have conducted only limited comparison of the simulations against field data; there is a far larger field database available for calibration and experimentation than could be fully utilized in the scope of this work. These are areas for further work beyond the end of this project.

A satisfactory basic LM was produced in which various approaches to simulating longwall hydrologic impacts were tested. Two major aspects of longwall impacts were addressed: simulation of the head drops due to the initial rapid increase in fracture porosity, and changes in K and S due to fracturing associated with subsidence. The approaches used here are strongly grounded in the conceptual models of these mechanisms. In the scope of this project, it was not possible to address a third aspect: changes of ground and layer elevations due to subsidence. Although it is possible to modify elevations through GV-MODFLOW, the approach would require substantial time-consuming manual alteration of the elevation data matrices at each discrete stress step, with likely problems of model instability. Again, this is an issue for future work.

It is good modeling practice to test separate parameter changes or new features independently. For example, tests were conducted of the simulation of increases in fracture porosity by a series of well sinks advancing in numerous stress periods in transient models without permeability change zones, even though later models would be made differently in order to include permeability changes. These tests are discussed below because of the importance of the approach. However, numerous LM's that were developed to test various refined boundary conditions, hydraulic property changes, well sinks, stress periods and other features are mostly not described. Similarly, model development involves numerous false directions, tests of procedures, revisions of errors, and basic software option testing. These are not included in this report. Problems included the LAYCON specifications (discussed below), difficulties with grid specification in the LM (attempts to create a non-uniform grid created problems with maintaining boundary conditions; a uniform grid was necessary), and grid-offset problems due to a subtle error in transcribing a map grid coordinate.

The maintenance of consistency between the RM and LM in this case is somewhat ambiguous. Unlike in a contaminant migration problem, we are not keeping the same flow field, but are

changing many structural features of the model, including the permeability values. The RM serves as a physical framework from which the LM site geometry, property distributions and boundary heads are specified through the TMR conversion, but may be difficult to link back in to the modified LM. Nevertheless, in general we have followed the principle of not changing property values from the calibrated RM except as necessary for applying the mine-related changes.

5.1 Procedure for setting up LM from RM in GV

Summary of GV procedure. The basic process for generating a local TMR model from the RM in GV is fairly straightforward. It takes two stages: first, export TMR data from an existing GV model (the RM); second, start a new model by importing the TMR data. The appropriate menu commands are described in the GV manual. However, the procedures are described here in some detail because they help illustrate the TMR concept.

Export TMR data. The RM is run to completion and the LM area is approximately delineated by drawing a window on the solved RM map/grid screen using the mouse. The coordinates can be refined later. GV gives the option of assigning either constant head, constant flux, or general head boundaries along the LM edge cells.

Specific command sequence:

-- Run the RM to completion.
-- Select **Grid>Export TMR**
-- Drag a window on the on-screen solved RM map to cover the area of the LM sub-model.
-- Fill in the options on the TMR dialog box:
    Set #rows and #columns (default is 100 x 100; this model used 116 x 158)
    Refine minimum and maximum RM-grid coordinates of the LM by the dialog box. The "snap to grid" option may then be used to extend the coordinates of the LM edges to the nearest row and column coordinates in the RM [it was not used in this case because of the need to pre-define grid cell sizes].
-- Specify edge boundary types for each face (N, S, E, W) [constant head in this case].
-- Did not use "reinterpolate bottom elevations" option, which jumbled the elevations.
--Save TMR data to a file (has a .tmr extension)

Set up the new LM model

- **File>New**
- On dialog box, select "**Import TMR**"
- Enter or browse for the name used for the .tmr file.
- Click OK on the dialogs and allow the program to construct the LM

The new file is saved as a standard .gwv model file. Further menu and screen commands allow the LM to be linked to a background topographic (or other) base map.

Regional Model used for TMR transformation. The calibrated Regional Model (renamed RM-1000) was used as the base regional model for the TMR refinement. This model had been successfully calibrated using DRAIN boundaries in the upper layer to reduce excessive simulated heads in the early tests; however, further changes in the DRAIN boundaries were needed.

Details of Regional Model RM-1000 boundaries, per layer:
(CHB = constant head boundary, NFB = no-flow boundary)

L1: edge CHB's; Rend Lake CHB; DRAINs established.
L2: southern edge CHB for higher K zone, otherwise NFB
L3: small section of southern edge CHB, otherwise all NFB.
L4: CHB's in sandstone on most of 3 sides; NFB's in low K zones.
L5: local CHB, otherwise NFB
L6: CHB's along major areas where sandstone at sides, some NFB
L7: NFB all edges; area east of Rend Lake Fault inactive.
L8: same as L7.
Rend Lake Fault Zone: simulated in the calibrated RM by permeability changes in the upper layers.
Warnings noted: some L1 DRAIN elevations are below bottom elevation of L1.

Layer Condition. Layer conditions are defined in the MODFLOW-88 BCF package by the LAYCON number. L1, the top layer, is LAYCON-1, the unconfined condition. Because it was likely that some layers would switch to an unconfined condition during mining, an initial attempt was made to set up other layers as LAYCON-3 (variably unconfined/confined – MODFLOW calculates variable transmissivity and selects the appropriate storage coefficient). This caused serious computational problems in the TMR conversion from the RM to the LM, and was abandoned in early test runs in favor of the simpler LAYCON-0 (confined) setting. However, it was later found that the LAYCON-3 would work if it was defined in the LM after TMR conversion and this setting was ultimately used with MODFLOW-88 for all final LM simulations.

On the other hand, MODFLOW has known stability problems when attempting to rewet cells that dry out during a simulation. The newer commercial variant MODFLOW-SURFACT is designed to handle unsaturated and dewatered conditions. It has recently been applied to the deep fractured /dewatered zone above a proposed Australian longwall mine with demonstrated improvement over standard MODFLOW (Merrick, 2009). The SURFACT software is supported as an extra-cost add-on in the GV suite but was not available for this project. None of the simulations in the current project required this feature but it could be useful in future work involving more wide-ranging simulations.

Calibrated heads in the RM base model. The calibrated regional model RM-1000.gwv was used as the base run from which the LM was developed. Scattered dry cells in L1 occurred in the RM, especially clustered in central higher elevations, but these are considered hydrogeologically reasonable (the water table is in L2 in some locations).

Simulated test values (m AMSL) at Panel-4 centerline (P350 site) in RM-1000 base model

L1 = 131.97	L4 = 126.72	L7 = 126.28
L2 = 132	L5 = 126.73	L8 = 126.67
L3 = 129.32	L6 = 125.88	

These are reasonable calibrated values at the principal test site. Approximately the same values (+/- 0.06 m) were obtained in tests of the model with MODFLOW-88 and MODFLOW-2000, and with L2 set as either LAYCON-0 or LAYCON-3 options in the RM (see above), though the LAYCON-3 selection would not successfully convert into the LM in the TMR process.

5.2 Local Model Geometry

The four longwall panels are about 183 m wide, separated by three barrier zones each about 61 m wide. Panels 1 and 2 are each 1,737 m long, Panel 3 is about 1,645 m and Panel 4 is 1,584 m long. Thus, the footprint of the longwall section is 1,737 m (EW) x 915 m (NS), or about 1.6 km^2. The limit of subsidence based on the observed 23^o angle of draw at the site is about 93 m from the edge of the panel, extending the area of deformation to about 2.1 km^2. The maximum radius of influence of transmitted hydrologic effects was estimated as about 600 m from previous studies, increasing the minimum necessary area to the LM boundaries to about 7.2 km^2. The LM final area was 7.3 km^2 with dimensions 3,160 m (EW) x 2,320 m (NS).

The LM consisted of 146,624 cells arranged as a grid of 158 columns x 116 rows of uniform cell size 20 m x 20 m. The 8-layer configuration and same layer thicknesses were used directly from the RM. The basic LM grid and area are shown in Figure 5.1.

LM Coordinates:
* Site offset coordinates: X = 321419.46 Y= 4224431.7
* LM linked to the base topographic map thus:
  Commands: **File > Map > Bitmap**
  Select map file [= Rend Lake_RegionalModel2.bitmap]
  Map origin coordinates: X = 317080 Y = 4222220
  Stretch coordinates: H = 6729 W = 8858
* This model was saved as LMM-1001.gwv and used for later LM work.

5.3 Development of the Steady-State Pre-mining LM.

In order to maintain consistency between the RM and the LM at the unmined steady-state stage, no changes were made to the hydraulic property values database transferred from the RM to the LM in the TMR process. However, adjustments to boundary conditions were made as follows:

External Constant Head Boundaries. The edges of the LM were set to constant-head boundaries in each layer by the TMR conversion program. The values of constant heads were the solved

head values at those locations determined by the RM. The edge boundary conditions link the RM with the LM and were thus generally not altered. However, a few dry-cell CHB's were deleted to eliminate error messages. In an early set of simulations, in an attempt to reduce persistent high heads in L1 and L2 the outer-edge CHB's in the low permeability zones were altered to no-flow boundaries. This did improve the head values, but because of concerns about boundary consistency, the approach was later rejected in favor of including the internal DRAIN boundaries in L2.

Internal Constant Head Boundaries. Internal CHB's that had been artificially placed in L1 cells in the ephemeral edges of Rend Lake in the RM design caused warnings in the LM because some of the heads were below the redefined bottom elevations of redrawn cells in the finer LM grid. These boundaries were redundant hydrogeologically and were deleted. This made no apparent difference to the steady-state unmined simulation.

Drains. GV transfers the internal drain boundaries from the RM to the corresponding cell locations in the LM, adjusting the conductance terms for the different cell areas. In the RM-1000 base model, the drain boundary was specified only in L1. However, many of the drain cells had elevations lower than the digitized bottom elevations of L1, generating warnings in the model compilation stage but no obvious problems in the RM. However, the DRAIN boundary cells were copied from L1 into L2 in a successful attempt to lower persistent excessive simulated heads in the surficial layers of the LM.

Head Adjustments. Initial trial runs of the LM showed steady-state heads in the top layers (L1-L3) at the Panel 4 test site that were consistently high compared to those in the calibrated RM, by about 5 m. Heads in the aquifer (L4-L6) and lower layers were similar to those in the RM. Standard MODFLOW and MODFLOW-2000 produced the same results.

Heads (m AMSL) at Panel 4 centerline site: models LMM-1000 and LM2-1000

L1 = 137.67	L4 = 126. 88	L7 = 126. 35
L2 = 137.66	L5 = 126.42	L8 = 126. 70
L3 = 132.18	L6 = 125. 95	

In the first LM tests we reset constant-head edge boundaries to no-flow boundaries (NFB's) in the low permeability units (selected zones of L2, all L3, some L4-L6, all L7 and L8) to reflect dominant vertical flow in these units. The heads in L1-L3 reduced by about 4 m (though were still slightly high).

Heads (m AMSL) at Panel 4 centerline site, using NFB's in low permeability units.

L1 = 133.39	L4 = 126.73	L7 = 125. 95
L2 = 133.41	L5 = 126.31	L8 = 126.01
L3 = 130.01	L6 = 125.89	

This model was saved (as LM2-1012) and used in the early experimental simulations. However, because of concerns about RM-LM consistency, the later LM models returned to the original

constant-head boundaries imposed by the TMR conversion, and reproduced lower heads using drains in the L2 layer as noted above.

5.4 Transient simulation and storage coefficients

MODFLOW-88 normally requires input of the confined storage coefficient as storativity values (S, dimensionless) whereas MODFLOW-2000 requires input as specific storage (Ss, dimension L^{-1}). To simplify switching between versions, GV provides an option of inputting storage as Ss regardless of the model variant, and makes the appropriate calculations. Thus, Ss values were used. Initial values were determined from:

(a) Representative values for various lithologies tabulated in Younger et al. (2002).
(b) Values of pre-mining storativity determined in pumping tests in well P350 over Panel 4 that ranged from $5x10^{-5}$ to $7x10^{-4}$. Specific storage equals storativity divided by aquifer thickness, which is about 23 m at the site. Thus the average Ss values for the aquifer range from $2.2x10^{-6}$ to $3x10^{-5}$ m^{-1} and a base value of $1x10^{-5}$ m^{-1} was applied to the sandstone units.

Base storage coefficient values were assigned according to the same property zones as the K values (saved in Model LM2-1015):

Zone	Lithology	Ss
1	Till (L1)	1x10-3
2	Weathered Shale (L2)	1x10-5
3	Shale (L3)	1x10-6
4	Shale (L4)	1x10-6
5	interbed sh/sst (L5-6)	1x10-6
6	Lower shale (L7)	1x10-7
7	Limestone (L8)	1x10-6
8	shallow sandstone (L2)	1x10-5
9	Sandstone (L3-6)	1x10-5
10	Fault zone (L3-5)	1x10-5

5.5 Simulation of transient increase in fracture porosity

Analysis of Mechanism. The primary cause of head drops during subsidence is rapid increase in fracture and bedding-plane porosity in the relatively short tensional phase. This creates new void space into which ambient water drains, lowering heads – typically very rapidly in confined bedrock aquifers. As space opens in a confined unit, the head in a unit-area (A=1) column will drop according to

$$S = V/(A*dH) \text{ or } \quad dH = V/S$$

Where S = storage coefficient (storativity),

V = volume of new voids = volume of water "drained" from the medium,
dH = head drop.

Since S is small in confined units, dH is correspondingly large even for small losses of water from the porous/fractured medium into the new void space.

Model Approach. MODFLOW has no direct mechanism for simulating this mechanism and it has not previously been simulated in any known model of longwall mining. Porosity is not a parameter in the MODFLOW groundwater flow equations, except as implicitly contained in the storage coefficient. Simply changing S could not reproduce the dilation head loss.

However, the effect of loss of water from the existing porous medium into the new void space can be replicated by simulated wells that are switched on during active subsidence. This procedure is readily accommodated in the MODFLOW structure stress-step and well definition structure. In GV, wells can be treated either as internal boundary conditions located in the center of specified cells, or as analytical elements located by site coordinates independent of the grid configuration. The former approach was used in this study,

The volume of new void space generated by the sudden fracture dilation and bedding plane separation is not known, but rough estimates can be made. At the Rend Lake field study site, individual bedding separations of up to about 10 cm were observed due to subsidence. However, we do not know the areal extent of individual opening, the average and cumulative apertures of sets of openings, or their distribution through the geologic units. Openings may be concentrated as a few large openings at lithologic contacts - for example, in post-subsidence core-hole T402 on Panel 4 centerline, openings of several cm were observed at a few contacts of strong/weak materials such as limestone/shale. On the other hand, the sequence comprises multiple beds and contacts even within the same geologic unit, and the field evidence (including packer tests) of increases in permeability throughout the sandstone aquifer unit in the subsidence area does indicate some broad distribution of openings as well.

The loss of water into the rapidly opening void space is simulated by well sinks operating for a limited time. (Similarly, the partial closure of openings in the compressional second phase of subsidence may be simulated by short-term well sources, i.e. recharge wells, in that zone. This was modeled in the final operational simulations but not in these trial runs.) The equivalence between the void opening and the imaginary wells requires specification of three values:

(a) Total volume of additional void space in each grid cell. An initial estimate of the combined aperture of openings in L6 sandstone was 5 cm. Every cell assigned openings would thus develop an additional fracture volume of 0.05 m x 20 m x 20 m, or 20 m^3.

(b) Time period over which this volume of water is removed from the porous medium. As a first approximation based on the period of most rapid subsidence (Appendix A), the rapid fracture opening was assumed to occur during a 4-day period in each successive location. Thus, the 20-m^3 volume was expressed as a discharge rate of -5 m^3/day for each well.

(c) Locations over which the effect is distributed. Not every cell would necessarily have significant fracture opening. For this exercise, 50% coverage of the subsiding area was assumed,

distributed in alternate columns across the panel. However, in the final demonstration model, the wells are distributed in simpler and more reasonable rectangular zones across the entire tensile subsidence area. For the purpose of this test simulation, well sinks were applied only to L6 (the lower, channel sandstone bench).

Test simulation. This section describes simulations made purely to test the well sink approach, using the advance of Panel 3. No attempt was made at this stage to include the effects of previous panels 1 and 2 or the change in hydraulic properties caused by mine subsidence. The panel is mapped in the GV MODFLOW program with a series of well zones in the L6 sandstone that are switched on and then off in successive stress periods.

Because this stage was simply a test of the well simulation approach, no changes in K or S were specified. Where no changes in hydraulic properties complicate the situation, the advance of the mine subsidence front and associated zone of rapid porosity increase can be simulated in discrete steps within a single MODFLOW run using multiple Stress Periods. The face position is advanced in stages. A set of well sinks representing the loss of water into the new void space is assigned to the subsidence zone following the face line. Each zone consisted of two columns (40 m) of which the front column contained a line wells across the width of the panel (9 rows).

Panel 3 (183 m x 1,645 m) was approximated by 9 rows (180 m) and 82 columns (1640 m). An advance rate of 10 m/day was assumed (an interpretation error – the average advance rate of Panel 3 in reality was 17 m/day, used in the final demonstration models – but for the purpose of this trial simulation the discrepancy is not important. Discounting the end grid columns, the panel advance was simulated in 40 steps of 4 days and 40 m each, taking 164 days to complete the panel. An additional steady-state initialization step (an option in MODFLOW-2000) brings the total to 41 stress steps. In each of the transient steps, the wells in the subsidence zone were pumped at a rate of -5 m^3/day per cell.

Results. As expected, the simulation (Model LM2-1015A) produced a stepwise traveling elongated “cone of depression” around the active well column, surrounded by a larger composite cone of depression that was infilling behind (in the region of earlier well sinks) and developing ahead (Figure 5.2). The simulated heads at various positions in the model for layer L2 (weathered upper bedrock), L4 (upper sandstone) and L6 (lower sandstone) are shown in Table 5.1.

Table 5.1 Heads (m AMSL) over Panel 3 simulated by well-sink models LM2-1015A

Layer	Cell: End step:	Panel 4 Mid (40, 74)	Panel 3 start (53, 16)	Panel 3 mid-zone (53, 73)	Panel 3 end (53, 38)
L2	41	133.2	124.5	134.2	138.6
U. Bedrock	23	133.2	124.5	134.2	138.6
	1	133.2	124.5	134.2	138.6
L4	41	125.4	123.6	125.0	124.4
U. Sst	23	125.6	122.8	125.3	127.0
	1	126.7	124.3	126.5	127.7
L6	41	121.4	123.6	121.0	**105.3**
L. Sst	23	117.4	122.8	**103.9**	125.1
	1	125.85	124.3	125.0	127.0

These results show:

(a) A potentiometric low at the center of active subsidence areas (in bold) with a central drawdown of about 21-22 m in L6.

(b) Earlier impacted zones gradually recover after well sink moves on.

(c) The upper sandstone (L4) is only slightly impacted by sinks in the lower sandstone. At step 23, the drawdown at the center of the cone of depression in mid-panel 3 is 21.1 m in "pumped" L6, whereas in L4 it is 1.2 m at the same location. Field observations (Miller, 1996) during pumping tests in well P350 with a packer between L4 and L6 showed minimal response in L4 from pumping in L6 at the pumping well. This response (even with an unfractured L5 confining unit) is somewhat large compared to the well pumping test, but for subsidence impacts over a broader area a more noticeable effect would be expected.

(d) No effect of L6 sinks is seen in L2, which is to be expected when the L3 shale remains unfractured.
(e) Well sinks in L6 on Panel 3 cause a simulated drawdown of about 8.5 m on the centerline site on adjacent mid-Panel 4.

(f) Several simulations were also run with coarser steps/stress periods of 10 days instead of 4 days, with corresponding adjustment of the nominal pumping rates to maintain the same water loss volume. As expected, the coarser approach spreads the cone of depression over a larger area

while missing the finer delineation of the deeper potentiometric low in the subsiding zone. It might be appropriate for a preliminary set-up of previous mining (e.g. Panels 1 and 2 in this study) but not for detailed simulation of the main period of interest.

Comparison with Field Data. Although no attempt was made to calibrate this test model (it neglects changes in permeability and storage coefficient caused by subsidence), the results can be usefully compared to field data.

It is difficult to separate the fracture porosity dilation component of head drops from the transmitted drawdown effecting field data because both are occurring simultaneously. We assume that the most rapid head drop that occurs in the brief period before the potentiometric minimum at maximum tension is primarily the result of porosity dilation. From the hydrograph behavior over panels 3 and 4 (Figures 5.3, 5.4) at their respective tensional phase periods, the head drops due to the porosity increase and immediate drawdown ahead of subsidence are between about 7 and 12.5 m (Table 5.2). At least about 4.6 m of the 7.3 m drop at Panel 4 can be attributed to direct subsidence (fracture/bedding plane opening) during subsidence at that site.

Table 5.2. Field head changes estimated from hydrographs, Jefferson County study

Piezo. (response)	Starting Level ft BGL	Ending Levels ft BGL	Head drop (drawdown) ft (m)	Period days	Rate m/d
P300	- 70 ft	-93 ft	23 ft (7 m)	36	0.2
Over barrier pillar between Panels 2 and 3					
P301	-83 ft	-124 ft	41 ft (12.5 m)	20	0. 6
Panel 3 centerline					
P350 & adjacent sandstone piezometers (P302-304) on Panel 4					
P3 adjacent	-85 ft	-102 ft	15 ft (4.5 m)	30	0.15 (adjacent)
P4 advance	-95 ft	-113 ft	18 ft (5.5 m)	60	0.1 (advance)
Panel 4 subs.	-113 ft	-137 ft	24 ft (7.3 m)	12	0.6 (adv & subs)
Panel 4 rec.	-137 ft	-128 ft	-9 ft (-2.7 m)	6	-0.45 (compression)

Central depression: The well-sink simulation produced maximum drawdown of about 21 m in the center of the elongated cone of depression, which is around 3-4 times too high compared to observed drawdown. However, this preliminary test model did not include subsidence-induced enhancement of permeability, and the "pumping rate" was based on a very uncertain estimate of new fracture volume and the time to develop it. Considering these limitations, the simulation is considered reasonable for a simple test run.

Transmitted drawdown: The mid Panel 4 well site (represented here at cell (40,74)) was closest to the Panel 3 subsidence at the step 23. It shows a simulated drawdown of 8.5 m; this compares to field data showing about a 5.2 m drawdown from Panel 3. The Panel 3-4 area was already impacted by Panels 1 and 2 when monitoring started, so the true static levels and total drawdown are unknown. However, the estimate again seems to be in the right magnitude.

To test the simulation of recovery, additional recovery stress periods #42 (30 days in 15 time steps) and #43 (300 days in 20 time steps) were added to the model (LM-1019A, complete simulation). No wells were operating in periods #42 and #43. Results in L6 showed a full recovery sometime between 30 and 300 days (Table 5.3):

Table 5.3 Recovery Simulation, Well Test Model

End step	mid P4	Start P3	End P3
	(40, 74)	(53, 116)	(53, 38)
	heads (m AMSL)		
#1 (steady state)	125.85	124.3	127.0
#23 (nearest P4)	117.4	122.8	125.1
#41 (160 days)	121.4	123.6	105.3
#42 (30 day rec)	123.6	123.8	124.1
#43 (300 day rec)	125.84	124.3	126.95

Summary and conclusions. The use of well sinks and stress periods in MODFLOW is a reasonable approach to simulating the transient drop in potentiometric level caused by the rapid increase in fracture porosity during subsidence. The nominal pumping rate can be assigned from the value of V/T where V is the estimated average volume of new fracture openings and bedding separation in the cells representing the subsidence, and T is the estimated time over which the porosity increase occurs.

V is not known but can be crudely estimated from field strain measurements in boreholes, if available, or from reasonable expectations of bedding separation in a stratigraphic interval. Note that a 3 m coal extraction producing 2 m ground subsidence everywhere over the panel leaves an average of 1 m of new void space per unit area column of the overburden. Even though most is taken up in the caved and deep fractured zones, there is still likely to be significant new space developing rapidly in the upper bedrock layers.

These results can be somewhat compared to observed rapid head drops in piezometers directly over the subsiding panel. Although it is difficult to separate the head drops due to porosity increase from those due to transmitted drawdown from approaching or adjacent areas of subsidence, an approximate determination can be made. In the Rend Lake case, the porosity increase component seems to be a head drop averaging about 0.6 m/d for an average mine advance rate of about 17 m/day, through a period of several days leading to a total head drop of 7-12 m.

Without simulation of changes in hydraulic properties, the well-sink representation of the fracture porosity increase can be conveniently set up in a continuous model run using the stress period capability of MODFLOW. Each defined set of wells is switched on for one stress period representing a stepwise advance of the mine front, then switched off as the next set of wells operates for the next stress period. The heads develop continuously through the series of stress periods to the end of the selected mining period. The development of the elongated cone of depression, actually a composite of the successive cones of depression, reflects the development of drawdown in one zone while the drawdown in earlier zones is diminishing.

If changes in hydraulic properties are being simulated, this continuous stress-period approach cannot be used. MODFLOW does not permit the change of hydraulic properties during a continuous simulation. Instead, changes in hydraulic properties must be simulated by a series of separate simulations in which the final heads of one simulation are input as the initial heads of the next, and the user manually makes the changes in permeability between each simulation. The well-sink simulations of the increase in fracture porosity are included in that process. This is a more laborious but still workable process.

5. 6 Simulation of stresses and hydraulic property changes.

As noted in sections 2.1 and 3.2, stresses due to mine subsidence substantially change the hydraulic properties of the overlying strata even in the shallow zone far above mine drainage effects. Overall, values of permeability and storage coefficient increase, but the specific effects vary in different lateral and vertical zones. For example, the lower “dilated” part of the constrained aquitard zone may develop substantial bedding-plane separation due to vertical tension and horizontal compression (Kendorski, 2006), which increases horizontal permeability and lateral drainage away from the site, while leaving vertical permeability unchanged and vertical leakage restricted. The zone’s Kh/Kz anisotropy ratio increases.

On the other hand, lateral zones of near-vertical tensile and shear fracturing along the edge of the subsidence trough will have substantial increases in both vertical and horizontal permeability. The elongated rib zone itself will provide a preferential pathway for groundwater flow, and the fractures will be preferentially oriented so that directional anisotropy (Kx/Ky) changes. This is not simulated in the present model but of course remains an issue for potential future work.

The changes will also vary with lithology (e.g. brittle sandstone versus malleable shale), position relative to the panel geometry, height above mining, depth below ground, and time, since the mine face is advancing and the overlying subsidence is developing through time.

Modeling Approach

There is no mechanism by which to change hydraulic properties during the dynamic runtime operation of a MODFLOW model. Thus, the problem is approached as simplified step-wise changes using a small number of discrete “stress zones” that advance with the underlying advancing mine face and change the hydraulic properties of the overburden strata in a systematic manner. Each face advance step is modeled as a separate run with manual adjustment of the

property zone position. The final head configuration from one run is input as the initial head configuration for the next run, maintaining the transient development.

The stress-zone concept is illustrated in Figure 5.5. The active mining area of the Local Model is subdivided into three traveling stress zones representing the dominant processes associated with each stage of the advancing subsidence front. Figure 5.6 shows the concept of stepwise advance of the package of stress zones as originally envisaged.

Zone A: The advance zone ahead (spatially and temporally) of the approaching face/tension zone exhibits a gradual slight subsidence (about 0.5 ft; Mehnert et al., 1997). Permeability and storage values probably increase. In early test simulations, this zone was modeled with small well sinks to simulate fracture openings. However, it was realized that these added little to the model (and were also speculative), thus in the main demonstration simulation the zone is modeled only as advance slight enhancement of K and S. Considering the results of the simulations, this zone is probably only of marginal effect and further work will include tests without it.

Zone B: The main active tensional zone located immediately behind the face position exhibits the most rapid changes in K and S, subsidence of ground and strata elevations (about a further 5 ft, 1.5 m), and rapid increase in fracture porosity. Panel 4 (P350) pumping tests showed that the sandstone permeability increases 1-2 orders of magnitude during this tensional phase (Booth et al., 1997), and storativity increases up to about an order of magnitude. Well sinks can be used to represent the increase in fracture porosity (as tested above) but hydraulic property zones must be changed manually in a discrete fashion.

Zone C: The compression/settlement zone exhibits minor subsidence (about a further 0.5 ft, 0.15 m) but with partial reversals of the previous increases in the hydraulic parameters. Reverse well sinks (recharge wells) in the model can represent the closure of fracture and bedding plane openings, pushing water levels back up. As Zone C advances through the interior of the subsidence trough, it "overwrites" the interior part of Zone B. The edges of the subsidence trough remain at Zone-B enhanced levels while the Zone C area has residual but lower levels of enhancement of hydraulic properties.

Data are available from the 1988-1995 studies that help to define the spatial extents, time periods, and magnitudes of these zones. The changes in the hydraulic parameters vary with location, but for the purpose of this model each stress step at each location is assumed to have uniform changes.

Procedure for setting up stress zones

The procedure for setting up the stress zones is fairly laborious because hydraulic properties cannot be changed in MODFLOW stress steps, but it is made easier by using the Property Zone option in GV. The process is essentially three stages:

(1) Defining the zones and values.
(2) Mapping the base (unaltered) zones into the GV model.
(3) Setting up the altered stress zones in the longwall subsidence stress areas at each step.

(1) *Defining the zones and values*. An Excel spreadsheet defining the zones and properties was set up (Table 5.4) to make property modifications and serve as a guide to inputting data into the GV database. The spreadsheet data cannot be transferred directly into the GV property zone database; manual input is required. Four sets of zones are defined:

(i) The base set of unaltered permeabilities (Kx, Ky, Kz) and storage coefficient (Ss) values, taken directly from the calibrated RM (see above). This comprised ten zones (#1 - #10) representing different lithologies. Note that GV zones are not the same as layers. In some cases an entire layer is comprised of one zone (e.g. L8 is all limestone); in others, layers contain more than one zone (e.g. L5 includes areas of both Zone 5 shale and Zone 9 sandstone).

(ii) Stress Zone A: slightly raised (2x base) values ahead of the main subsidence area; specified as zones #11 - #20 (Thus zone #13 is the enhanced version of zone #3)

(iii) Stress Zone B: significantly raised values (10x base) in the main tensional subsidence area; specified as zones #21 - #30.

(iv) Stress Zone C: values lowered back from the tensional peak, though still residually enhanced (7.5x) relative to base values; specified as zone #31 - #40.

Any one lithology zone has four potential values: base, advance tension, main subsidence increase, and compressional. For 10 base zones there are 40 zones in total (the number of zones depended on the materials present in the RM calibration; 10 was coincidentally convenient because it made manual redefinition of zones in each step easier).

The information is inputted to the GV model via zone database definition tables according to the following sequence of instructions:

For each layer in the model:

*Props>select Hydraulic Conductivity
*Props>Property Values> database
Database table appears on screen.
* Specify number of zones (40, here)
* Enter the property values for each zone
OK
*Props>Property Values>Edit zone colors. Arbitrary, but it helps to have systematic colors for the different materials and sufficiently distinguishable colors for the different ones of the same lithology that will be easier to see when adjacent on the grid/map screen.

(2) *Mapping the base (unaltered) zones into the GV model*. The hydraulic conductivity zones were mapped from the RM to corresponding positions in the appropriate layers in the LM during the TMR conversion process. No further definition for base K values is needed at the LM level.

Because the RM was in steady state, no storage coefficients had been specified. For the transient LM, however, the Ss values must first be defined (see Table 5.4). The storage zones can then be copied to the same mapped positions as the hydraulic conductivity zones by the commands:

*Props>select Storage/porosity
*Props>Set Value or Zone>Copy
A dialog box appears allowing the user to copy the K zones (not the K values) as S zones.

(3) *Setting up the stress zones in the longwall subsidence areas at each new advance step*. This is a key step in the modeling of the subsidence impact, hence the procedure in GV is described below:

* Open the previous stress-step simulation model (e.g. LM-1105).
* Save it immediately under the next new name (e.g. LM-1106) to avoid erroneously overwriting the previous model. Also immediately, change the MODFLOW Root File names to avoid overwriting the previous model's Root Files:

Model>MODFLOW>Packages>
Enter a new "Root File Name" (normally same as the file, LM-1106); OK

It is also convenient to set the initial head input file as the head output file from the previous model, at this point:

Model>MODFLOW>Package Options>Initial Heads>
Enter the previous file as the new File Name (…LM-1105.hds).

* Select one layer (e.g. L8) then

Props>select Hydraulic Conductivity
Props>Set Value or Zones>Window
Draw the additional stress area (e.g. A) window with the mouse and use the dialog box to set the appropriate K property zone number.
Repeat for zones B and C.

* Repeat for each layer; and save the model!
* Copy the new K zone configuration into the S zones using the Props> Set Value or Zone>Copy command.

The next step is to reset the well-sink locations and specifications for the new configuration:
* Open B icon and select BC's>wells
* Select layer in which wells (representing fracture porosity increase) will operate, in this case L6:

BC's>insert>window>
Draw window of the tension-zone (zone B) wells over the area chosen; OK
In the dialog box, uncheck "steady-state condition" (if checked) and select "transient data"
Enter the stress period beginning and end ((1) and (1) in this model)
Enter pumping rate (-3 m^3/d was chosen for the zone B wells); OK
Select color and label; OK

*Repeat the process for the Zone C recharge wells

Repeat the process for other layers selected to have well simulations (L4 in this model).

* Make sure all Model names are specified correctly, and save model.
* Run this model and note results, save, continue with next stage model

5.7. Demonstration Model

The stress-zone modification approach and possible variations were tested in a number of preliminary models, not described here. The following section addresses only the final demonstration model presented with the project report. Although preliminary tests had been made using both MODFLOW-88 and MODFLOW-2000, the final version was operated entirely in MODFLOW-88. Operation in MODFLOW-2000 may be possible but has not been tested.

Field Data. The ISGS conducted detailed surveying of ground elevations by monuments on a longitudinal centerline over Panel 3 and on a transverse line across Panels 3 and 4.

Face Advance Rates. Face advance rates were reported (Mehnert et al., 1997) for both panels 3 and 4 as 40-70 ft/day (12-21 m/d) with an average of 55 ft/d (17 m/d). Panel 3 began in June 1988 and was completed on 15 December; panel 4 began on 23 November 1988 and was completed in late March 1989 (Mehnert et al., 1997); it undermined well P350 and the piezometer line in early February 1989.

Transverse profile. Maximum tensile strain over Panel 4 was 125 ft (38 m) from the edge of panel 4, the tensile zone being 112.5 ft (34 m) wide. The maximum compression was 150 ft (46 m) inside the panel. Maximum tension over Panel 3 was at about 96 ft (29 m) in from the edge, or 63 m out from the centerline. The principal subsidence occurred within the panel map location but the chain pillars between panels also experienced some cumulative successive subsidence.

Longitudinal profile. Longitudinal profiles over Panel 3 showed gradual ground movements starting at a point about 300 ft (91 m) ahead of the face position. Rapid subsidence began when the face had just (0-30 m) undermined the instrumented site and ended when the face was about 400 ft (122 m) past it. Slight adjustments including ground rise (negative subsidence) continued until the face was about 600 ft (183 m) past the site. Slight but measurable subsidence continued for about three years (although effects on hydrology would probably have been negligible).

Representative Stress Zones in the current demonstration model.

The particular configuration of stress zones in a study will vary depending on the particular conditions, mine geometry and advance rate, etc. In this demonstration study, the standard configuration used over Panels 3 and 4 is based on the field data discussed above.

Observations over panel 3 at the Rend Lake site (Mehnert et al., 1997) had shown separations of 0.2 ft in the upper overburden, measured by Sondex instrumentation, at locations as far as 437 ft (133 m) ahead of undermining. Continued and changing strains developed at different

overburden levels as the face approached. For example, the centerline TDR (time-domain reflectometry) cable broke in tension at the top of the main sandstone unit when the face was at 38 ft (12 m) distance. The longitudinal subsidence profiles showed that slight ground subsidence started well in advance of the zero (undermined) face position, but rapid subsidence started at variously 18 to 49 m behind (after) the face, and reached maximum rates in the 60-90 m range. When the face was about 30 m past the instrumentation, overburden beams of approximately 30 m thickness were separating (Mehnert et al., 1997). Major subsidence had largely completed by the time the face was about 120 m past the instrumentation, and interpretation of the water-level rebounds indicates that compression and settlement was happening around this time.

The stepwise representation of these processes therefore involves an advance zone (A) of minor tension and hydraulic property changes ahead of the face, a maximum tensile and K increase zone (B) behind the face and a compressional rebound zone (C) behind that, as indicated in Figure 5.5. The precise positions of the changeovers and maximum stresses relative to the face position vary from place to place as the panel advances, and also at different levels in the overburden. The stress zones used in the model represent a "typical" configuration based on the site data, discretized for efficient and practical model application.

Figure 5.7A and B show example K zones in successive stress steps in the advance of Panel 3 in one layer. The configuration is repeated in the other layers, with appropriate K zones, and also for the Ss zones. The three-zone package is moved in discrete steps as the panel advances. Behind, it leaves a lengthwise increasing area of compressional Zone C in the interior of the subsidence trough over the panel and residual tension Zone B along the edges. The advance rates for both panels 3 and 4 averaged 17 m/day, equivalent to 5 grid columns (100 m) in 6 days. Note that the length of a mine-face advance step is not necessarily the same as the length of zones A, B or C – it is the whole package that moves forward in a step.

Zone A — About 80 m (4 columns) longitudinally; across the whole panel transversely.

K and Ss increased by 2x from the base state in most layers.

No well sinks simulated.

Zone B — About 120 m (6 columns) longitudinally, and out 1-2 rows transversely on the lateral sides of the panel. It starts one column (20 m) behind the position of the mine face, in accordance with field observations.

K and Ss generally increased by 10x (one order of magnitude) in most layers, with some variation by lithology. The K and S of the drift were not changed but the possibility is coded. The thick shale in Layer L7 was coded to increase Kh but not Kz or Ss, since it is likely part of the constrained-dilated zone.

Well sinks (negative Q) represent fracture porosity increases in the Mt Carmel Sandstone (Layers L4 and L6). There are increases and impacts in other units, but for this model only the sandstone aquifer was specified. Wells are configured in

the interior 6 rows of the zone. Discharge rates (continuing for 6 days) of -3 m^3/d from L6 and -1.5 m^3/day from L4 were specified (L4 is thinner than L6 and therefore would probably have less overall fracture/bedding opening).

Zone C: About 80 m (4 columns) lengthwise; 1-2 rows in from the lateral edge of the panel.

K and Ss remain residually enhanced at 7.5x the base state, with some variation in lithology as above.

Well sources (positive Q values) represent the partial recompression of fracture openings. Wells are configured across the entire zone. Recharge rates were specified as +1.5 m^3/d in L6 and +0.75 m^3/d in L4.

Table 5.4. Property Zones for K and Ss.

	Hydraulic Conductivity		Storage		
Base	m/d	m/d			
Kh/Kv = 10	Kh	Kv	Ss		
Zone 1	0.432	0.0432	1.00E-03	Layer 1	glacial till
Zone 2	0.0864	0.00864	1.00E-05	Layer 2	weathered shale
Zone 3	0.0000864	0.000000864	1.00E-06	Layer 3	shale
Zone 4	0.0000864	0.000000864	1.00E-06	Layer 4	shale
Zone 5	0.0000864	0.000000864	1.00E-06	Layers 5, 6	interbedded shale
Zone 6	0.0000864	0.000000864	1.00E-07	Layer 7	lower shale
Zone 7	0.00432	0.000432	1.00E-06	Layer 8	limestone
Zone 8	0.432	0.0432	1.00E-05	Layer 2	near surface sandstone
Zone 9	0.0864	0.00864	1.00E-05	Layers3-6	sandstone (Mt. Carmel)
Zone 10	0.00864	0.432	1.00E-05	Layers 3-5	Fault Zone
Partial enhancement in stress zone A			2X base value		
Zone 11	0.432	0.0432	1.00E-03	Layer 1	glacial till
Zone 12	0.1728	0.01728	0.00002	Layer 2	weathered shale
Zone 13	0.0001728	0.000001728	0.000002	Layer 3	shale
Zone 14	0.0001728	0.000001728	0.000002	Layer 4	shale
Zone 15	0.0001728	0.000001728	0.000002	Layers 5, 6	interbedded shale
Zone 16	0.0001728	0.000000864	0.0000002	Layer 7	lower shale
Zone 17	0.00864	0.000864	0.000002	Layer 8	Limestone
Zone 18	0.864	0.0864	0.00002	Layer 2	near surface sandstone
Zone 19	0.1728	0.01728	0.00002	Layers 3-6	Sandstone (Mt. Carmel)
Zone 20	0.00864	0.432	1.00E-05	Layers 3-5	Fault Zone
Full enhancement in stress zone B			10X base		
Zone 21	0.432	0.0432	1.00E-03	Layer 1	glacial till
Zone 22	0.864	0.0864	0.0001	Layer 2	Weathered shale
Zone 23	0.000864	0.00000864	0.00001	Layer 3	shale
Zone 24	0.000864	0.00000864	0.00001	Layer 4	shale
Zone 25	0.000864	0.00000864	0.00001	Layers 5, 6	interbedded shale
Zone 26	0.000864	0.000000864	0.000001	Layer 7	lower shale
Zone 27	0.0432	0.00432	0.00001	Layer 8	limestone
Zone 28	4.32	0.432	0.0001	Layer 2	near surface sandstone
Zone 29	8.64E-01	0.0864	0.0001	Layers 3-6	Sandstone (Mt. Carmel)
Zone 30	0.00864	0.432	1.00E-05	Layers 3-5	Fault Zone
Partial enhancement in stress zone C			7.5X base value		
Zone 31	0.432	0.0432	1.00E-03	Layer 1	glacial till
Zone 32	0.648	0.0648	0.000075	Layer 2	Weathered shale
Zone 33	0.000648	0.00000648	0.0000075	Layer 3	shale
Zone 34	0.000648	0.00000648	0.0000075	Layer 4	shale
Zone 35	0.000648	0.00000648	0.0000075	Layers 5, 6	interbedded shale
Zone 36	0.000648	0.000000864	0.00000075	Layer 7	lower shale
Zone 37	0.0324	0.00324	0.0000075	Layer 8	limestone
Zone 38	3.24	0.324	0.000075	Layer 2	near surface sandstone
Zone 39	0.648	0.0648	0.000075	Layers 3-6	Sandstone (Mt. Carmel)
Zone 40	0.00864	0.432	0.00001	Layers 3-5	Fault Zone

Demonstration simulation models

The sequence of models used in the full demonstration simulation is:

LM-1101M Steady-state starting model setting up initial heads

This is the modified LM produced from the RM conversion, described in section 5.1. Because each of the mine advance stages is run as a separate model in which the initial heads are input from the previous model's final heads, the sequence needs this steady-state starting model to provide the first initial heads. The hydraulic conductivity zones and values are those transferred in from the calibrated RM. This model (LM-1101M) is an unmined LM without any hydraulic property changes or any well sinks defined.

MM-1104W3 Transient development of Panels 1 and 2.

We have no information about hydrologic conditions during mining of Panels 1 and 2 and therefore used a very simplified model that allows a continuous transient run. The hydraulic properties are set for both panels 1 and 2 in post-mining configuration (panel interiors are Zone C, perimeter Zone B) for all bedrock layers for the entire mining period. Mining is simulated in only 5 periods for each panel, each period being 20 days and each having a broad zone of well sinks representing the fracture porosity impacts spread over the 20-day stress period (Q = -1 m^3/d for each cell in L6 and -0.5 m3/d in L4) (Figure 5.8). This is a very crude model of the development of Panels 1 and 2 but avoids an excessive amount of time-consuming manual step-configuration (see Procedure above) for panels for which control is minimal.

The MM-1104W3 model operates in a single continuous transient run starting with the steady-state head configuration (input from LM-1101M) and developing each of the 10 stress zones in turn (5 per panel) through to the 200 day point. The final head configuration is a broad cone of depression with a low point near the western end of completed Panel 2, but extending very broadly across the LM study area (Figure 5.9).

MM-1106A to MM-1106M Mining of Panel 3

MM-1106A through 1106M represent the progressive mining of Panel 3 in individual runs for 100-m (5 column) advances every 6 days. Each model is a single transient stress period of 6 days, subdivided for computational purposes into 10 time steps with 1.2x multiplier (the default setting). The final head configuration from each model run becomes the initial head configuration for the next model. Hydraulic properties are changed in advancing stress zones at each run and wells represent the opening and partial closing of fractures and bedding planes in the tensile and compressional stress zones, as discussed above.

MM-1107A – MM-1107D Simultaneous mining of Panels 3 and 4

Panel 3 is completing at its western end, while Panel 4 is starting at its eastern end. Each panel advances 100 m (5 columns) in 6 days and the run specifications are the same as above. Hydraulic properties are changed in both panels in the advancing stress zones with each model run, and wells are applied in both active subsiding zones.

MM-1107E to MM- 1107P Mining of Panel 4

As above, except that Panel 3 has finished and Panel 4 continues mining.

MM-1107R Recovery

Model MM-1107R is a transient model representing the post-mining period starting with the end of mining of Panel 4 and hence of this longwall section. The model is run out to approximately 1800 days in 80 time steps. Other recovery models were also run.

In total, the demonstration sequence contains 1 steady-state LM, one multi-period transient LM representing Panels 1 and 2, 29 single-period transient models representing each advance of Panels 3 and 4, and one single period transient model representing the recovery. Each model is dependent on input data from the previous model. However, once run, the model output is stored and can be examined without running the model again (Plot>Import Results).

Results of the Demonstration Model

The results of the demonstration model are summarized in Table 5.5; columns indicate the following:

-- Model name
-- Mining stage (Panel and advance step)
-- Output Stress Period and Time Step
-- Simulation time (days)
-- Heads (m AMSL) in L6 at mid-panel centerline locations for the four panels 4, 3, 2 and 1 along column 73 (location of well P350 on Panel 4).
-- Heads (m AMSL) in the center of the active subsidence zone/cone of depression. This changes location with each stress step model run.

In summary, Table 5.5 shows that

(a) The heads across the study area broadly decline through time as the mined-out area increases, although heads at individual locations fall and rise as each subsidence area approaches and then moves past.

(b) The heads in the active subsidence area/active cone of depression gradually get lower through time, from about 120.5 m at stage P1-1 (Panel 1, step 1) to about 112 m at stage P4-16, with occasional slight rises due to local variations and position in the overall field.

(c) The 1800-day recovered heads are only about 0.1 m higher than the 723-day recovered heads, indicating an approximate steady state has been reached. A separate 3600-day recovery model showed a similar negligible head difference.

(d) The heads on Panels 1-3 stabilized about 1 m lower than their starting steady-state heads; the final head on the Panel 4 site was approximately the same as the starting head. This is probably due to the entire mined area developing an order of magnitude higher K in all bedrock units, broadening out local head differences over the impacted area.

The simulated head distributions at the mid-point and completion of Panel 4 are shown in Figures 5.10 and 5.11. Hydrographs of the mid-panel centerline heads (Col. 73) for the whole simulation are shown in Figure 5.11.

* Each panel has a potentiometric minimum when an active subsidence zone/mine face is close to the column-73 mid-panel position.

* The panel with the actively subsiding zone has the lowest heads (deepest cone of depression)

* Each cone of depression impacts the other panels, except that Panel 1 does not impact Panel 4 and Panel 4 does not impact panel 1 in this simulation, at a distance between sites of about 740 m. There is a noticeable impact between P1 and P3, P2 and P4, etc. at distances of 500 m. If these simulated drawdown figures were real (they are generally too low, as discussed below) they would indicate a radius of influence >500 m but <740 m, which fits with the initial estimate of 600 m.

* The simulated subsidence-zone drawdowns in Panels 1 and 2 are less than those in Panels 3 and P4. However, Panels 1 and 2 were simulated in model MM-1104W3 more coarsely than the models simulating Panels 3 and 4. Thus, in L6 the well sinks for 1104W3 were distributed as -1 m^3/d per cell x 20 days rather than -3 m^3/d per cell x 6 days, creating a less intense cone of depression. No recharge wells were simulated in the Panels 1 & 2 model. A full representation (for future work) would include shorter advance time periods as in the P3 and P4 models, together with simulation of the progressive permeability change.

	Table 5.5 Simulated heads at mid-panels in Layer 6 - Rend Lake Demo Model								
Model	Stage	Period	TS	Day	mid-P4	mid-P3	mid-P2	Mid-P1	cone
					Layer-6	L-6	L-6	L-6	L-6
					(40,73)	(53,73)	(65,73)	(77,73)	
LM-	s/state	1	0	0	125.9	126.6	126.5	126.5	123.5
1104W3	P1	1	1	0.77	125.9	126	126.05	126.2	123.8
	P1-1	1	10	20	125.8	125.7	125.7	125.7	120.5
	P1-2	2	1	20.8	125.7	125.7	125.6	125.6	121
	P1-2	2	10	40	125.2	124.1	124	124	119.5
	P1-3	3	10	60	124.3	123	121.8	120.2	119.2
	P1-4	4	10	80	123.6	122.2	120.95	120.2	119
	P1-5	5	10	100	123.2	121.2	121.2	121.2	118.2
	P2-1	6	10	120	122.9	121.8	121.2	121.2	117.6
	P2-2	7	10	140	122.3	120.7	119.95	120.2	115.8
	P2-3	8	10	160	121.3	118.5	116.1	118	115.2
	P2-4	9	10	180	120.95	118.3	116.5	117.5	115
	P2-5	10	10	200	120.9	119	118.1	118.2	114.1
1106A	P3-1	1	1	200.2	120.95	119	118.1	118.2	117.6
1106A	P3-1	1	10	206	120.9	119.1	118.2	118.4	117.6
1106B	P3-2	1	1	206.2	120.9	119.1	118.25	118.34	117.9
1106B	P3-2	1	10	212	121	119.3	118.5	118.6	116.2
1106C	P3-2	1	10	218	120.9	119.45	118.8	118.9	114.7
1106D	P3-4	1	10	224	120.9	119.5	119	119.1	114.3
1106E	P3-5	1	10	230	120.6	119.3	119	119.2	113.5
1106F	P3-6	1	10	236	120.2	119	118.9	119.2	113.3
1106G	P3-7	1	10	242	119.6	118.1	118.65	119.1	112.95
1106H	P3-8	1	10	248	118.9	116.4	118.2	119	112.8
1106I	P3-9	1	10	254	118.1	114	117.6	118.8	112.7
1106J	P3-10	1	10	260	117.6	112.7	117.1	118.6	112.7
1106K	P3-11	1	10	266	117.7	116.5	117	118.5	112.6
1106L	P3-12	1	10	272	118	116.5	117.4	118.4	112.7
1106M	P3-13	1	10	278	117.9	116.5	117.2	118.35	110.5
1107A	P3-14	& P4-	.	284	118.2	116.8	117.4	118.2	111.9
1107B	P3-15	& P4-		290	118.5	117.35	117.7	118.3	112.3
1107C	P3-16	& P4-		296	118.6	117.6	117.9	118.4	114.1
1107D	P3-17	& P4-		302	118.6	117.7	118	118.4	113.75
1107E	ended	P4-5		306	118.2	117.7	118	118.4	113.1
1107F		P4-6		312	117.7	117.6	118	118.5	112.8
1107G		P4-7		318	116.3	117.4	118	118.5	112.4
1107H		P4-8		324	114	117	118	118.6	112
1107I		P4-9		330	112.5	117.1	117.9	118.6	112.5
1107J		P4-10		336	113.7	116.5	117.9	118.6	111.8
1107K		P4-11		342	115.6	116.7	117.9	118.6	111.8

1107L		P4-12		348	116.1	117	118	118.7	111.7
1107M		P4-13		354	116.7	117.3	118.1	118.8	111.8
1107N		P4-14		360	117.2	117.6	118.3	118.8	111.8
1107O		P4-15		366	117.5	117.8	118.4	118.9	111.8
1107P		P4-16		372	117.9	118.1	118.5	119	112
1107R	Rec T=	0.245	2	372.245	117.9	118.1	118.5	119	
		1.2	40	373.2	117.9	118.1	118.6	119	
		18.9	55	390.9	118.9	118.9	119.1	119.4	
		47	60	419	120.15	120.1	120.2	120.4	
		117.7	65	489.7	122.2	122.2	122.2	122.35	
		290.7	70	662.7	124.5	124.5	124.5	124.6	
		723.4	75	1095.4	125.6	125.6	125.6	125.6	
		1800	80	2172	125.7	125.7	125.7	125.75	
		end			Stabilized				

Comparison with Field Data

Figure 5.11 shows the hydrograph of the simulated heads at mid-panel 4 (cell 40, 73). The period from about 200 to about 500 days – the simulation of panels 3 and 4 - is very similar in overall shape to the corresponding periods in the observed hydrographs from well P350 and adjacent piezometers (Figure 5.12 and 5.4), from summer 1988 through summer 1990. The precise timing of hydrograph events during mining differs because the simulated mine advance rate was specified as uniform 17 m/d, whereas the actual advance varied irregularly between 12 and 21 m/d. The precise response values also differ (see Table 5.6). Many factors potentially affect this. For example:

* Well simulation of fracture porosity increase is based on very uncertain guesses of the volume of new void space, the time taken to develop it, and the distribution of the openings. Drawdown is proportional to (simulated) discharge, hence the drawdown results are more or less linearly sensitive to the m^3/d well discharge specification,

* No account was made of the void openings in units other than L6 and L4 Mt Carmel sandstone.

* The specified changes in K and Ss in each of the geologic units in the tensional and compressional subsidence phases are very uncertain. Only in the Mt Carmel are they guided by field data, and those values were obtained only from a limited site.

* There is no simulation of ground and layer subsidence.

Given all this, it is quite promising that the general shape of the simulated hydrographs bears a good relationship to the field case. Precise values can be adjusted by varying the well parameters and hydraulic property changes, but the overall behavior of the model is completely in accordance with expected and observed field behavior.

	Table 5.6 Comparison of mid-Panel 4 Simulated and Observed Responses					
	Simulated			Observed		
	head	day	Rate	head	day	rate
Initial	121.0	212		108	50	
s =	-3.4	48	0.07	-5	40	0.125
Low; resp. to P3	117.6	260		103	90	
s =	+1.0	36	0.03	+2	50	0.04
Recover after P3	118.6	296		105	140	
s =	-6.1	34	0.2	-14	65	0.215
Min; on P4 subs	112.5	330		91	205	
s =	+3.1	12	0.26	+2	10	0.2
Recovery (1)	115.6	342		93	215	
s =	+6.6	148	0.05	+14	275	0.05
Recovery (2)	122.2	490		107	490	

6. Discussion of Model Development and Results

Objectives

The main objective of this project was to develop an approach by which the readily available groundwater flow model MODFLOW could be applied to simulate the hydrogeologic impact of longwall mining and subsidence in the shallower layers above the mine. The project used the Groundwater Vistas ® interface (GV) to the MODFLOW codes.

The project proposal restricted the model to the upper part of the overburden in order to avoid the problems of intense fracturing, mine drainage and variable saturation of the deeper zone. This is possible because the shallow layers are almost always protected from mine drainage effects by a low permeability confining "constrained" zone at intermediate levels in the overburden.

The principal issues to address were thus:

(1) ***The high hydraulic gradients and complex detail of mine-related overburden features such as hydraulic property variations***. This was addressed by the use of TMR, using the conversion feature in GV that transfers the basic physical and hydraulic framework from a coarser regional model to a more refined local model.

(2) ***Changes that occur over longwall mining that significantly affect the groundwater flow system***. These can be summarized as

(a) Rapid increase in fracture openings and bedding separation in the early tensile phase of subsidence causes rapid head drops, especially in confined bedrock aquifers.

(b) Increases in permeability and storage coefficients of one or two orders of magnitude in the subsidence trough over the panel, followed by partial reduction during the compressional and settlement phases.

(c) Subsidence of ground and layer elevation, up to about 2 m above the 3-m extraction in the study area.

Approach and Model Development

This project developed a modeling approach to 2(a) by using well sinks to simulate the rapid loss of water into the new void space, and to 2(b) by discrete advances of the mine in short discrete steps, each requiring manual adjustment of the position of the stress zones that specify the new values of hydraulic conductivity and storage coefficient. Definition of the stress zones is made using the Property Zone feature of GV.

Each subsidence front is associated with a traveling package of three stress zones: an advance zone of slight changes (A), a tensional zone of major changes during the principal subsidence phase (B), and a compression phase in the late subsidence stages (C). Active zones B and C

incorporate well-sink and well-source simulations respectively. The final configuration of a completed subsidence trough is a central residual zone C of partial property enhancement, surrounded by a peripheral residual zone B of greater residual enhancement. The approaches are innovative but are based on an established conceptual model of the hydraulic/deformational mechanisms.

We did not simulate ground and layer subsidence in this model. It should be possible to change the elevations in GV at each discrete advance step by making cell-by-cell adjustments in the property matrix database, but this process will be laborious and we suspect that it may cause stability problems in the model. This is a task for future experimental work.

A Demonstration Model was constructed to simulate the hydrologic behavior over four panels of a longwall mine at Rend Lake, Illinois, for which extensive field data were available from an earlier field study. The process of model construction and operation involved:

(a) Construction and calibration of a "regional" pre-mining model, in this case about 53 km^2. This is a significant task but not intrinsically innovative; established methods were used.

(b) Creation of a Local Model (7.3 km^2) framework using the TMR conversion feature in GV.

(c) Development of the necessary models that form the LM sequence, including an initial steady-state phase generated by TMR from the RM, a coarse transient model of the development of Panels 1 and 2, and about 30 detailed step models of the advance of Panels 3 and 4. These developments also required numerous test simulations of individual components such as the well-sink approach, prior to the demonstration model presented here.

Results

The overall pattern of simulated potentiometric levels was very similar to values observed over Panel 4 during the 1988-1995 study. The precise timing and values of the simulated responses were not exactly equivalent (simulated drawdowns were about half those observed), but they were in the right range and could be adjusted to a better solution in a calibration process with the appropriate combination of K and S modifications and well-sink values. The model is considered successful as a demonstration of techniques that can be used to apply MODFLOW to longwall mining.

The well-sink approach was successful in simulating the transient cone of depression that forms in the subsiding area due to the rapid opening of bedding planes and fractures. This is a simple way to represent a key mechanism that has not previously been modeled in the longwall situation. The precise values of drawdown would still require calibration-type adjustments of the well-sink parameters and K and S modification factors. Nevertheless, the simulated values were in an appropriate general range of observed drawdown both at the center of the subsiding area and as transmitted to adjacent panels. Although parameters are unknown, there is some theoretical basis in estimated "discharge" values based on reasonable volumes of new open fracture space developed over the limited time period of rapid subsidence.

The concept and use of stress zones in discrete steps to modify the hydraulic properties as the mine face and subsidence front advances is also new and was also successful procedurally. It is a viable though time-consuming way to apply MODFLOW to the longwall mine subsidence problem. Again, the difficulty is the uncertainty about the magnitudes and distribution of property changes. The general pattern of the simulated heads in the demonstration model was consistent with field observations and expectations, but reproduction of precise values at specific locations would need more calibration than was possible in this project. Calibration problems include the highly multivariate situation; in addition to the usual calibration variables of K and S, the longwall simulation includes the magnitude of K and S changes in each of the stress zones, the values used in the well-sink simulation of transient openings, and the vertical (layer) and lateral geometry of all these zones.

The major difference between the simulated and actual situation is the overall head elevation above datum. The simulated heads are consistently some 10 m higher than the field heads at all times except the final static level. Whether this is a problem of incorrect initial levels, insufficient impact of Panels 1 and 2, or excessively high storage values is a matter for further work. At the beginning of the 1988-1995 study, the heads had already been lowered by mining. The steady-state regional model was calibrated assuming that the sandstone water level 18 years after the end of mining ahs returned to the initial static level. These levels were then input to the steady-state initial LM. However, the initial heads may already have been lower at the start of longwall mining. In addition, the overall potentiometric depression produced by mining appears to intersect the edge boundary conditions of the LM. The simulated radius of influence may be farther out than expected and it may be that more of the RM would need to be included in the LM construction.

The discrete stress-zone approach to hydraulic property modification works, but because MODFLOW does not have a mechanism for including runtime changes via stress periods in a continuous transient simulation, it is necessary to intervene manually intervention between each discrete panel-advance run. Although this adds enormously to the time to develop a complete model simulation (about 20 minutes to make the changes to each subsequent advance model), it would be quicker to make subsequent changes once the basic models have been produced, and even much of the routine development stage could be carried out by junior staff in consulting companies or by undergraduate student help in universities.

In conclusion, the modeling approach developed in this project is firmly grounded in the conceptual model of the mechanisms involved and has succeeded in applying MODFLOW to the problem of simulating the hydrologic effects of longwall mining. Further calibration of the demonstration model of the Rend Lake site would be necessary for further work specifically for this site. The techniques demonstrated could readily be related to other individual sites, which would require adequate site information. The bulk of the effort would be in developing the initial regional model (a conventional modeling activity) from which the local model could then be produced. The actual process of TMR creation of the local model would follow the existing procedures in GV and further refinement of the LM for the specific site would be fairly straightforward following the procedures developed here.

7. Future Work

This project was conceived as a pilot demonstration of a modeling technique to apply to longwall mine hydrology, and also as the possible basis of further research to incorporate more sophisticated iterative TMR techniques. However, there still remain several issues to resolve or expand on in the model as developed. A more complete sensitivity analysis and calibration study of the local model would be required for further work on the hydrogeology of the Jefferson County/Rend Lake study area, but not for application of the methods to other areas. Further calibration would primarily involve adjustment of the simulated well-sink "pumping" rates, experimentation with modification factors for the hydraulic properties in each of the three hydraulic conductivity stress zones associated with subsidence, and modifications of storage coefficients.

Well sinks in other layers. Both specifically for this site and more generally for model clarification, further work could be done on including the well-sink simulation in other geological layers. The rapid transient increase in fracture porosity has been simulated only in L4 and L6 (the upper and lower sandstone). This process is potentially also occurring in other bedrock units, especially at strong/weak contacts. It had originally been intended to simulate major bedding plane dilation in L8 (Carthage Limestone) because significant bed separation had been observed at the limestone/shale contact in the post-subsidence cored borehole at the centerline of Panel 4. However, it was quickly obvious that this was not a meaningful option within the present study, because trial simulations of a short-term well sink in L8 produced rapid dewatering, a steep-sided cone of depression, and local drying in L8, while causing no impact at all in the aquifer because of the thick shale confining unit represented by L7. This result probably does reflect the hydrological regime. Sudden fracture and bedding plane openings in the limestone or other low permeability isolated units will cause rapid dewatering and possibly negative pressures (Booth, 2007) from which the sandstone aquifer is protected by the L7 shale unit. However, some further experimentation would be desirable.

Other areas. The model procedure as developed could be applied immediately to other areas. However, this would require adequate site information from field investigation. The bulk of the modeling effort would be the conventional development of the initial regional model. The delineation and application of the local model would then be relatively straightforward provided that sufficient calibration data are available.

Elevation Changes. This project did not reach the intended goal of simulating elevation changes due to subsidence. As with hydraulic properties, there is no direct mechanism in MODFLOW for dynamically incorporating elevation changes in the model runs; they would need to be modified in every discrete step separate run. Unlike hydraulic properties, however, elevation changes cannot be simulated through GV's property zone approach but would have to be changed cell by cell in the elevation data matrix for each layer. The procedure is possible in theory but liable to be laborious in execution. It would require detailed changes for each discrete stress step using the Math tool in the GV Matrix Editor for top and bottom elevations for all layers, according to the subsidence pattern.

More significantly, changes in the elevations of each layer would create complex consistency problems with specified elevations of constant head boundaries, drain boundaries, rivers (if included), and in some cases the unconfined/confined and dry/wet conditions of cells between runs. Because of all these issues, it was realized that incorporating the elevation changes will take much more work and experimentation with GV than was possible in this project. It is an issue for future work.

RM-LM linkage. At this stage, we have not returned to the RM to incorporate changes produced by the LM during the mining simulation. There is no reverse-TMR mechanism in Groundwater Vistas to make changes in the RM based on developments in the LM. The RM would need to be substantially revised as a separate modeling project to incorporate any changes. It is therefore probable that more sophisticated feedback between the LM and RM would need to go beyond the use of GV.

Literature Cited

Anderson M.P. and W.W. Woessner, 1992. *Applied Groundwater Modeling*. Academic Press, San Diego: 381 pp

Bertsch, Lawrence P., 1997. The Effects of Longwall Mining on Groundwater Chemistry at Two Sites in Southern Illinois. M. S. Thesis, Northern Illinois University, DeKalb, IL.

Booth C.J., 2002. The Effects of Longwall Coal Mining on Overlying Aquifers. In: Younger P.L. & Robins N.S. (eds.) *Mine Water Hydrogeology and Geochemistry*, Geological Society, London, Special Publications 198: pp 17-45.

Booth, C.J., 2007. Confined-unconfined changes above longwall coal mining due to increases in fracture porosity. Environmental & Engineering Geoscience, vol. XIII, no. 4, pp. 355-367.

Booth C.J. and L.P. Bertsch, 1999. Groundwater Geochemistry in Shallow Aquifers Above Longwall Mines in Illinois, USA. *Hydrogeology Journal* 7 (6): 561-575.

Booth C.J., P.J. Carpenter, R.A. Bauer, 1997. *Aquifer Response to Longwall Mining, Illinois*. U.S. Department of the Interior, Office of Surface Mining, Library Report No. 637, Grant/Co-op Agreement GR196171, 400+ pp.

Booth C.J., E.D. Spande, C.T. Pattee, J.D. Miller, L.P. Bertsch, 1998. Positive and Negative Impacts of Longwall Mining on a Sandstone Aquifer. *Environmental Geology* 34 (2/3): 223-233.

Buxton H. and T.E. Reilly, 1986. A Technique for Analysis of Ground-water Systems at Regional and Subregional Scales Applied on Long Island, New York. USGS Water Supply Paper 2310, p. 129-142

Harbaugh, A.W., Banta, E.R., Hill, M.C., and McDonald, M.G., 2000, MODFLOW-2000, the U.S. Geological Survey modular ground-water model -- User guide to modularization concepts and the Ground-Water Flow Process: U.S. Geological Survey Open-File Report 00-92, 121 p.

Hutcheson S.M., J.A. Kipp, J.S. Dinger, L.V.A. Sendlein, D.I. Carey, G.K. Secrist, 2000a. Effects of Longwall Mining on Hydrology, Leslie County, Kentucky: Part 2: During-mining Conditions. Kentucky Geological Survey, Lexington, KY: Report of Investigations 4: Series XII, 34 pp.

Hutcheson S.M., J.A. Kipp, J.S. Dinger, L.V.A. Sendlein, D.I. Carey, G.K. Secrist, 2000b. Effects of Longwall Mining on Hydrology, Leslie County, Kentucky. Part 3: Post-Mining Conditions. Kentucky Geological Survey, Lexington, KY: Report of Investigations 6: Series XII, 21 pp.

Hunt R.J. and J.J. Steuer, 2000. Simulation of the Recharge Area for Frederick Springs, Dane County, Wisconsin. USGS Water-Resources Investigation Rept. 00-4172, 339 p.

Hunt R.J., J.J. Steuer, M.T.C. Mansor, T.D. Bullen, 2001. Delineating a Recharge Area for a Spring Using Numerical Modeling, Monte Carlo Techniques, and Geochemical Investigation. *Ground Water* 39 (5): 702-712.

Johnson K.L., 1992. Influence of Topography on the Effects of Longwall Mining on Shallow Aquifers in the Appalachian Coalfield. In: Peng S.S. (ed.): Proc. 3d Workshop on Surface Subsidence Due to Underground Mining, Morgantown, WV., June 1992. West Virginia University, Morgantown, p. 197-203.

Keating E.H., V.V. Vesselinov, E. Kwicklis & Z. Lu, 2003. Coupling Basin- and Site-Scale Inverse Models of the Espanola Aquifer. *Ground Water* 41(2): 200-211.

Kendorski, F. 2006. Effect of full-extraction underground mining on ground and surface waters: a 25-year retrospective. 25th Inter. Conf. on Ground Control in Mining, West Virginia University, Morgantown, WV.

Keys J.N. and W.J. Nelson, 1980. The Rend Lake Fault System in Southern Illinois. Illinois State Geological Survey, Circular C513, 23 pp.

Kim J-M, R.R. Parizek, D.Elsworth 1997. Evaluation of Fully-coupled Strata Deformation and Groundwater Flow in Response to Longwall Mining. *Int. J. Rock Mech. Min. Sci*. 34 (8): 1187-1199.

Leake S.A. and D.V. Claar, 1999. Procedures and Computer Programs for Telescopic Mesh Refinement Using MODFLOW. USGS Open-File Report 99-238, Tucson, AZ

Leake S.A., P.W. Lawson, M.R. Lilly, D.V. Claar, 2003. Assignment of Boundary Conditions in Embedded Ground Water Flow Models. *Ground Water* 36 (4): 621-625.

Liu J. and D. Elsworth, 1997. Three-dimensional Effects of Hydraulic Conductivity Enhancement and Desaturation around Mined Panels. *Int. J. Rock Mech. Min. Sci*. 34 (8): 1139-1152.

Matetic R.J., J. Liu, D. Elsworth, 1995. Modeling the Effects of Longwall Mining on the Ground Water System,. US Bureau of Mines, Report of Investigations RI 9561, Pittsburgh, PA: 14 p.

Matetic R.J. and M.A. Trevits,1992. Longwall Mining and its Effects on Ground Water Quantity and Quality at a Mine Site in the Northern Appalachian Coal Field. Proc. NGWA Focus Conference on Eastern Regional Ground Water Issues, Boston, MA October 1992, p. 573-587.

McDonald M.G. and A.W. Harbaugh, 1988. A Modular Three-dimensional Finite-Difference Ground Water Flow Model. Techniques of Water Resources Investigations 06-A1, USGS: 576 p.

Mehl S., M.C. Hill. SA Leake, 2006. Comparison of Local Grid Refinement Methods for MODFLOW. *Ground Water* 44 (6): 792-796.

Mehnert B.B., D.J. Van Roosendaal, R.A. Bauer, P.J. DeMaris, N. Kawamura, 1997. *Final report of subsidence investigations at the Rend Lake Site, Jefferson County, Illinois.* Illinois State Geological Survey, IMSRP-X (38 pp + Apps); and ISGS Open-File Report 1997-7, 119 p.

Merrick N.P., 2009. Comparable modelling of longwall mining effects using Standard-MODFLOW and MODFLOW-SURFACT in the Southern Coalfield, New South Wales, Australia. In: Milne-Holme W.A. (ed): Groundwater in the Sydney Basin, Proc. International Association of Hydrogeologists symposium, Sydney, NSW, Australia, 4-5 Aug. 2009, p. 236-245.

Miller, Joseph D., 1996. Hydrogeologic Characterization of a Heterogeneous Sandstone Aquifer Overlying a High Extraction Longwall Coal Mine: M.S. Thesis, Northern Illinois University, DeKalb, IL.

Pattee, Charles T., 1994. Long-term Hydrogeologic Impact of Longwall Subsidence on a Shallow Bedrock Aquifer in Illinois. M.S. Thesis, Northern Illinois University, DeKalb, IL, 210 pp.

Rauch H.W. 1989. A Summary of the Ground Water Impacts from Underground Mine Subsidence in the North Central Appalachians. Chapter 2 in: Coal Mine Subsidence Special Institute, December 1989, Pittsburgh, The Eastern Mineral Law Foundation, p. 2.01-2.31.

Singh M.M. and F.S. Kendorski, 1981. Strata Disturbance Prediction for Mining beneath Surface Water and Waste Impoundments. In: Peng S.S. (ed.) Proc. 1st Conf. on Ground Control in Mining, Morgantown, WV, July 1981, p. 76-88.

Székely F., 1998. Windowed Spatial Zooming in Finite-Difference Ground Water Flow Models. *Ground Water* 36 (5): 718-721.

Spande, Erik D., 1990. Effects of Longwall-Induced Subsidence on Hydraulic Properties at a Site in Jefferson County, Illinois. M.S. Thesis, Northern Illinois University, DeKalb, IL, 245 pp.

Trent, B.A., 1996. Effects of Longwall Mine Subsidence on Agricultural Soils and Hydrology, p. 106-117 in: Trent, B.A., R.A. Bauer, P.J. DeMaris, W. Kawamura: Findings and Practical Applications from the Illinois Mine Subsidence Research Program, 1985-1993. Illinois State Geological Survey, IMSRP-XII, 146 pp.

Ward D.S., D.R. Buss, J.W. Mercer, S.S. Hughes, 1987. Evaluation of a Groundwater Corrective Action at the Chem-Dyne Hazardous Waste Site Using a Telescopic Mesh Refinement Modeling Approach. *Water Resources Research* 23(4): 603-617.

Werner E. and J.C. Hempel, 1992. Effects of Coal Mine Subsidence on Shallow Ridge-Top Aquifers in Northern West Virginia. In: Peng, S.S. (ed.): Proc. 3d Workshop on Surface Subsidence Due to Underground Mining, Morgantown, WV., June 1992. West Virginia University, Morgantown, p. 237-243

Winters W.R., 2004. Numerical Modeling of the Irwin Syncline, Westmoreland County, Pennsylvania. Hydrologic Issues Workshop, Appalachian Region Technology Transfer: Office of Surface Mining (US Department of Interior): Morgantown, WV, August 3-5.

Younger P.L., S.A. Banwart, R.S. Hedin, 2002. *Mine Water: Hydrology, Pollution, Remediation.* Kluwer Academic Publishers, Dordrecht, Netherlands, 442 pp.

Figures

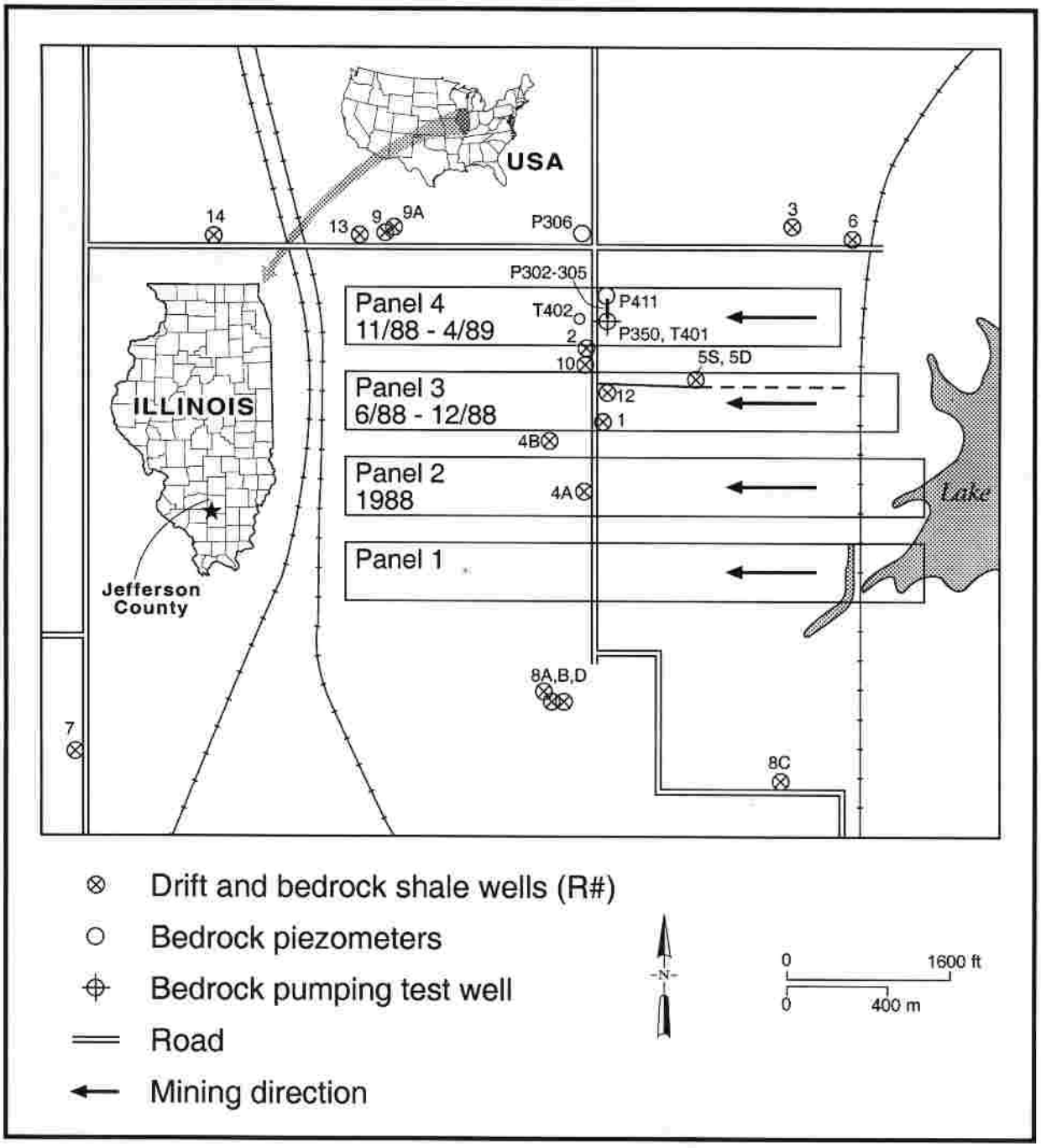

Figure 1.0 Location and map of study site, showing the four longwall panels and location of principal field instrumentation.

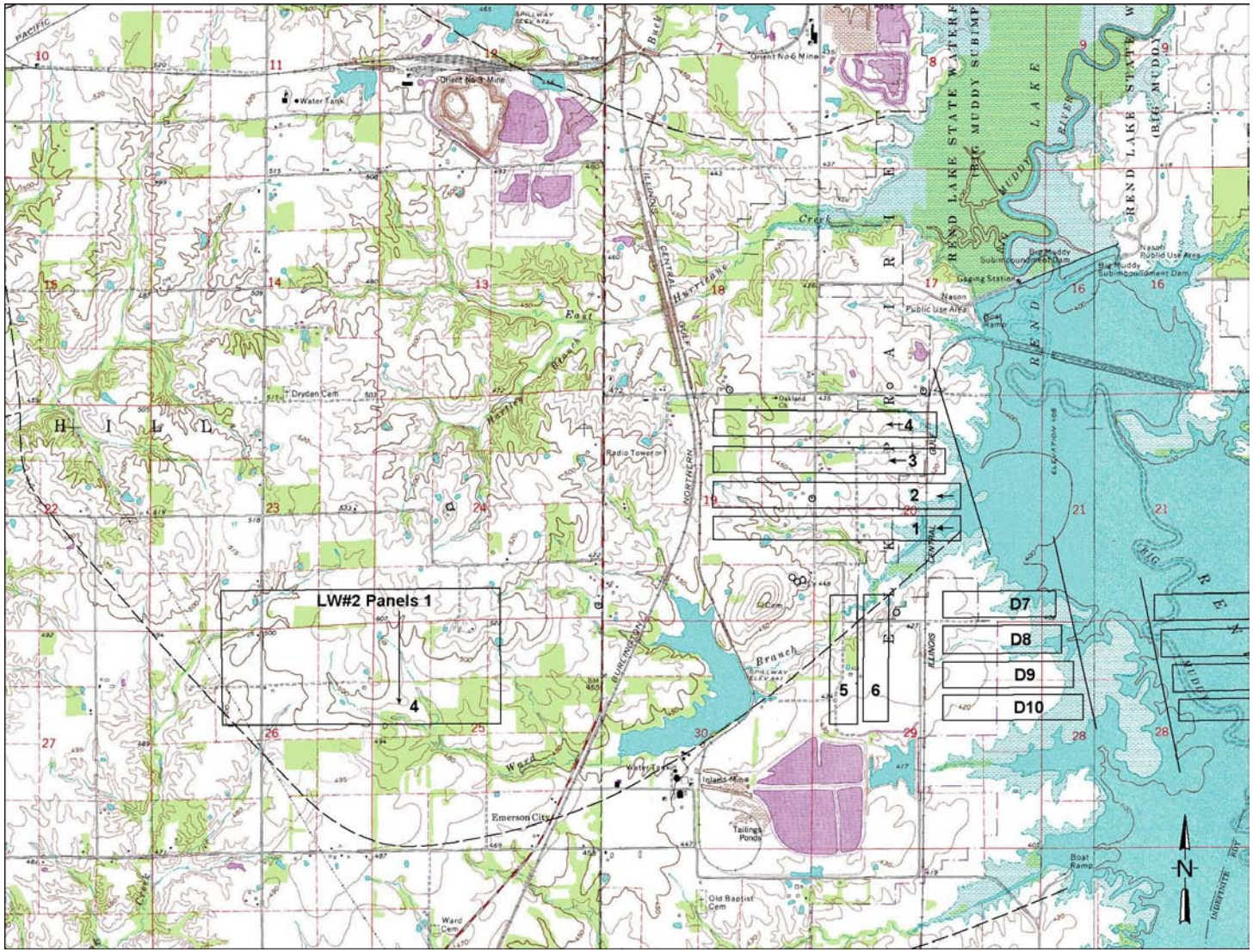

Figure 3.1 Map of the study area from USGS 7.5-min topographic maps (Waltonville and Ina, Illinois). Panels 1-4 were the first longwall section. Panels 1 and 2 are 1,737 m long.

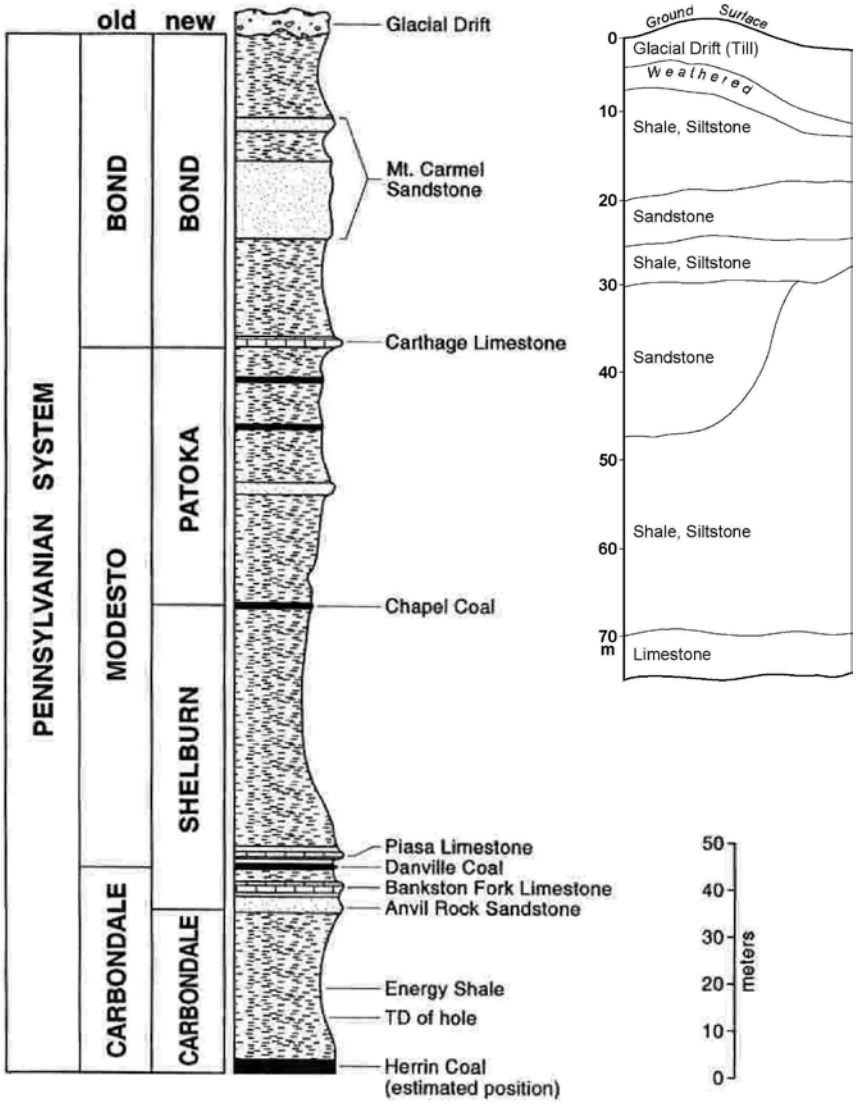

Figure 3.2 Stratigraphic Column of the Jefferson County Site. Full column is approximately 230 m; inset shows modeled units from the drift down to the Carthage Limestone.

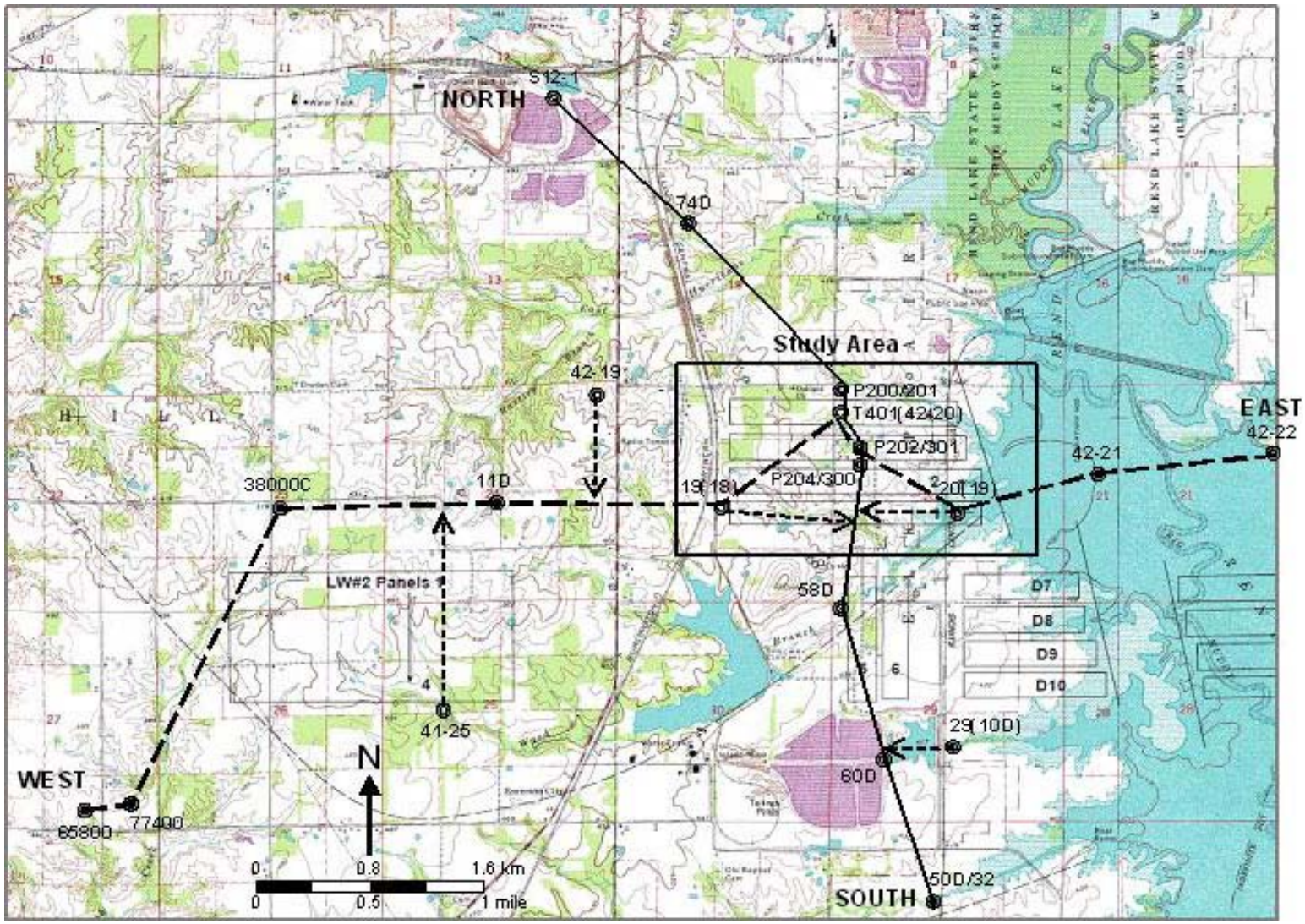

Figure 3.3 Location of Cross Sections: North-South (solid line) and West-East (dashed line) cross sections. Dashed arrows indicate projection lines from outlying borings to the cross-section lines.

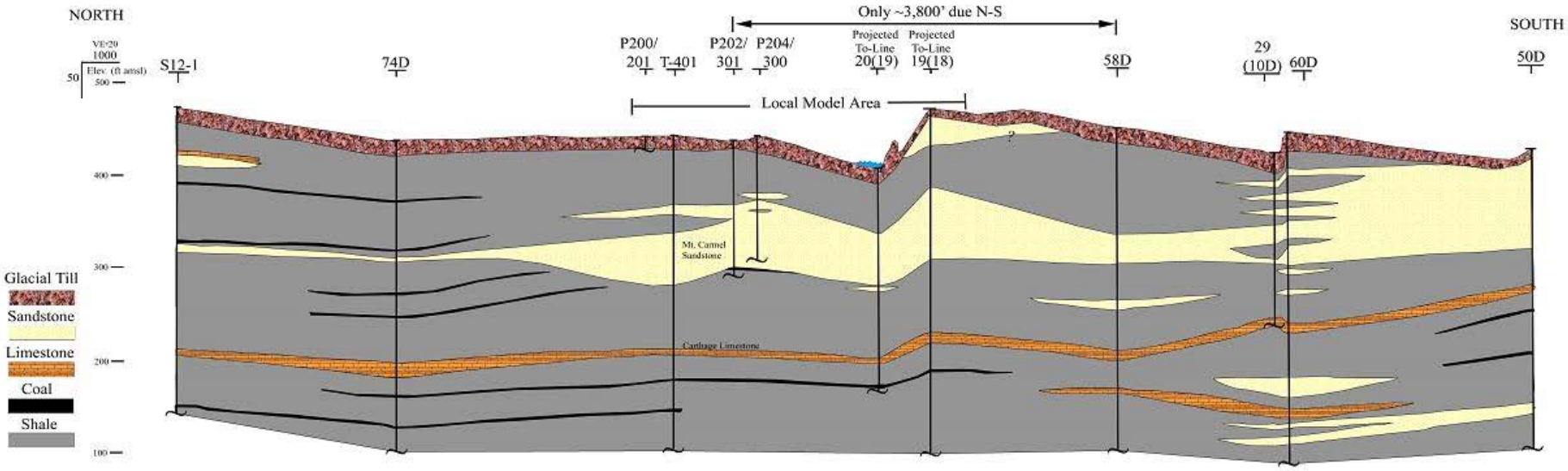

Figure 3.4 Lithologic N-S Cross Section across Regional Model Area; Local Model shown in center.

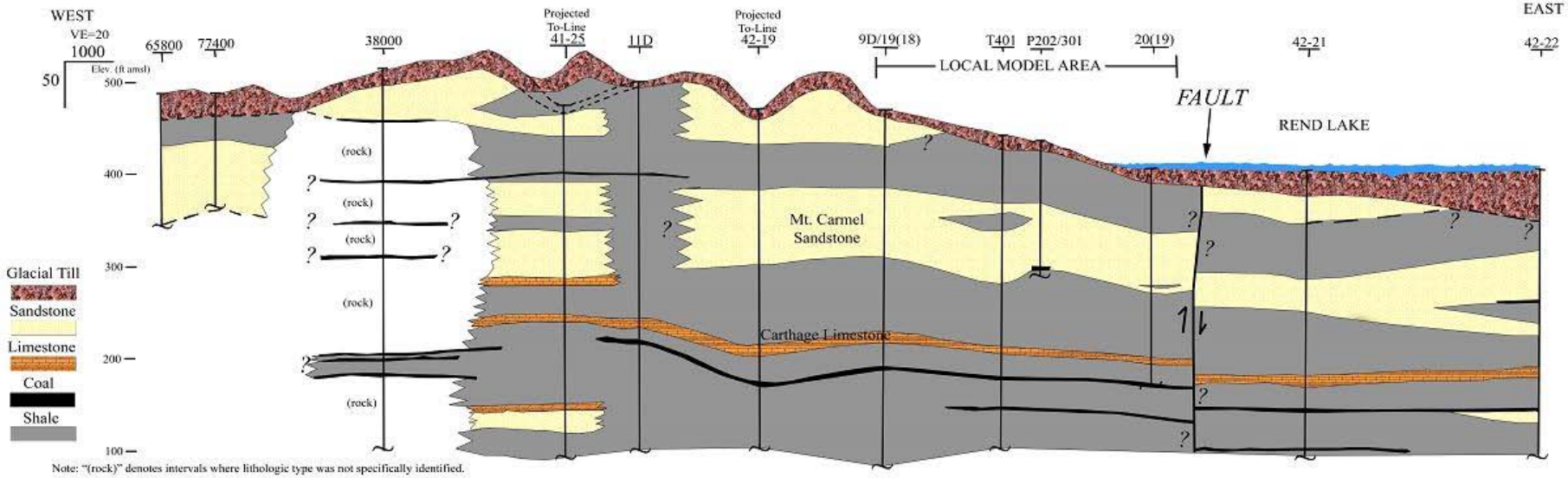

Figure 3.5 Lithologic W-E Cross Section across Regional Model Area; Local Model shown in center.

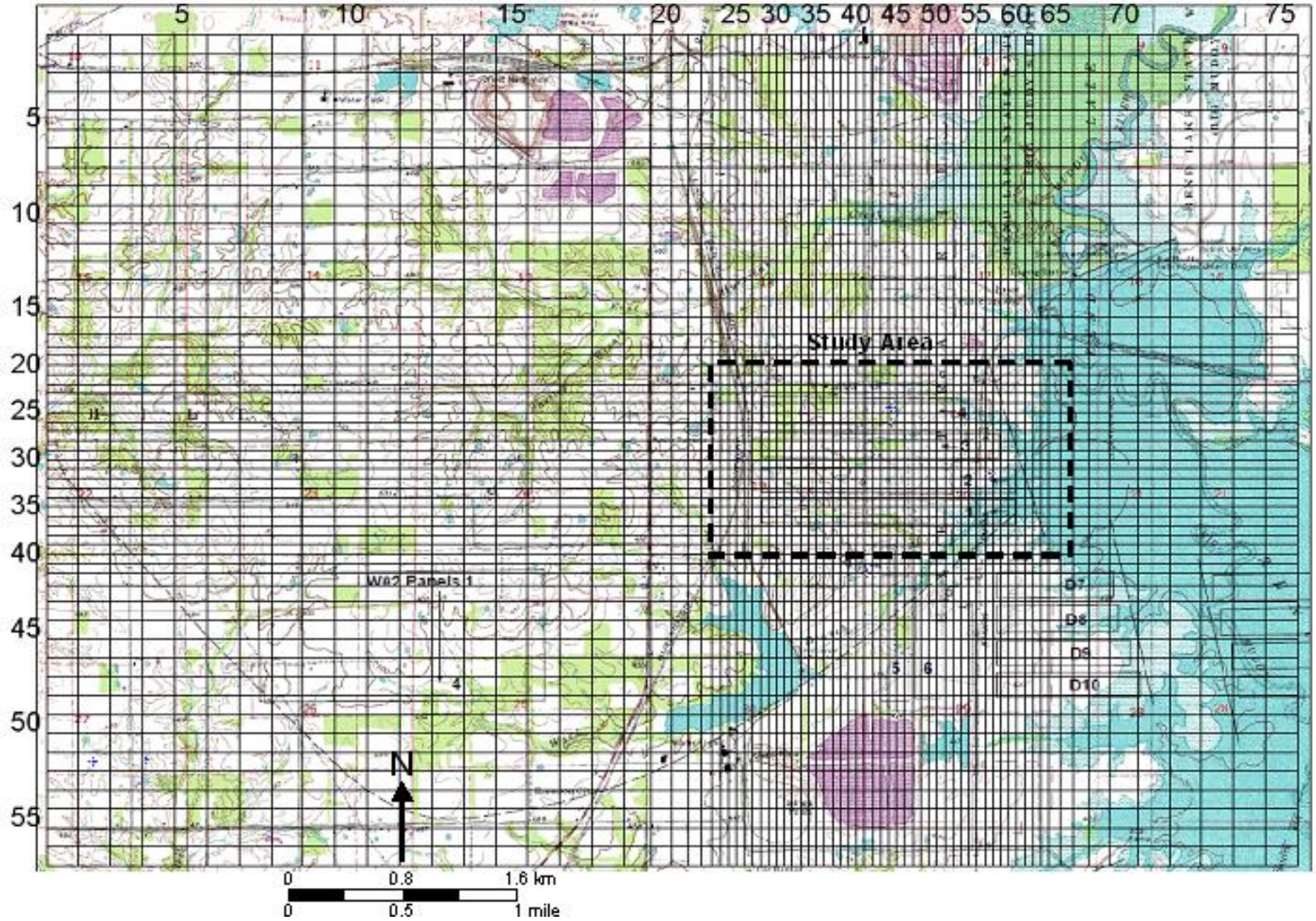

Figure 4.1 Regional Model: Variably spaced FD grid, 57 rows x 78 columns.

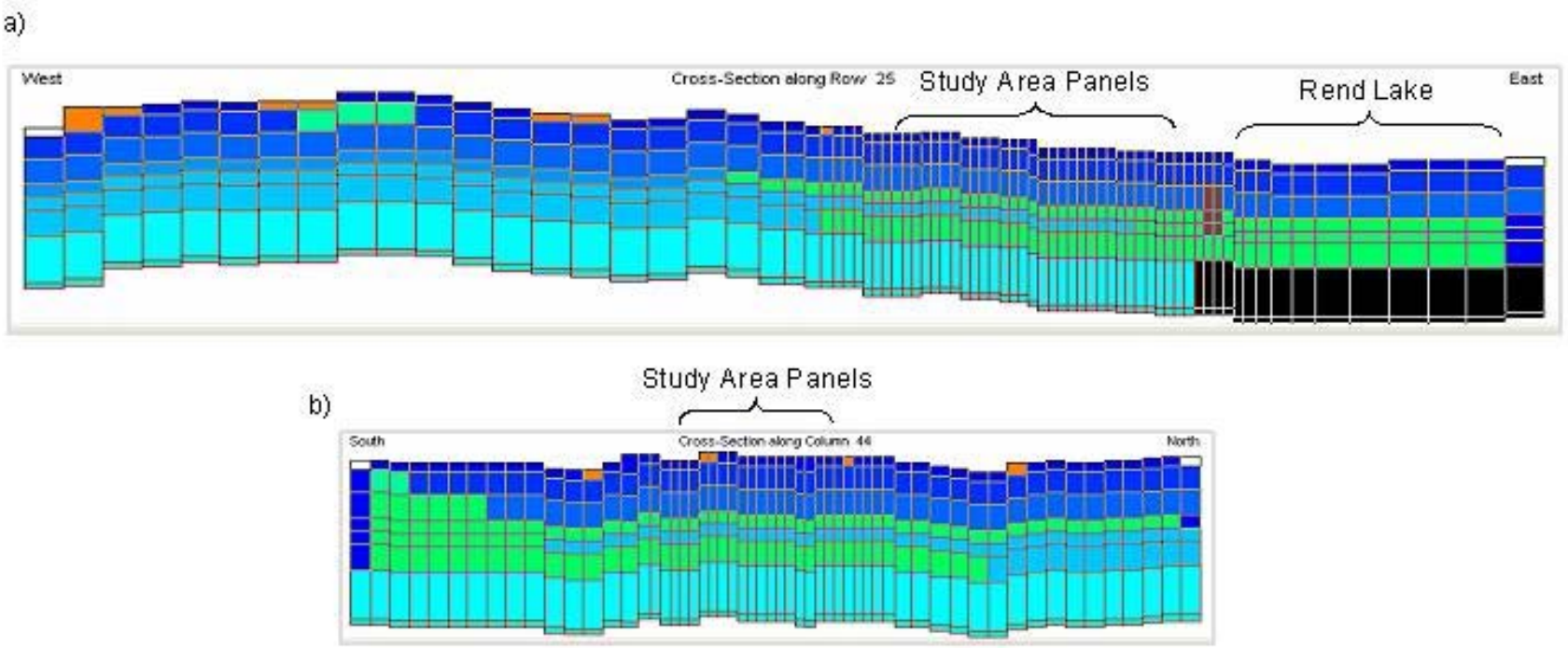

Figure 4.2 Regional Model: Cross Sections (a) W-E along row 25 and (b) S-N along column 44. Rend Lake Fault System represented by dark brown cells in W-E section; layers 7 and 8 east of Fault are inactive (black cells). Lower permeability units (till, shale, limestone) are in blue and higher permeability units (sandstone) are in green. Constant-head boundaries of sandstone are dark blue; stream-drain cells in surficial layer are orange.

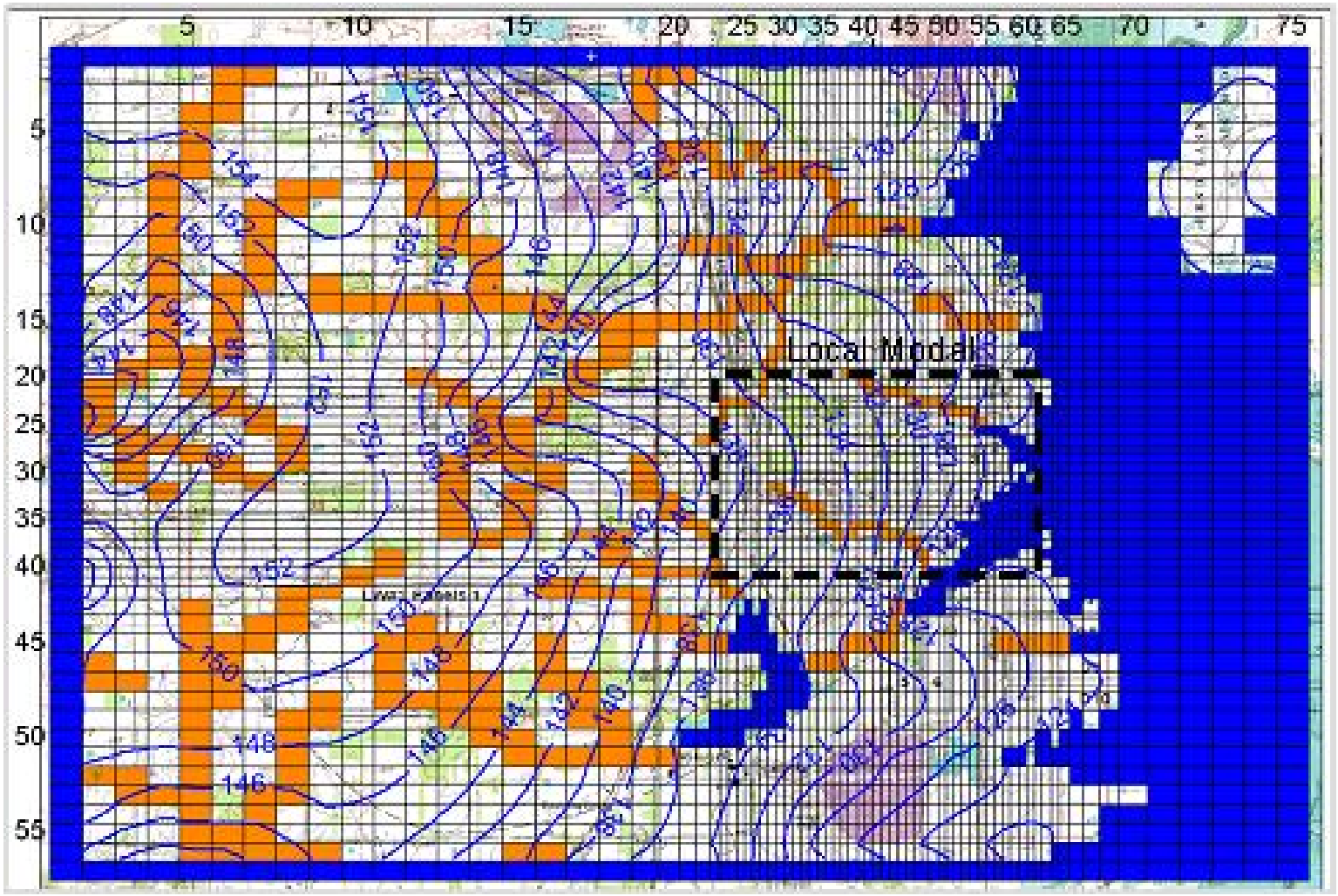

Figure 4.3A Regional Model: Contours of simulated heads in Layer 1. Contour interval 2 m, elevations in m AMSL. Constant head cells are in dark blue and stream-drain cells are in orange.

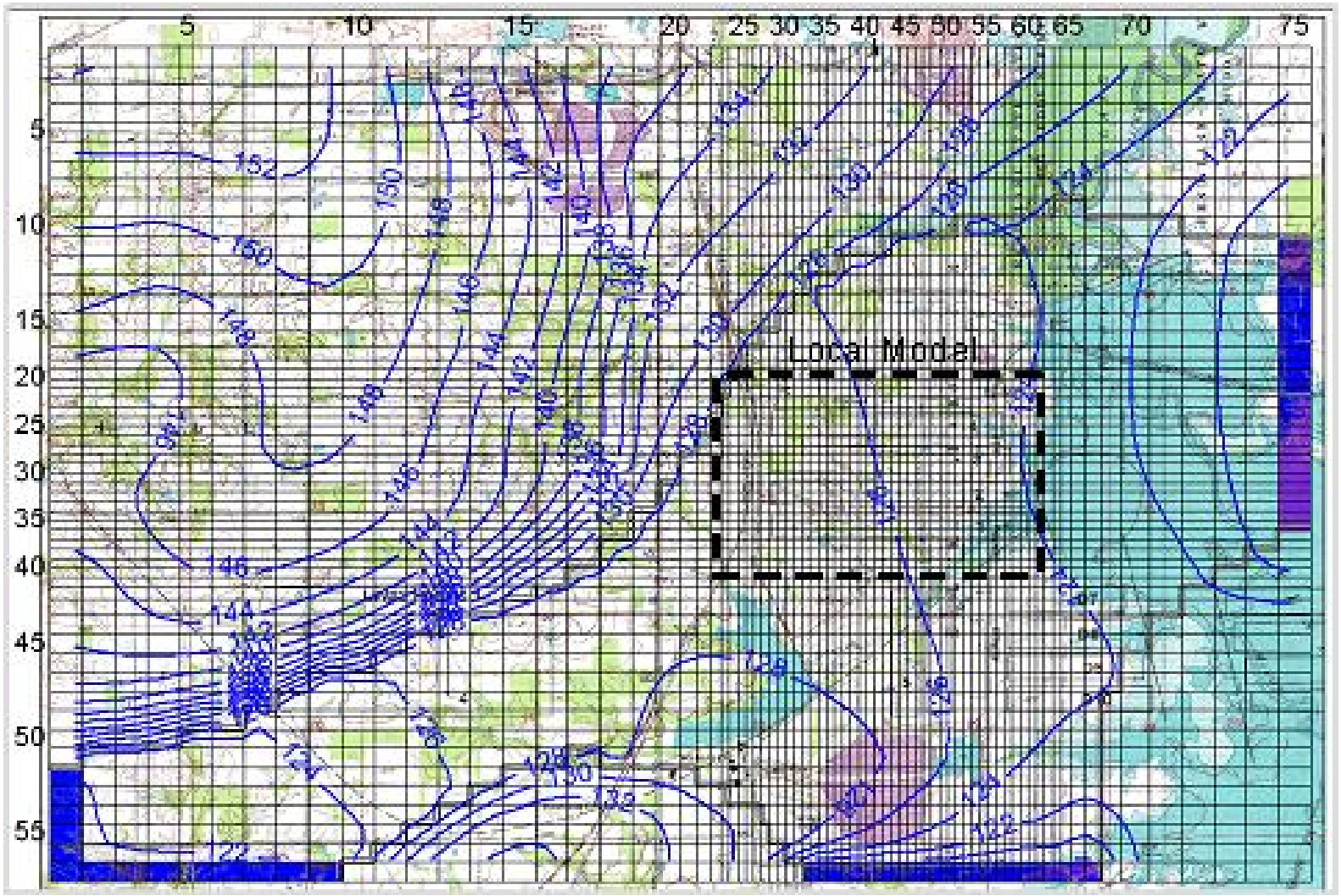

Figure 4.3B Regional Model: Contours of simulated heads in Layer 6. Contour interval 2 m, elevations in m AMSL. Constant head cells are in dark blue.

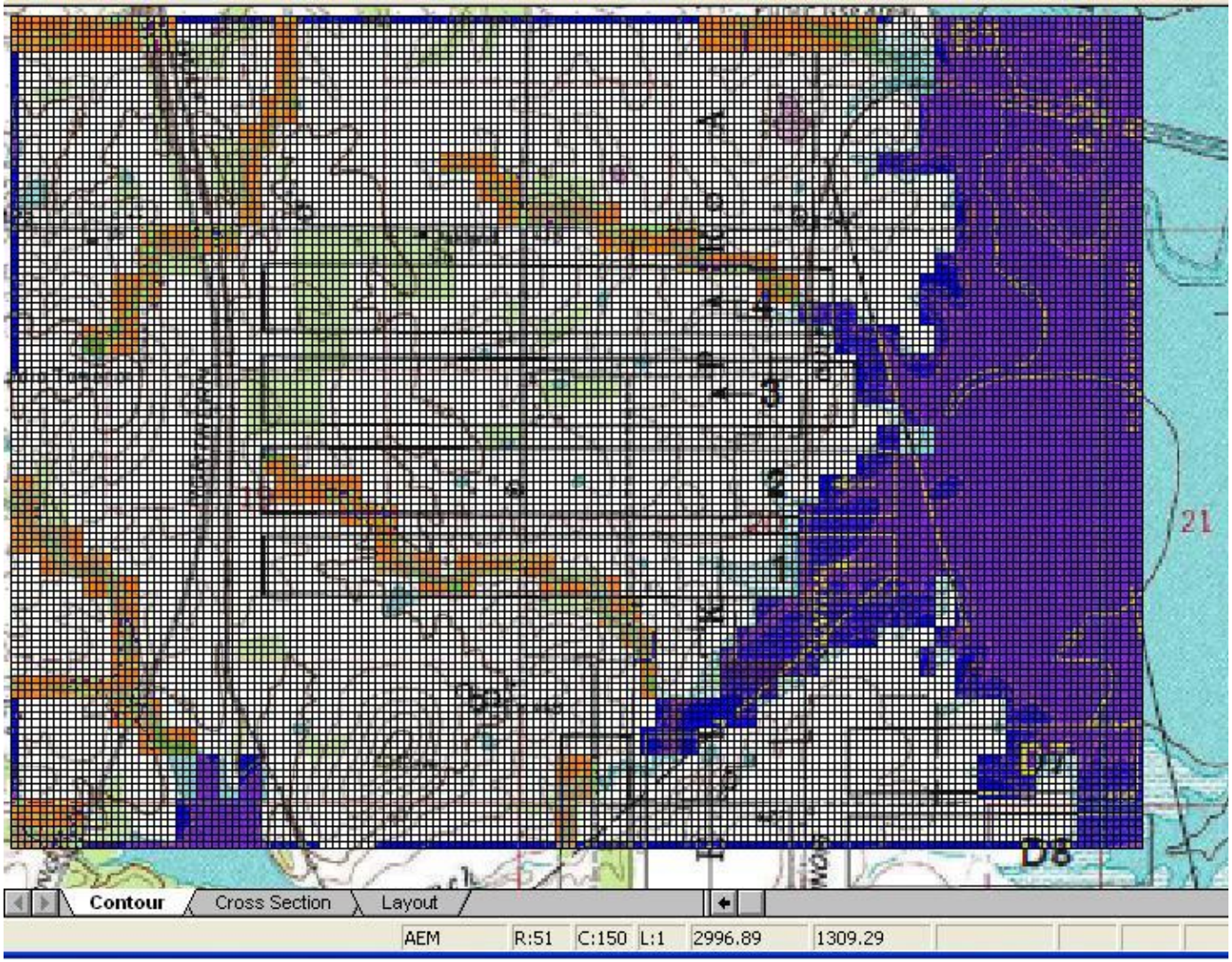

Figure 5.1 Map of the Local Model Area. Grid cells are 20 m x 20 m. Boundaries (Layer 1) shown as stream-drain (orange) and constant head (dark blue).

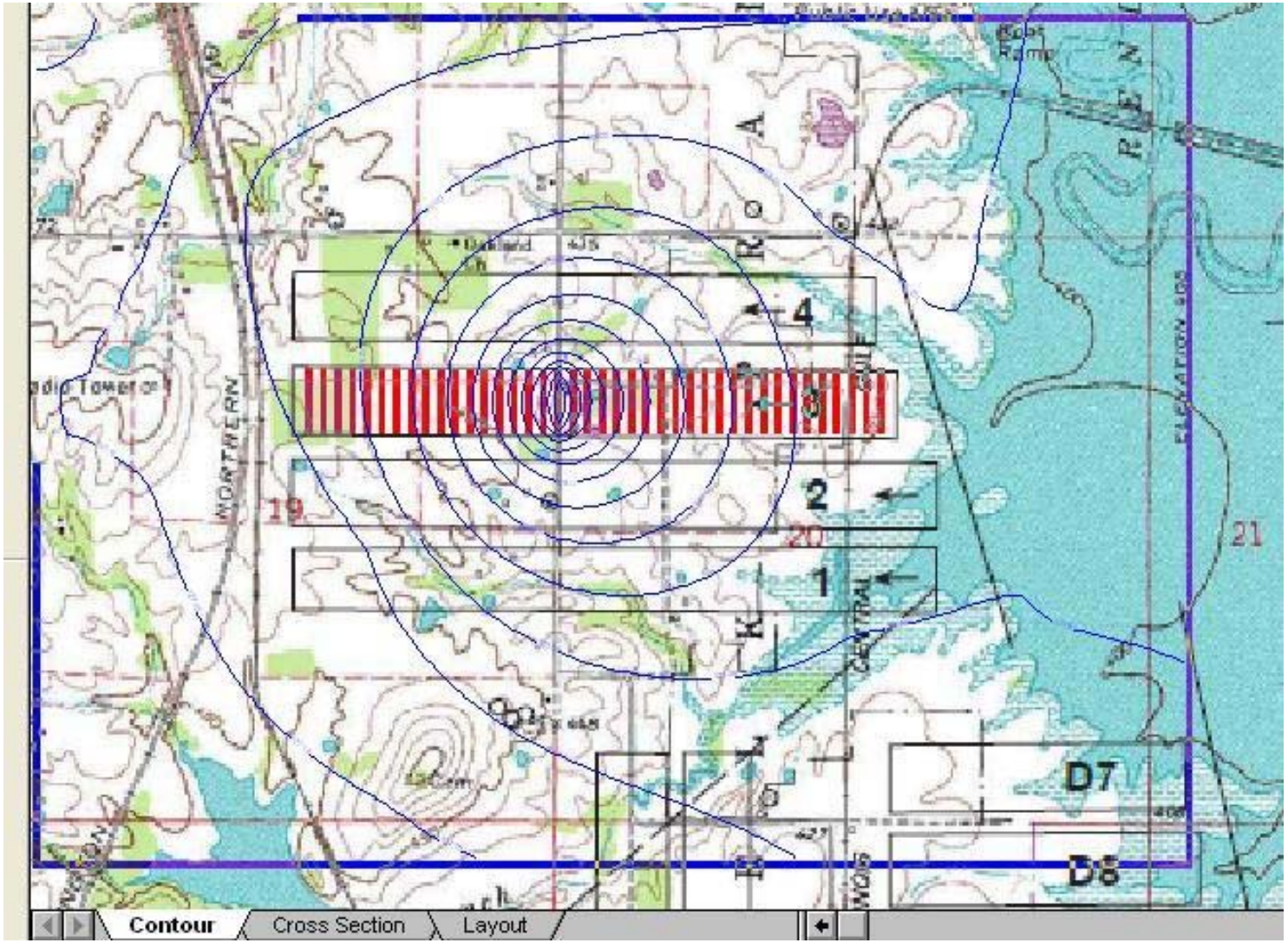

Figure 5.2 Cone of depression produced by test simulation (LM2-1015A) of the "well sink" concept: Layer 6, Step 24 (closest to well P350 on Panel 4).

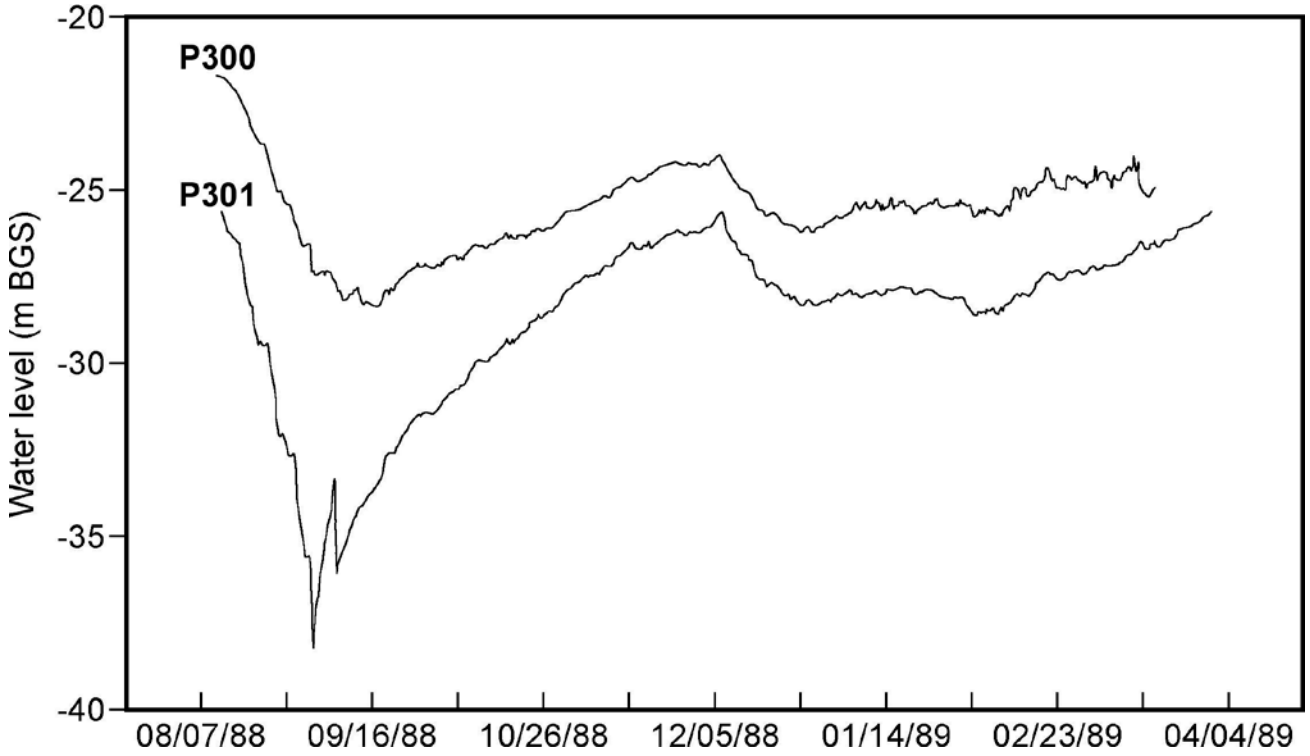

Figure 5.3 Hydrograph of heads over Panel 3 in piezometers P300 (barrier) and P301 (centerline) during mining of Panel 3 (after Mehnert et al., 1997).

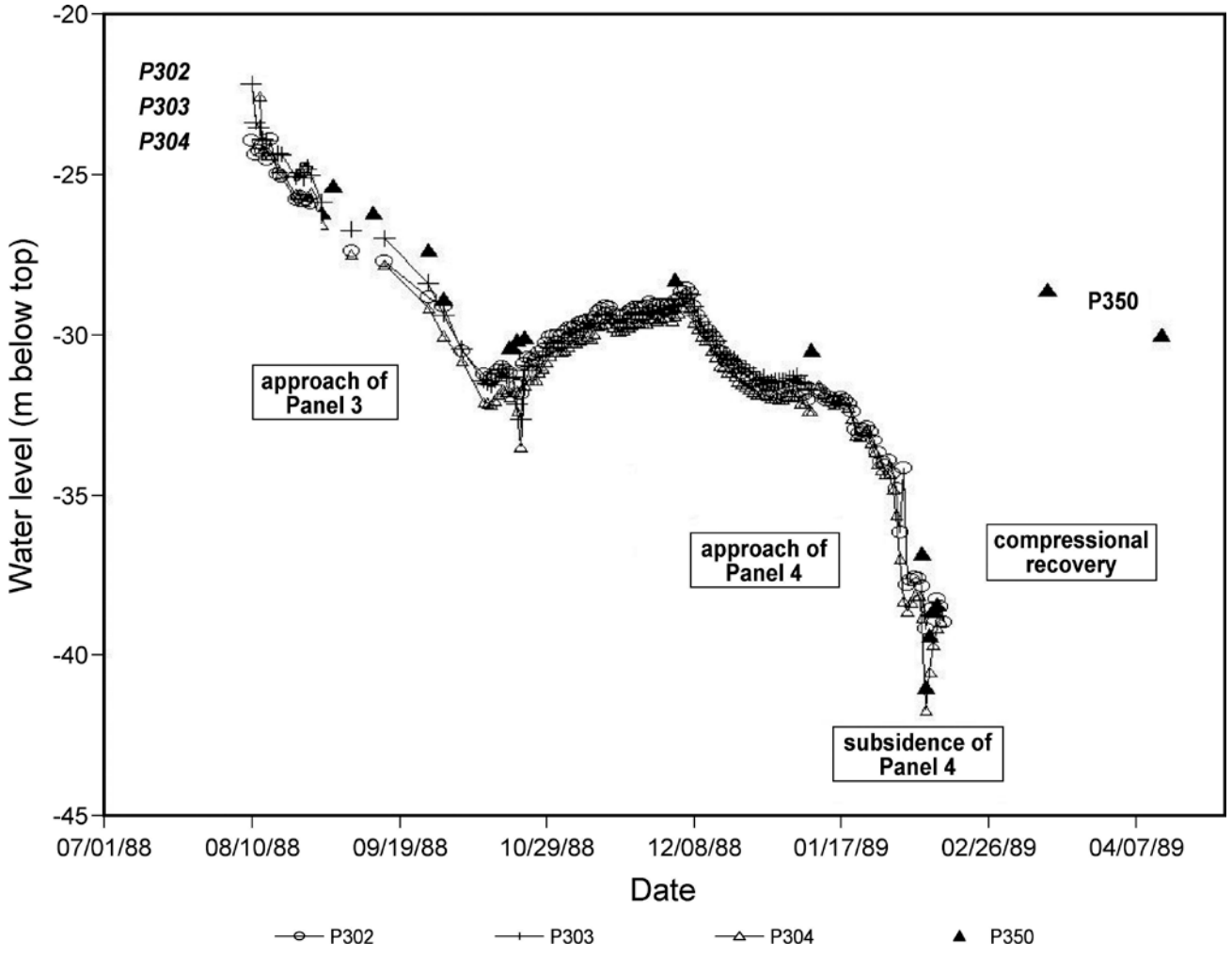

Figure 5.4 Hydrograph of piezometric levels over Panel 4, 1988-1989.

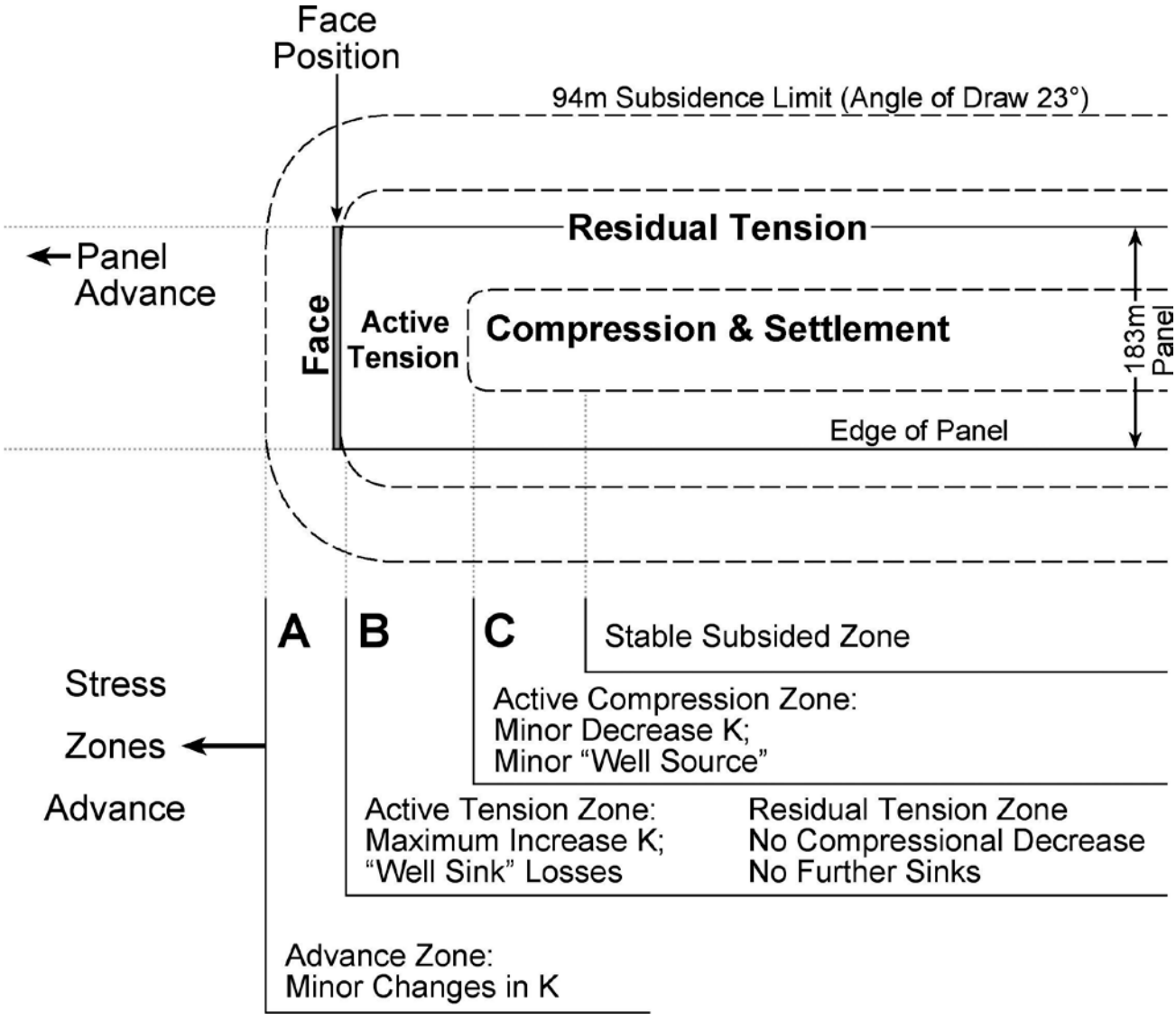

Figure 5.5 Concept of stress zones over and around subsidence front.

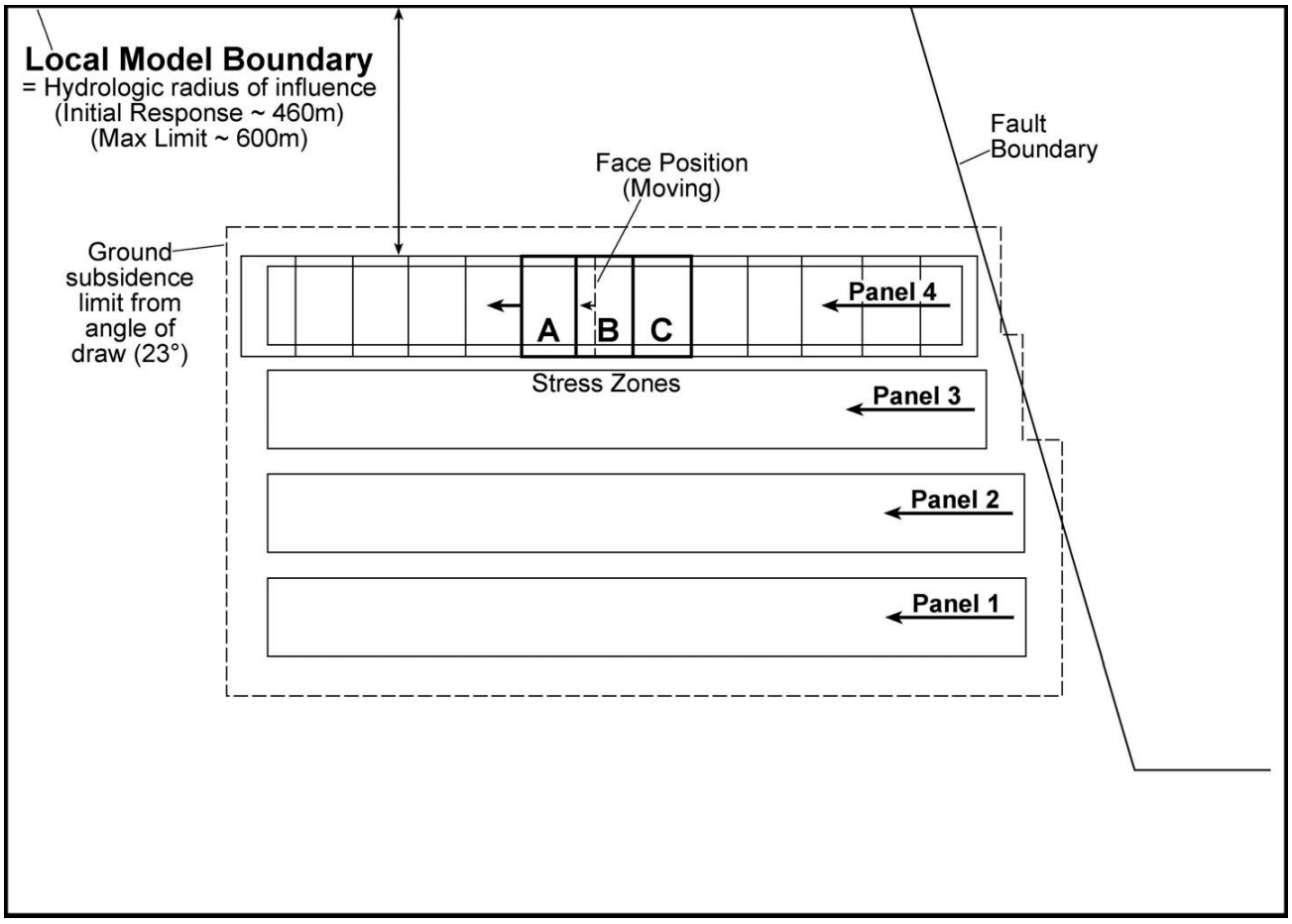

Figure 5.6 Stepwise advance stress zones along model panel.

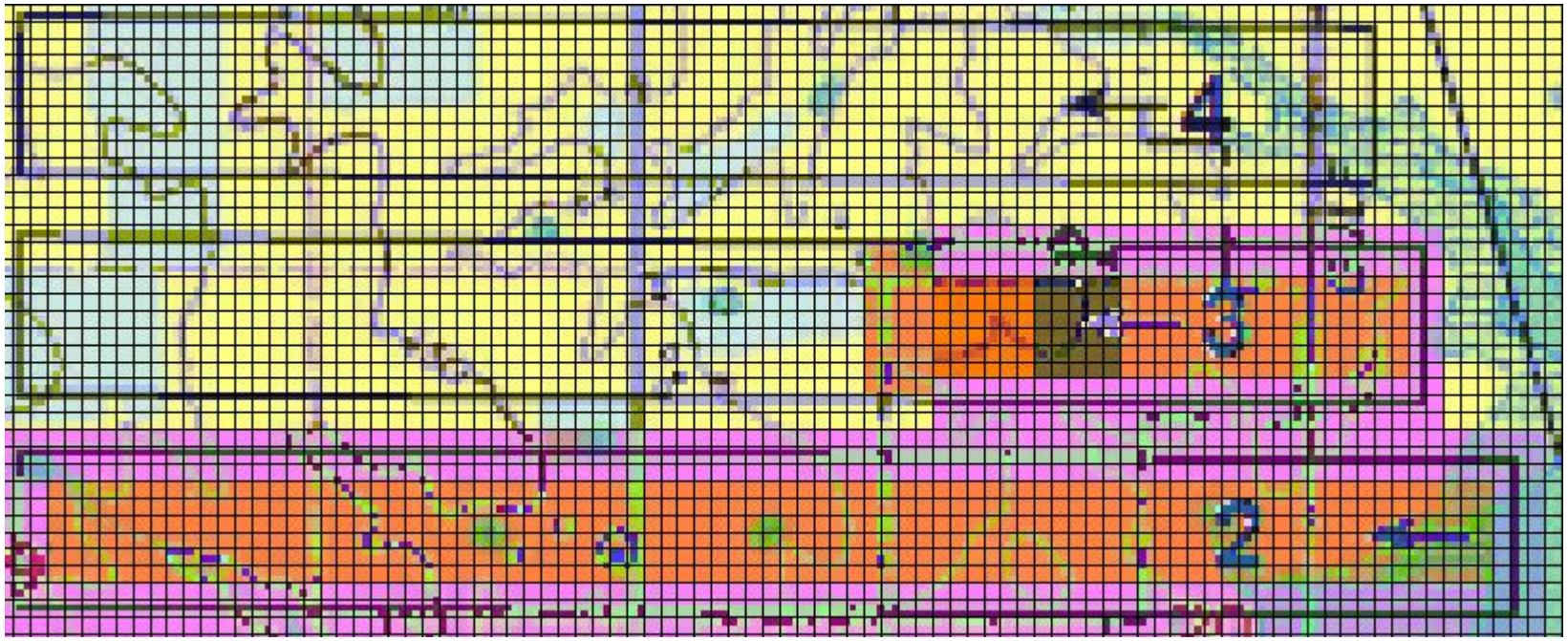

Figure 5.7A Positions of permeability stress zones in L4 at example successive advance positions of Panel 3: A (model MM-1106F).

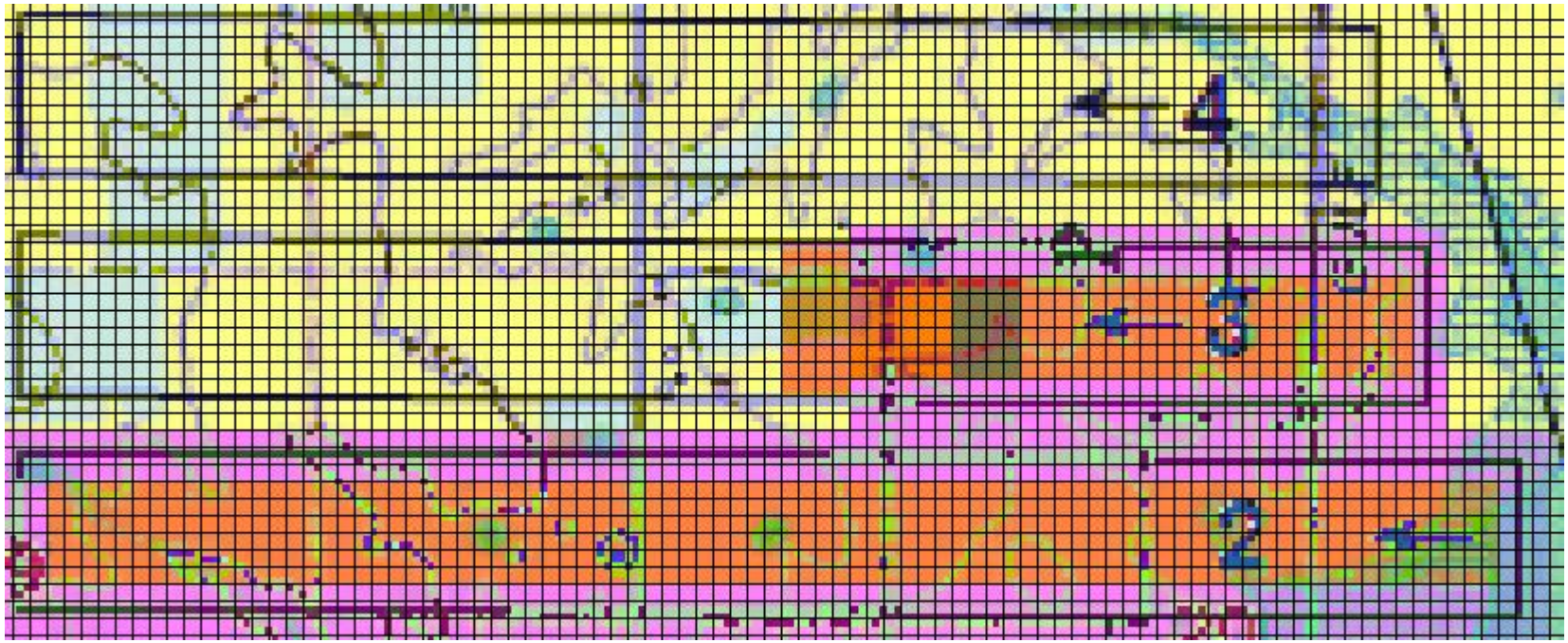

Figure 5.7B Positions of permeability stress zones in L4 at example successive advance positions of Panel 3: B (model MM-1106G).

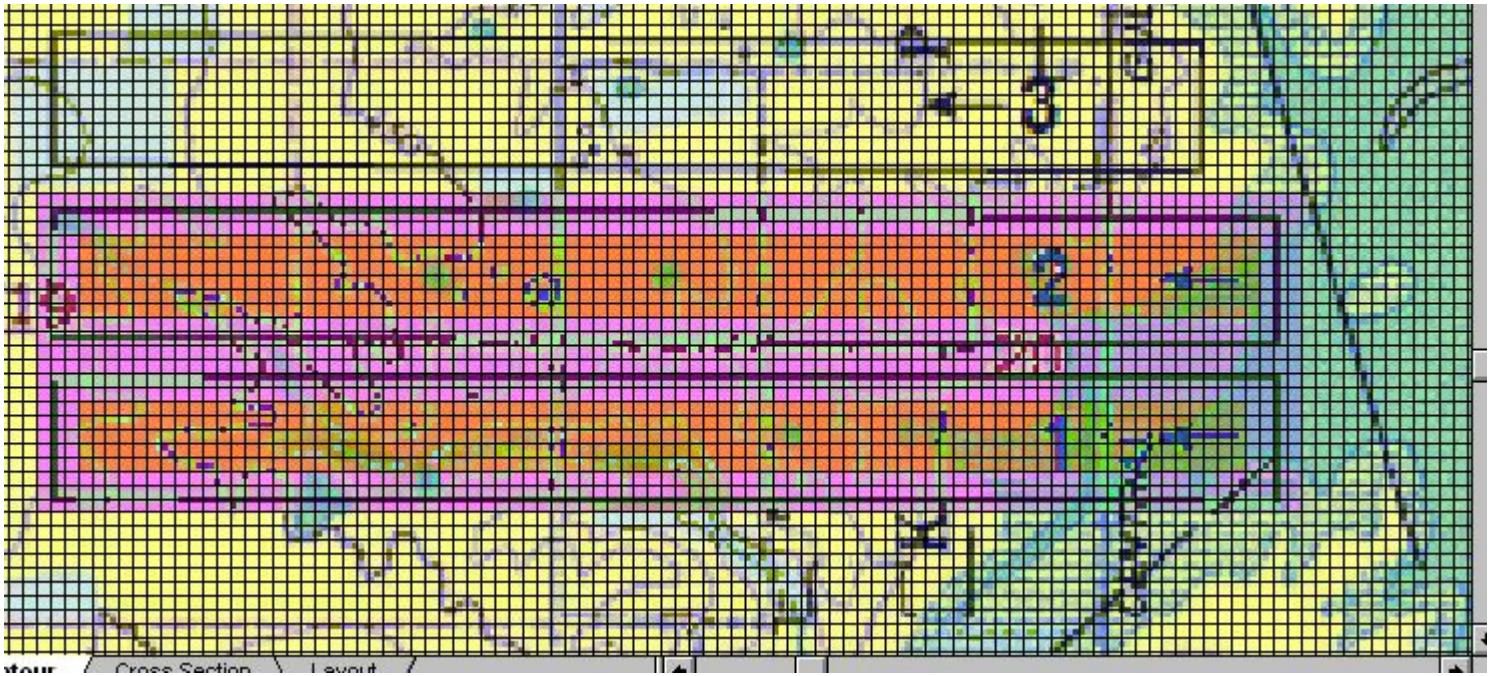

Figure 5.8A Representation of hydraulic conductivity zones for Panels 1 and 2 in Layer 6 in Model MM-1104W3.

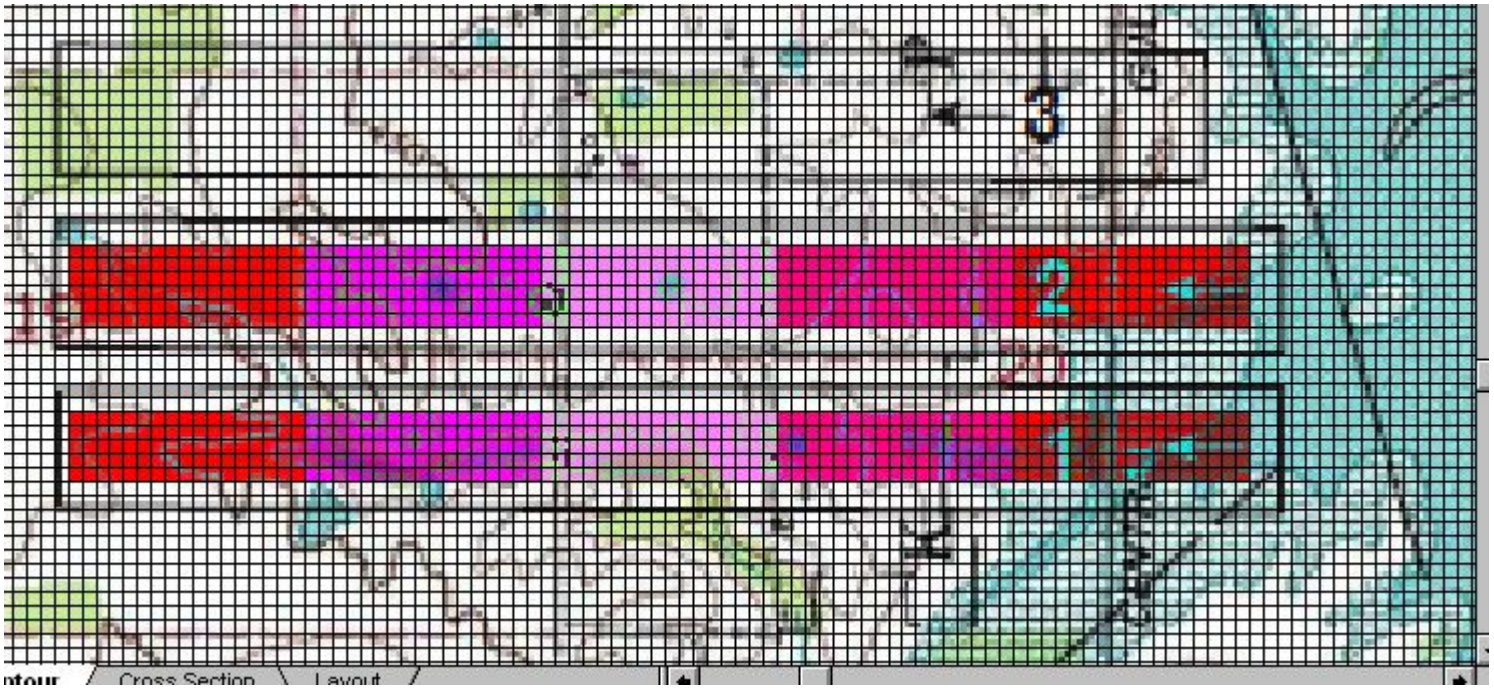

Figure 5.8B Representation of stress steps for Panels 1 and 2 in Layer 6 in Model MM-1104W3.

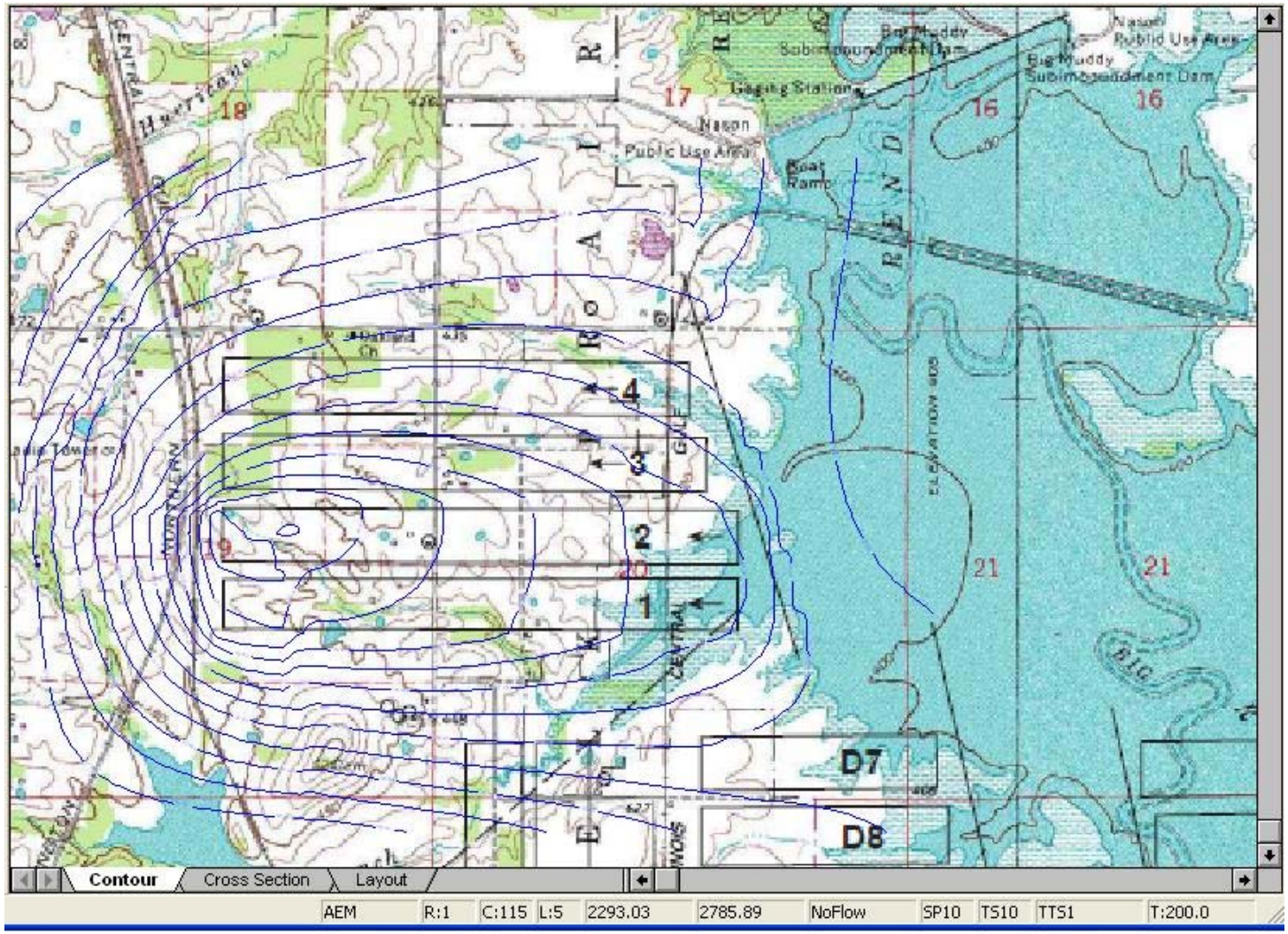

Figure 5.9 Simulated head distribution in Layer 6 at completion of Panels 1 and 2, Model MM-1104W3. Contour interval = 1.0 m, lowest contour = 115.0 m AMSL.

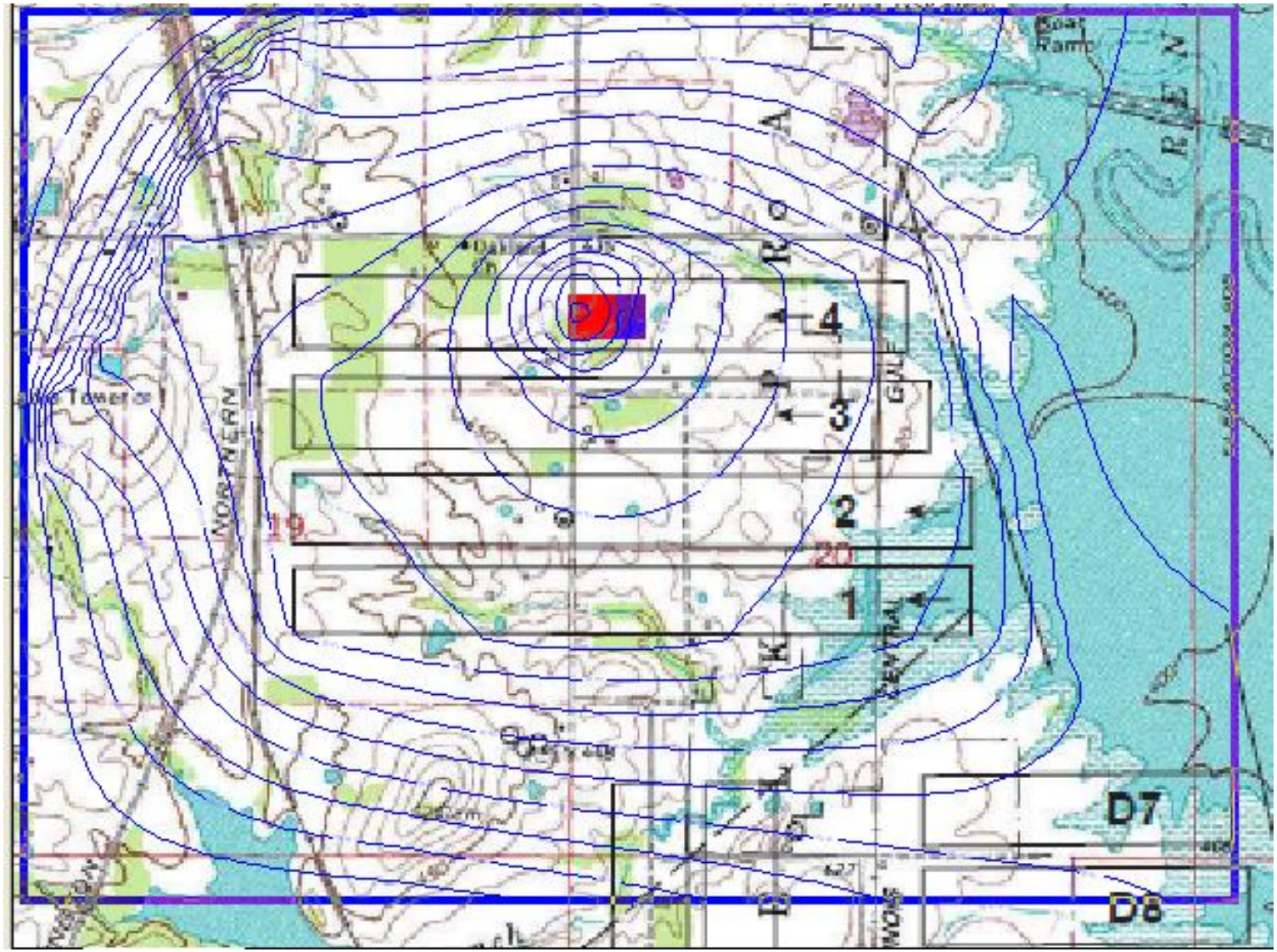

Figure 5.10 Simulated head distribution in L6 at Panel-4 mid-advance position. Contour interval = 1.0 m., lowest contour = 112 m AMSL.

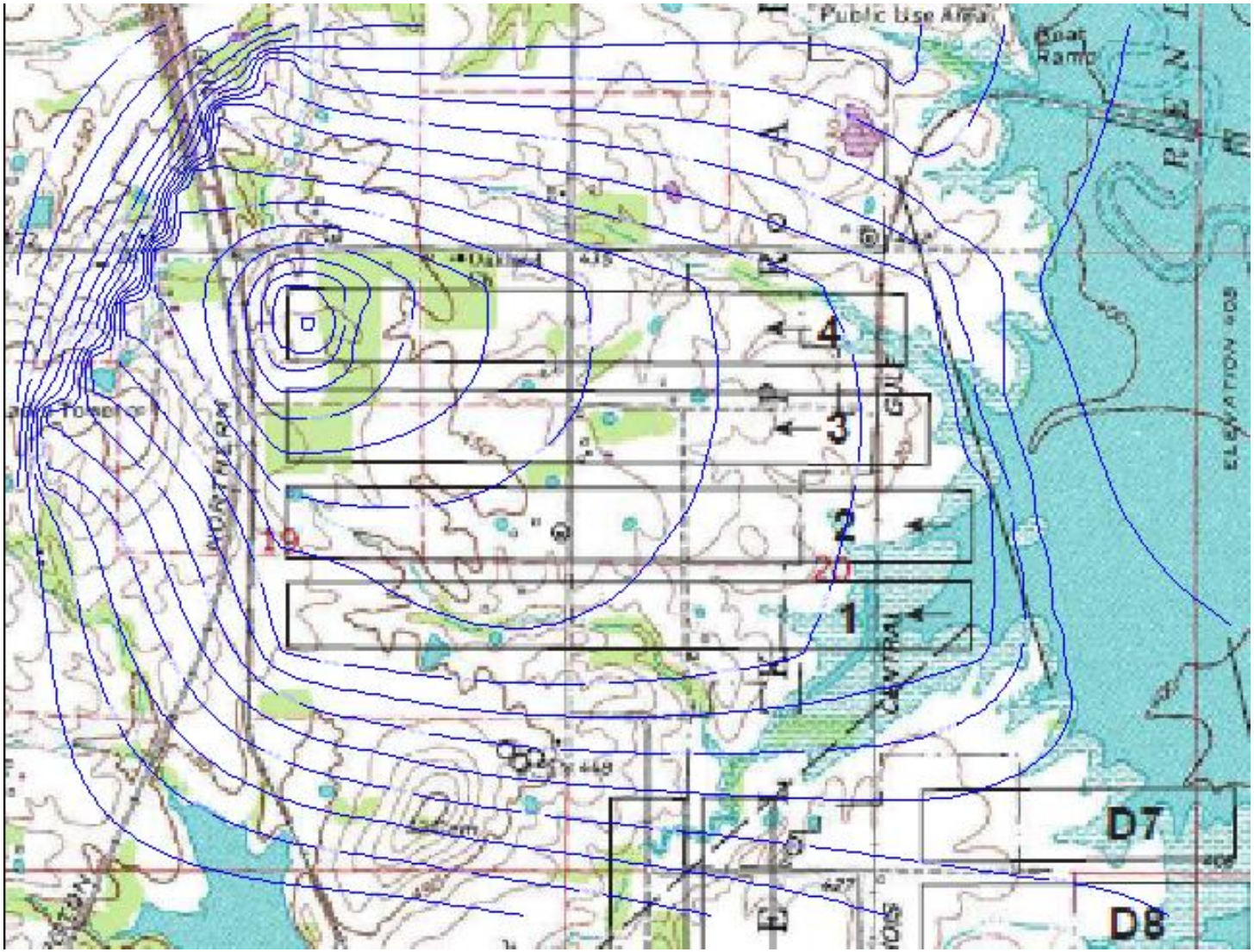

Figure 5.11 Simulated head distribution in L6 at completion of Panel 4. Contour interval = 1.0 m., lowest contour = 112 m AMSL.

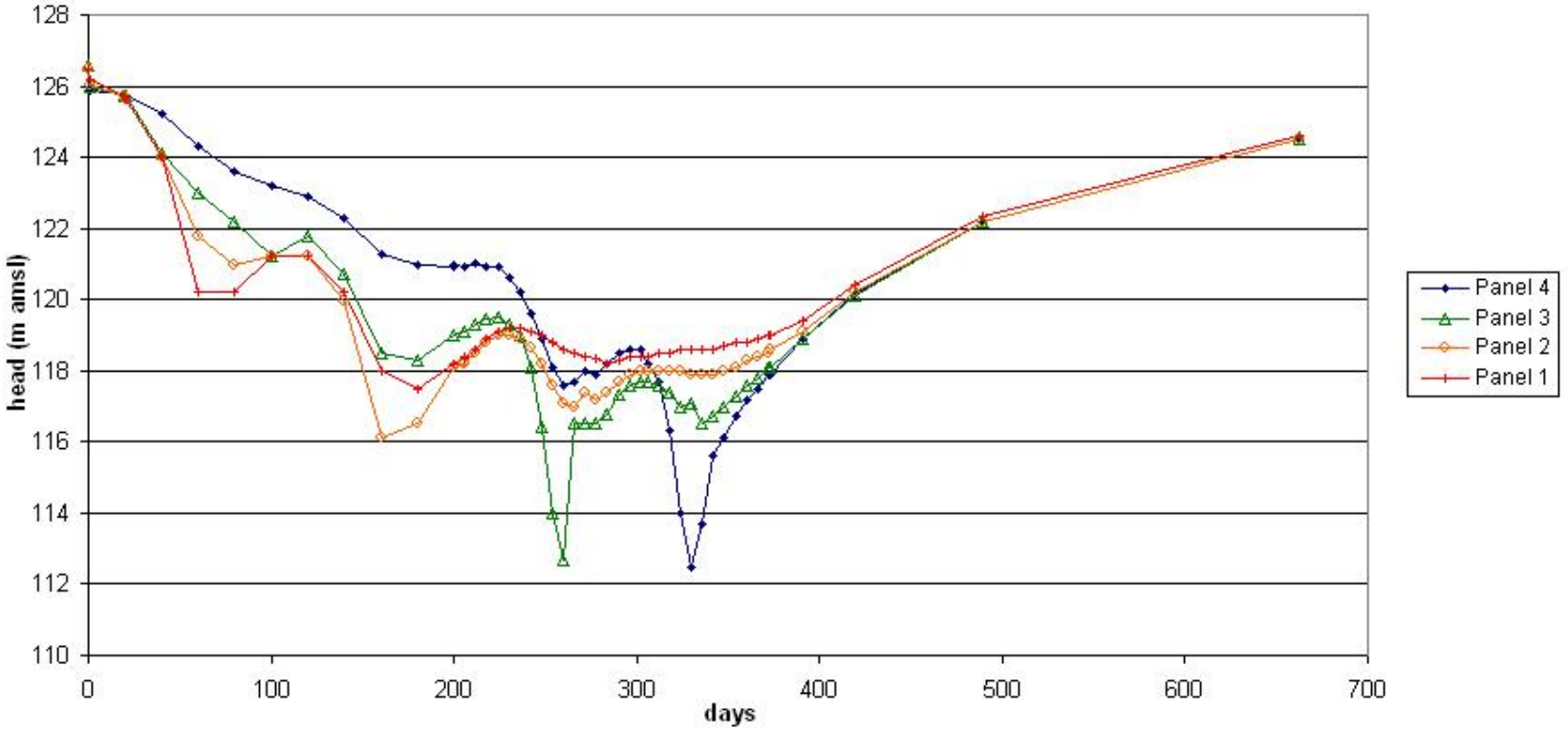

Figure 5.12 Hydrographs of simulated heads at mid-panel points for the entire simulation period.

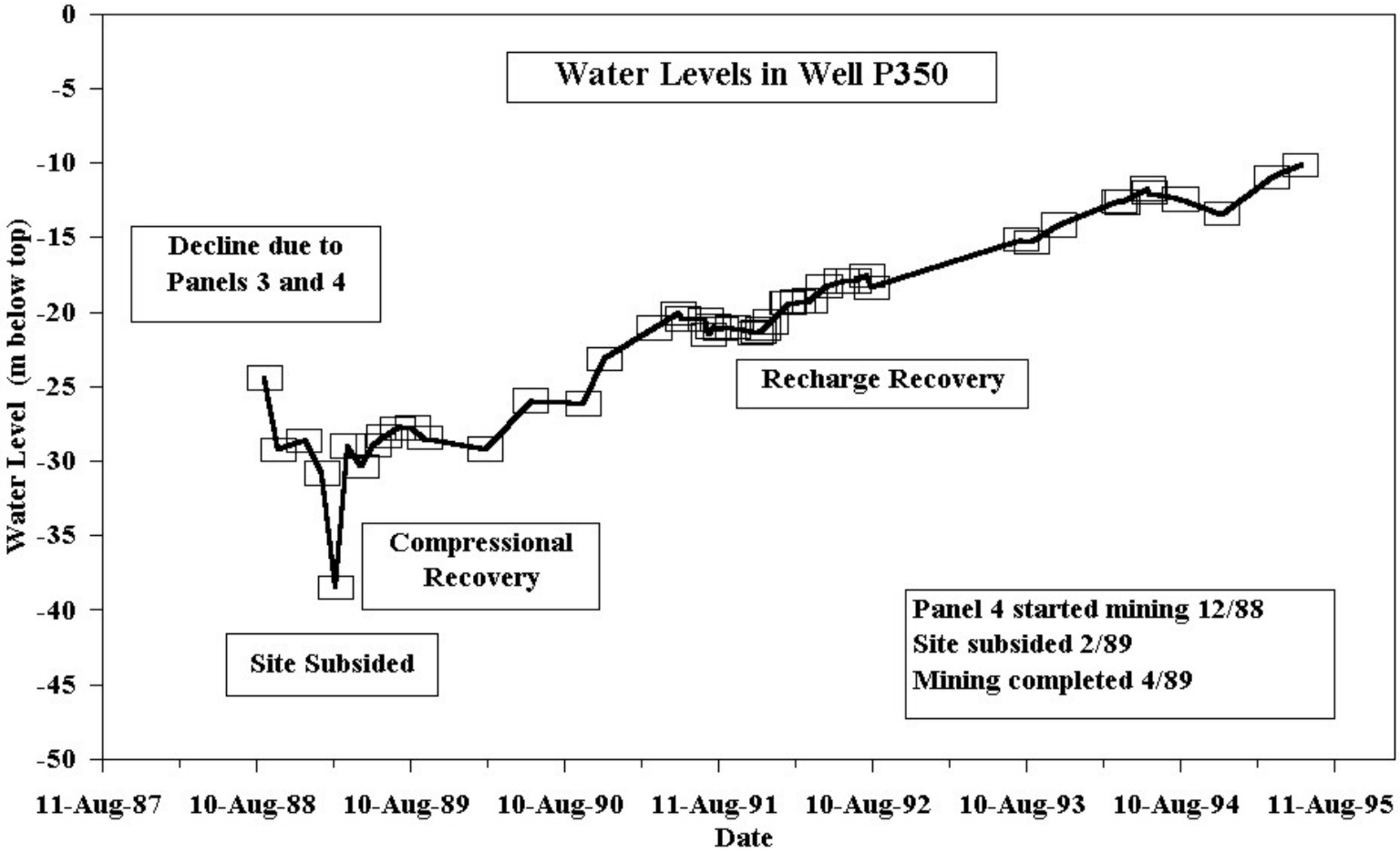

Figure 5.13 Hydrograph of well P350 (Panel 4) for entire monitoring period, 1988-1995.

APPENDIX A: MONUMENT DATA

Appendix A1: Longitudinal Monuments (Data from Mehnert et al., 1997)

Appendix A1		INFORMATION SUMMARIZED FROM MEHNERT ET AL. (1997), ISGS										
				Elevations ft amsl								
Monument #	Ft from zero	Centers of 20m grid	Baseline	Monument #	8/9/88	8/17/88	8/31/88	9/8/88	9/23/88	9/27/88	10/11/88
134	0	0	434.912	134	434.914	434.971	434.6166	431.5359	429.1678	429.1215	429.0056
136	70	65.61	435.077	136	435.0716	435.1215	434.0834	430.4428	429.2871	429.2393	429.1341
138	140	131.22	434.678	138	434.6517	434.6958	431.7338	429.4334	428.7602	428.7216	428.6164
140	210	196.83	433.963	140	433.9277	433.9687	430.0627	428.9147	428.4738	428.4479	428.349
141	245	262.44	433.248	141	433.2225	433.2471	429.1285	428.294	427.9262	427.9024	427.8057
143	315	328.05	432.034	143	432.0035	431.9928	426.7391	426.3059	426.0373	426.0247	425.9162
145	350	393.66	430.876	145	430.8381	430.7387	425.6515	425.3959	425.185	425.1655	425.0684
146	385	459.27	432.424	146	432.1645	432.0257	427.1301	426.9709	426.7882	426.7687	426.6805
147	455	524.88	433.29	147	433.1602	432.1138	428.1088	427.998	427.8461	427.8279	427.745
148	525	590.49	432.099	148	431.8841	429.7221	427.0961	427.003	426.8816	426.8665	426.7621
149	595	656.1	429.889	149	429.5145	426.0786	424.7483	424.6415	424.5399	424.5308	424.4108
150	665	721.71	428.337	150	427.3387	423.8289	423.1568	423.0604	422.9667	422.952	422.847
151	735	787.32	427.621	151	425.1837	422.9035	422.4993	422.4179	422.3351	422.3159	422.2263
152	805	852.93	427.196	152	423.4237	422.3665	422.1026	422.0237	421.9582	421.9247	421.8607
153	875	918.54	426.775	153	422.351	421.876	421.6848	421.6094	421.5545	421.5348	421.4472
154	945	984.15	425.309	154	420.5834	420.4026	420.2595	420.1806	420.1328	420.1143	420.0251
155	1085	1115.37	424.226	155	419.4984	419.4471	419.3278	419.2549	419.2165	419.1873	419.1205
156	1155	1180.98	424.212	156	419.7375	419.7433	419.6395	419.567	419.5331	419.5001	419.4439
157	1225	1246.59	423.136	157	418.5588	418.6244	418.5296	418.4636	418.4322	418.4062	418.3591
158	1295	1312.2	422.621	158	418.0016	418.0607	417.9718	417.913	417.8828	417.8548	417.8181

Appendix A2: Transverse Monuments (Data from Mehnert et al., 1997)

Appendix A2

INFORMATION SUMMARIZED FROM MEHNERT ET AL. (1997), ISGS

Monument #	Ft from zero	Centers 20m grid	Baseline ft amsl
M79	490	590.49	419.279
M81	455	459.27	419.282
M83	385	393.66	418.947
M85	315	328.05	421.289
M86	280	262.44	426.179
M88	210	196.83	434.581
M90	140	131.22	434.132
M92	70	65.61	433.891
M94	0	0	433.646
M96	70	65.61	431.281
M98	140	131.22	431.059
M99	175	196.83	432.453
M101	245	262.44	431.145
M103	315	328.05	431.587
M105	385	393.66	432.552
M107	455	459.27	433.92
M109	525	524.88	434.033
M111	595	590.49	432.807
M112	700	656.1	432.894
M113	735	721.71	433.889
M114	770	787.32	434.587
M116	840	852.93	435.042
M118	910	918.54	434.33
M120	980	984.15	432.596
M122	1050	1049.76	433.785
M124	1120	1115.37	435.105
M126	1190	1180.98	435.306
M128	1260	1246.59	435.448
M130	1330	1312.2	435.068
M131	1365	1377.81	435.353
M133	1435	1443.42	434.397

		Elevations ft amsl								
Monument #	9/1/1988	9/7/1988	9/14/1988	9/23/1988	10/11/1988	11/17/1988	1/17/1989	1/23/1989	1/26/1989	
M79							419.3027	419.3006	419.3043	
M81							419.311	419.2963	419.3002	
M83							418.9795	418.9456	418.9359	
M85							421.3042	421.2255	421.2002	
M86							426.1762	426.0575	426.0262	
M88							434.5214	434.174	434.11	
M90							433.9771	430.9117	430.6821	
M92							433.6127	428.9427	428.672	
M94							433.2875	428.2324	427.9586	
M96							430.9748	426.2551	425.9545	
M98							430.7891	428.0819	427.7752	
M99							432.1598	431.339	431.2557	
M101	431.1687	431.1765	431.1271	431.1407	431.0875	431.0771	430.8418	430.5911	430.543	
M103	431.5858	431.5928	431.5387	431.5344	431.4885	431.4794	431.2942	431.1219	431.124	
M105	432.5333	432.5519	432.4904	432.4715	432.4218	432.4069	432.2464	432.147	432.1166	
M107	433.894	433.8846	433.8187	433.7858	433.7274	433.712	433.5774	433.4888	433.4681	
M109	433.9733	433.9428	433.8357	433.7712	433.6938	433.6754	433.5502	433.4766	433.4597	
M111	432.7229	432.62	432.0185	431.764	431.6644	431.6676	431.5109	431.4477	431.4352	
M112	432.7483	432.4083	429.5975	429.058	428.916	428.8887				
M113	433.6972	433.1554	429.5756	429.0173	428.872	428.8329				
M114	434.3533	433.6527	429.6718	429.1195	428.9639	428.9287				
M116	434.7361	433.8704	429.8002	429.2404	429.0859	429.0419	428.9085	428.8755	428.8532	
M118	434.0474	433.2958	429.4588	428.8712	428.6992					
M120	432.2924	431.9483	429.4383	428.8547	428.6584					
M122	433.5461	433.3971	432.9412	432.5389	432.3215	432.2518	432.1467	432.1211		
M124	434.8563	434.7685	434.4259	434.0799	433.8589	433.797	433.6917	433.6671		
M126	435.1342	435.0598	434.7809	434.4661	434.2474	434.2442	434.0799	434.0605		
M128	435.271	435.2107	434.9559	434.6529	434.4359	434.4309	434.2748	434.3099		
M130	434.9153	434.8663	434.6262	434.3274	434.1131	434.1118	433.954	433.9736		
M131	435.1914	435.1349	434.91	434.6189	434.4052	434.4066	424.2439	434.2668		
M133	434.2705	434.2262	433.994	433.7314	433.5269	433.5289	433.3705	433.3898		

Monument #	2/1/1989	2/6/1989	4/11/1989	12/12/1989	11/14/1990	2/4/1991	5/9/1991	12/10/1991	4/15/1992	12/3/1992
M79	419.2978	419.2961	419.2923		419.3116			419.303	419.2707	419.2929
M81	419.2865	419.2791	419.2775	419.2744	419.289			419.2574	419.2052	419.1933
M83	418.9069	418.9001	418.899							
M85	421.1627	421.1469	421.1324							
M86	425.9778	425.9603	425.9383	425.8932	425.8839			425.8061	425.7108	425.6348
M88	434.0345	434.0224	433.9768	433.9261	433.8796					
M90	430.5448	430.5258	430.3995	430.278	430.0239		429.9449	429.9	429.8144	429.7709
M92	428.5129	428.4811	428.3237	428.2221	427.9			427.7649	427.6869	
M94	427.7943	427.7577	427.5952	427.4569	427.1689			427.0261	426.9673	426.9603
M96	425.7772	425.7416	425.5699	425.409	425.1396		425.0984		424.9383	
M98	427.6082	427.5652	427.3471	427.1678	426.8922				426.6932	
M99	431.1611	431.1229	430.8688	430.6705	430.3985	430.3579		430.2404	430.1906	

M101	430.4793	430.4452	430.1595	429.9551	429.6875			429.5187	429.47	429.4811
M103	431.072	431.0373	430.7525	430.5537	430.2836			430.1116	430.0654	430.08
M105	432.071	432.0498	431.7623	431.5768	431.3084	431.2573			431.0825	431.1032
M107	433.424	433.407	433.1267	432.9217	432.6629	432.6094		432.4836	432.438	432.4496
M109	433.4184	433.4065	433.1393	432.9562	432.6956	432.6517		432.5218	432.4811	432.4863
M111	431.4028	431.3953	431.1997	430.9688	430.7305	430.7183	430.5036	430.5542	430.5619	430.5353
M112										
M113										
M114										
M116				428.6704	428.5067	428.4704	428.4127	428.365	428.3326	428.3572
M118										
M120										
M122				431.9702	431.8177	431.7862				
M124				433.5442	433.3964	433.3519				
M126				433.9463	433.808	433.7702				
M128				434.164	434.0217	433.9927				
M130				433.8532	433.738	433.7018				
M131				434.1508	434.0256	434.0045				
M133				433.2868	433.1684	433.1489				